



**UNITED NATIONS
UNIVERSITY**

GEOTHERMAL TRAINING PROGRAMME
Orkustofnun, Grensásvegur 9,
IS-108 Reykjavík, Iceland

Reports 2009
Number 1

ABSORPTION REFRIGERATION SYSTEM AS AN INTEGRATED CONDENSER COOLING UNIT IN A GEOTHERMAL POWER PLANT

MSc thesis

Department of Mechanical and Industrial Engineering
University of Iceland

by

Tesha

PT. Pertamina Geothermal Energy
Menara Cakrawala (Skyline Building), 15th floor
Jl. MH. Thamrin No. 9, Jakarta 10340
INDONESIA

United Nations University
Geothermal Training Programme
Reykjavík, Iceland
Published in December 2009

ISBN 978-9979-68-266-0
ISSN 1670-7427

This MSc thesis has also been published in May 2009 by the
Faculty of Engineering – Department of Mechanical and Industrial Engineering
University of Iceland

INTRODUCTION

The Geothermal Training Programme of the United Nations University (UNU) has operated in Iceland since 1979 with six month annual courses for professionals from developing countries. The aim is to assist developing countries with significant geothermal potential to build up groups of specialists that cover most aspects of geothermal exploration and development. During 1979-2009, 424 scientists and engineers from 44 countries have completed the six month courses. They have come from Asia (43%), Africa (28%), Central America (15%), and Central and Eastern Europe (14%). There is a steady flow of requests from all over the world for the six month training and we can only meet a portion of the requests. Most of the trainees are awarded UNU Fellowships financed by the UNU and the Government of Iceland.

Candidates for the six month specialized training must have at least a BSc degree and a minimum of one year practical experience in geothermal work in their home countries prior to the training. Many of our trainees have already completed their MSc or PhD degrees when they come to Iceland, but several excellent students who have only BSc degrees have made requests to come again to Iceland for a higher academic degree. In 1999, it was decided to start admitting UNU Fellows to continue their studies and study for MSc degrees in geothermal science or engineering in co-operation with the University of Iceland. An agreement to this effect was signed with the University of Iceland. The six month studies at the UNU Geothermal Training Programme form a part of the graduate programme.

It is a pleasure to introduce the seventeenth UNU Fellow to complete the MSc studies at the University of Iceland under the co-operation agreement. Mr. Tesha, BEng. in Electrical Engineering, from PT. Pertamina Geothermal Energy, completed the six month specialized training in Geothermal Utilization at the UNU Geothermal Training Programme in October 2006. His research report was entitled "Utilization of brine water for copra drying in Lahendong geothermal field, Indonesia". After a year of geothermal research work in Indonesia, he came back to Iceland for MSc studies at the Faculty of Engineering – Department of Mechanical and Industrial Engineering of the University of Iceland in September 2007. In May 2009, he defended his MSc thesis presented here, entitled "Absorption refrigeration system as an integrated condenser cooling unit in a geothermal power plant". His studies in Iceland were financed by a fellowship from the Government of Iceland through the UNU Geothermal Training Programme. Tesha is the first Indonesian to complete his MSc studies on a fellowship from UNU-GTP. We congratulate him on his achievements and wish him all the best for the future. We thank the Faculty of Engineering of the University of Iceland for the co-operation, and his supervisors for the dedication.

Finally, I would like to mention that Tesha's MSc thesis with the figures in colour is available for downloading on our website at page www.unugtp.is/publications.

With warmest wishes from Iceland,

Ingvar B. Fridleifsson, director
United Nations University
Geothermal Training Programme

ACKNOWLEDGEMENT

This is the great opportunity to express my respect to all those who gave me the possibilities to complete this thesis. I am pleased to thank to The Government of Iceland through the United Nations University for the financial support; and to PT Pertamina Geothermal Energy for supporting and giving me the opportunity to complete this MSc programme.

My gratitude to Dr. Ingvar Birgir Fridleifsson - the director of UNU Geothermal Training Programme - and Mr. Lúdvík S. Georgsson - deputy director of UNU-GTP - for the fellowship; also to all the UNU-GTP staff, Ms. Dorte H. Holm, Ms. Thórhildur Ísberg and Mr. Markús A.G. Wilde for their continuous help.

I would like to thank to my advisors, Páll Valdimarsson and Thrándur Ólafsson for encouraging and supervising me. Thank you for the time and the discussions. I sincerely thank Mrs. Guðrún Helga Agnarsdóttir, for giving the administrative support and assistance. I am in debt to all teachers and professors at the University of Iceland. I also would like to extend my appreciation to all staffs and lecturers of Orkustofnun and Iceland Geosurvey (ISOR). I would also like to thank all UNU-Geothermal Training Programme fellows for our memorable time and friendship.

This thesis is especially dedicated to my family. Yes we can.

ABSTRACT

Geothermal energy is promising energy for any heat driven applications whether involving direct or indirect utilization processes. A separation process of a geothermal fluid mixture is mostly needed for indirect geothermal utilization, especially in power generation cycles. The separation process disposes of the liquid form of low grade thermal energy which could be utilized further for other direct and indirect utilizations such as a power plant bottoming unit, heating and cooling purposes or other heat driven processes, depending on how much of the available energy remains.

As the steam condensation process is one of the main keys for achieving high power generation efficiency, the temperature level of the condenser is very crucial. Condenser temperature regulates the lowest pressure that can be applied to the condenser, not counting the presence of non-condensable gases from geothermal fluids. Simulations for various cooling water temperatures indicate that the change in the condenser's pressure from 11.178 down to 8.651 kPa yields extra power of about 45 and 33 kW for single flash and double flash systems, respectively. In some cases, the preferred condenser pressure is not achievable due to the environmental factor, i.e. high ambient temperatures in tropical countries. Hence, the environment cannot serve plant systems with such a low temperature of the cooling water. Based on this fact, an artificial cooling system such as an absorption refrigeration system could be built in order to produce the preferred temperature of the cooling water. Heated cooling water from the outlet of a plant's condenser is first cooled by a regular cooling tower and then cooled again by the absorption system to produce a lower temperature of the cooling water.

An absorption refrigeration system (ARS) as a heat driven refrigeration system could be powered using geothermal brine water as its heat source. Single effect absorption refrigeration systems of two well-known refrigerant-absorbent pairs - Water-Lithium Bromide pair and Ammonia-Water pair - are modelled. Fed by a similar heat source, and providing the cooling load needed by the power plant condensing system, two main aspects are observed: the Coefficient of Performance and the area of heat exchangers needed to operate the absorption system. Two different scenarios are set for this integrated power and refrigeration system: fixed mass flow for both power plant and refrigeration system, and a dynamic mass flow scenario. In the dynamic mass flow scenario, some quantity of mass flow which was previously fed to the power plant system can be freely switched to the refrigeration system in order to accommodate such a refrigeration load.

Several combinations of temperature differences between the inlet and the outlet of an ARS evaporator and the evaporator's temperature were simulated to determine the optimum combination for the given heat resource. Other parameters, for example the weak-strong solution concentration difference, were also selected so that the absorption refrigeration system would work in high refrigeration efficiency with the least heat exchanger area.

TABLE OF CONTENTS

	Page
1. INTRODUCTION	1
1.1 Background.....	1
1.2 Description of study.....	1
2. GEOTHERMAL UTILIZATION	3
2.1 Introduction.....	3
2.1.1 Direct use.....	4
2.1.2 Electric power generation.....	4
2.1.3 Heat pump	4
2.2 Geothermal power plant.....	5
2.2.1 Single flash cycle.....	5
2.2.2 Double flash cycle.....	6
2.2.3 Organic Rankine cycle	7
3. REFRIGERATION SYSTEM	9
3.1 Absorption refrigeration system	10
3.1.1 Absorber	11
3.1.2 Generator/desorber	12
3.1.3 Condenser.....	13
3.1.4 Evaporator	13
3.1.5 Expansion valve	13
3.1.6 Solution heat exchanger	14
3.1.7 Solution pump	14
3.2 LiBr-H ₂ O absorption system	15
3.3 Crystallization problem.....	16
3.4 H ₂ O-NH ₃ absorption system.....	17
3.5 System efficiency.....	19
4. SYSTEM MODELLING	21
4.1 Refrigeration system	22
4.1.1 Single effect lithium bromide-water absorption system.....	22
4.1.2 Single effect water-ammonia absorption system.....	23
4.1.3 Calculation of heat exchanger area.....	25
4.2 Combination of power generation and refrigeration systems	25
4.2.1 Full resource utilization scenario.....	26
4.2.2 1MW power generation scenario.....	28
4.3 Non condensable gases	28
5. RESULTS AND DISCUSSIONS	29
5.1 Absorption refrigeration system	29
5.1.1 Weak and strong solution concentration differences.....	29
5.1.2 Solution temperature at the absorber's outlet.....	31
5.2 Electric power generation	32
5.2.1 Total electric power generation.....	32
5.2.2 Power plant condenser pressure	38
5.2.3 ARS investment cost	39
6 CONCLUSIONS.....	41
7 RECOMMENDATION FOR FUTURE WORKS.....	42
REFERENCES	43

	Page
APPENDIX A: Aqueous lithium bromide solubility	44
APPENDIX B: Model	45
APPENDIX C: Simulation results	47
APPENDIX D: Optimum design parameters	51
APPENDIX E: EES source code.....	55

LIST OF FIGURES

1. Geothermal utilization with respect to the temperature of geothermal fluid	3
2. Simplified layout of single flash geothermal power plant	6
3. Simplified layout of double flash geothermal power plant	6
4. Simplified layout of organic rankine cycle with recuperation unit	7
5. A simple compression refrigeration system.....	9
6. A simple absorption refrigeration system	9
7. Duhring plot for single effect absorption system	10
8. Single effect LiBr-H ₂ O absorption refrigeration system.....	12
9. A typical effect of a solution heat exchanger's effectiveness on COP of refrigeration	14
10. Equilibrium chart for Aqueous Lithium Bromide solutions	16
11. Aqueous lithium bromide phase diagram	16
12. Enthalpy-concentration diagram for water-ammonia solutions	17
13. Single effect H ₂ O-NH ₃ absorption refrigeration system	18
14. Single effect lithium bromide refrigeration with refrigerant heat exchanger.....	19
15. Effect of refrigerant heat exchanger on COP for various evaporator temperatures	20
16. Duhring plot for LiBr crystallization control	23
17. Single effect NH ₃ refrigeration with refrigerant heat exchanger	24
18. Basic design of integrated power generation and absorption refrigeration system.....	26
19. Model of double flash and water-ammonia absorption refrigeration system.....	27
20. Heat exchanger area for different refrigeration capacities and evaporator temperature	29
21. Effect of weak and strong NH ₃ concentration differences on system performance.....	30
22. Effects of weak and strong LiBr concentration differences on system performance.....	30
23. Performance for various NH ₃ strong solution temperatures at the outlet of the absorber.....	31
24. Performance for various LiBr weak solution temperatures at the outlet of the absorber.....	32
25. Relationship between cooling water temperature, condenser and generation capacity	32
26. Integrated single flash-single effect absorption refrigeration system	34
27. Integrated double flash-single effect absorption refrigeration system	34
28. Integrated organic rankine cycle-single effect absorption refrigeration system	35
29. Maximum possible net power output for combination of power and refrigeration system	36
30. Net power generation on various evaporator temperature and chilled water temperature.....	37
31. Net power-area ratio of integrated single flash and lithium bromide-water ARS.....	37
32. A temperature-entropy diagram for the steam	39

LIST OF TABLES

1. Thermodynamic properties of some candidate working fluids.....	8
2. Initial design parameters for single effect ARS scenario	22
3. Design parameters for lithium bromide absorption system	22
4. Design parameters for ammonia absorption system	24
5. U value for several heat exchange situations	25
6. Design parameter of U value for each unit of heat exchanger	25

	Page
7. General design parameters for integrated power and absorption system.....	25
8. Maximum possible net power output.....	36
9. ARS main parameters and the final results	38
10. Gas extraction process data.....	38
11. Estimation of total capital investment for single effect lithium bromide-water ARS.....	40
12. Estimation of ARS investment cost for 1MW power generation scenario	40

LIST OF SYMBOLS

A	Area [m^2]
ARS	Absorption Refrigeration system
COP	Coefficient of Performance
$\Delta T_{cooling}$	External temperature difference at the inlet and outlet of evaporator [$^{\circ}C$]
η_{pump}	Solution pump efficiency [-]
η_{rec}	Rectifier efficiency [-]
η_{rhx}	Refrigerant Heat Exchanger efficiency [-]
η_{shx}	Solution Heat Exchanger efficiency [-]
h_i	Enthalpy [kJ/kg]
$LMTD$	Log Mean Temperature Difference [$^{\circ}C$]
\dot{m}_i	Mass flow [kg/s]
Q_a	ARS absorber heat [kW]
Q_c	ARS condenser heat [kW]
Q_d	ARS desorber heat [kW]
Q_e	ARS evaporator heat [kW]
s_i	Entropy [kJ/kg.C]
T_i	Temperature [$^{\circ}C$]
U_i	Overall heat transfer [kW/ $m^2.C$]
v_i	Specific volume [m^3/kg]
W	Work [kW]
x_i	Solution concentration [%]; Steam Quality [-]

1. INTRODUCTION

Utilizing and managing all available energy resources in a smart and wise manner is unarguable regardless of its renewability, sustainability or lack thereof. Many efforts have been made to advantageously use any wasted and un-utilized energy.

Geothermal energy is a sustainable energy that could be utilized either directly or indirectly. Occasionally, a separation process of geothermal fluid mixtures is needed to extract the steam from the liquid. Low grade thermal energy is produced during the separation process and is considered wasted energy, awaiting further utilization processes or just injected back into the earth without any effort to harvest the heat. Hence, depending on its energy content, this low grade thermal energy could power heat driven processes such as district heating, balneology activity, drying and cooling processes or even be re-separated for other indirect utilization such as in a double flash power generation cycle.

Since the absorption refrigeration system needs thermal energy as the heat source, and geothermal brine water is full of thermal energy, a geothermal absorption refrigeration system using brine waste energy as the heat source could be a good combination to serve any refrigeration or cooling demands.

1.1 Background

A geothermal power plant has similar characteristics to a steam power plant; both systems employ a steam turbine to create mechanical work from steam. The steam quality and steam condensation process control the production capacity of mechanical work. Steam quality depends on the geothermal resource and the separation process, while the condensation is strongly related to the environment and cooling water availability.

In tropical and some other areas, high air temperature and the availability of low temperature cooling water emerge as obstacles to the steam condensation process. The steam condensation process is always completed in the condenser if designed properly. If it occurs at a higher temperature, the leftover steam within the condenser increases, which increases condenser pressure and lowers turbine capacity.

An absorption refrigeration system as a heat-activated thermal cycle seems to be a good combination of utilization for any geothermal resource where applicable, especially with a power generation system which disposes of low grade thermal energy. An absorption cycle uses a heat source which could include the low temperature geothermal resource or a waste heat resource from the geothermal power plant. This waste energy powers the absorption machine and the chilled water from the absorption machine feeds the plant's condenser, mutually benefiting both systems.

1.2 Description of study

Utilization of geothermal energy for electric power generation mostly involves a separation process that will turn geothermal fluid mixtures into two different fluid phases, pure steam and brine water. As waste energy from the power generation process, the remaining heat content in brine water is still high enough to run an absorption refrigeration cycle. Steam from the steam separator feeds a geothermal power plant and the brine water delivers its heat to a single effect absorption refrigeration system.

There are two well-known absorbent-refrigerant pairs of working fluid widely used in absorption technology: Lithium Bromide-Water and Water-Ammonia. Comparison of the performance of these two systems will be observed, operating from a dedicated geothermal heat source in cooperation with a power generation system and fed from the same heat source as the power generation system.

As a first step, a stand-alone single effect absorption refrigeration system is modelled and compared for both lithium bromide and ammonia systems. Each absorption parameter is observed and the possibility of an internal heat exchange process that might increase refrigeration performance is evaluated.

An integrated power generation and absorption system is then modelled and simulated where both systems are designed to support each other and operate side by side. The waste heat from the power generation process feeds the Absorption Refrigeration System heat demand and the ARS supplies cooling water to the power plants. Absorption technology will be employed to produce a lower temperature of cooling water from the available resource and then pass it on to the power plant's condenser.

The aim in lowering the temperature of the cooling water is to accommodate a situation where it is hard to find a low temperature water resource, especially in tropical countries. The lack of low water temperature availability will affect the steam condensation process and will, moreover, decrease efficiency and power production. This study tries to reveal the possibilities of using geothermal ARS to produce lower cooling water temperature, even though the ARS needs its own heat sink system. By lowering the temperature of the cooling water, there should be some enhancement in the capacity for power generation. The improvement of production capacity will be observed along with the rise of the investment cost caused by the refrigeration unit.

A brief analysis of the absorption refrigeration system utilization for an air conditioning system will also be discussed in the last chapter of this report.

All modelling concepts, such as power generation, absorption cycle and cooling load calculations, used in this report are based on steady state analysis.

2. GEOTHERMAL UTILIZATION

Geothermal utilization deals with harvesting the energy content within geothermal fluid directly or indirectly. The type of geothermal resources determines the method of its utilization. A high temperature resource (dry steam/hot fluids) can be gainfully utilized to generate electric power, whereas the moderate-to-low-temperature resources (warm-to-hot water) are best suited for direct uses (Gupta & Roy, 2007). Despite the advantage of geothermal as a promising energy resource, some natural problems should not be neglected such as volcano eruptions and earthquakes since the geothermal resource is located in this type of environment.

2.1 Introduction

Geothermal, which means earth heat, is an energy resource that can be found anywhere in the world. Earth heat is a potential energy resource and is considered to be a relatively clean and renewable energy resource. Based on this perspective of temperature, it can be grouped as low temperature and high temperature geothermal resources. There is no exact boundary in category determination of geothermal resources, but it is common to name a resource which has a temperature gradient lower than 150°C per 1km depth as a low temperature geothermal resource and a high temperature geothermal resource for a system with a temperature gradient higher than 200°C per 1 km depth. A middle temperature geothermal resource can be virtually named for other resources in between. There are three main methods in utilizing geothermal resources: direct use, electric power generation and heat pumps.

A broad classification of the various direct uses of geothermal fluids on the basis of temperature requirements has been suggested by Lindal (1973). The Lindal diagram has been widely used and can be used as a rough estimation in order to utilize geothermal fluids as shown in Figure 1. Geothermal utilization should include good reservoir management and monitoring together with preventive action to protect the utilization process from corrosion, scaling and any chemical problem that might come naturally from geothermal fluids.

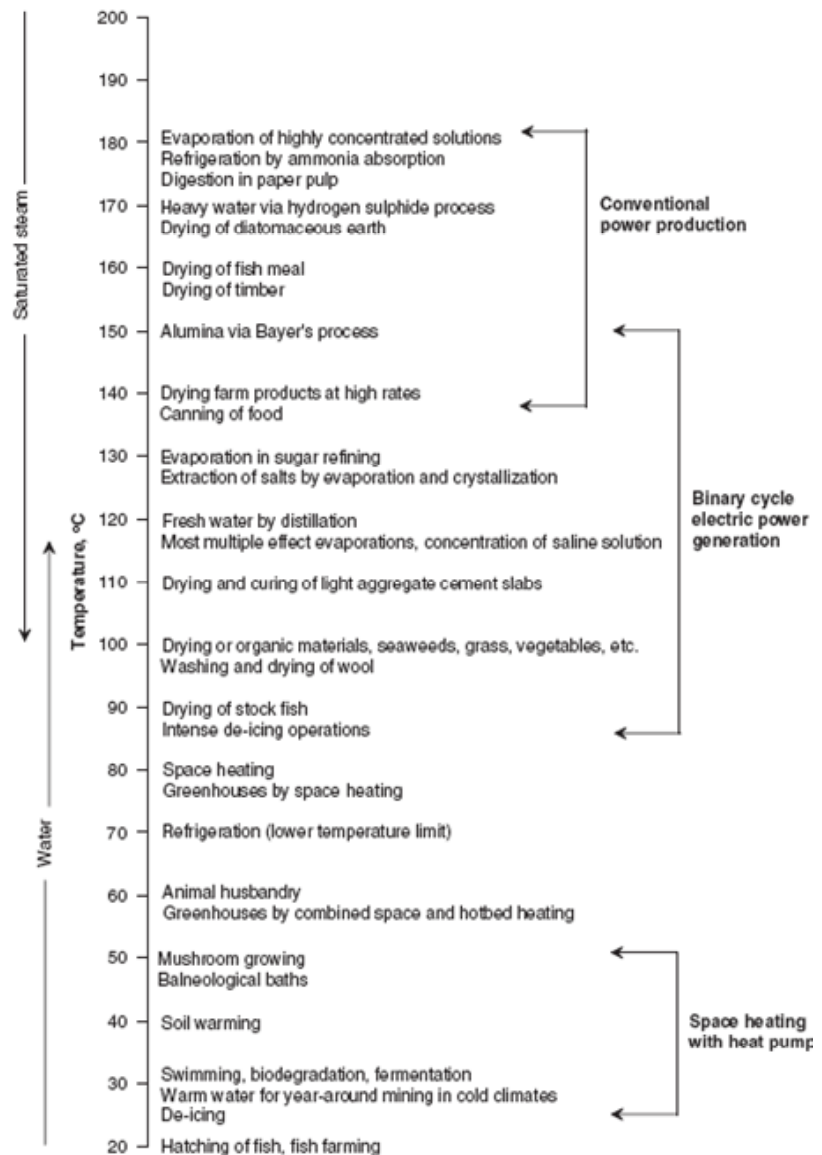


FIGURE 1: Geothermal utilization with respect to the temperature of geothermal fluid (Gupta & Roy, 2007)

2.1.1 Direct use

Direct uses of geothermal energy mainly utilize the geothermal hot water to provide heat directly for many purposes such as bathing and district heating. Hot water might come from geothermal wells, springs or a separation process of geothermal fluid mixtures. Direct use of geothermal energy refers to the use of the heat energy of low to moderate temperature geothermal waters without conversion to some other form of energy such as electrical energy or without any use of heat pump technology.

Conventional direct uses of geothermal fluid have been used for long periods of time where communities utilize hot springs for bathing and balneology. Nowadays, in modern direct use systems, the hot water is produced from a drilled geothermal well involving preliminary and conceptual design of a direct use project together with reservoir testing and evaluation. Most geothermal direct use systems use heat exchangers to keep the geothermal fluid separate from the working fluid that conveys the heat from geothermal fluids to the application. Development of direct use systems, especially when heat exchangers are not used, requires careful corrosion engineering if the most cost effective material selections and design choices are to be made.

The use of high enthalpy geothermal resources for the generation of electric power continues to be more popular even though the economic as well as environmental benefits of using moderate-to-low enthalpy fluids for direct use are still promising. Indeed, moderate-to-low enthalpy is widely applied in non-tropical regions where space heating demand is very high, not to mention the use of geothermal fluid for industrial purposes such as agricultural and drying processes. However, one problem in the developmental process of direct use beside of the cost related issue is the fact that geothermal waters can only be transported in a limited range and distance due to heat loss along the transmission line.

2.1.2 Electric power generation

Electric power generation utilizes high temperature geothermal resources ($>200^{\circ}\text{C}$) where the extracted steam drives turbines to create mechanical work. There are some energy conversion systems during electric power generation such as the separation process of geothermal fluid, creating mechanical energy, generating electricity from mechanical energy and disposing of the geothermal fluid after the power generation process.

A geothermal electric power generation process is basically similar to a steam power generation process with a steam creation process distinct for both power generation systems. Steam, in geothermal power generation systems produced from geothermal wells, could be either in the form of dry steam or liquid-steam mixtures. Dry steam from a geothermal well could be used directly to generate power, while flashing and a separation process are needed for liquid-steam mixtures of geothermal fluid. Multi-stage flashing power generation cycles are mostly used for liquid dominated geothermal resources.

However, by using recent power generation technologies, it is now possible to generate electric power from a lower temperature geothermal resource ($\sim 100^{\circ}\text{C}$) using a binary-cycle method. Performance and capital cost of a flashing cycle depend on a large, expensive low pressure steam turbine; in a binary cycle, they rely on the primary heat exchanger and condenser.

2.1.3 Heat pump

A heat pump is another technology of direct uses and usually applies for heating and cooling of buildings. Heat pump technology works against the natural condition of heat flows from higher temperature to lower temperature. To bring the heat from a lower to a higher temperature, work must be added to the system. Ground-source heat pumps use the earth or ground-water as a heat source in winter time and as a heat-sink in summer. The heat pump circulates water or other working fluids through pipe loops which are buried a few meters down in the ground and makes use of the temperature difference between a relatively stable ground temperature and atmospheric temperature to

remove heat from the building during summer and pump heat into the building during winter. Basically, heat pump technology can provide either heating or cooling effects to a confined space.

2.2 Geothermal power plant

A geothermal power plant and a steam power plant are basically steam driven power generating systems; the distinction between the two is in the method in which the steam is produced. A man-made steam is employed in a regular steam plant cycle. On the other hand, steam develops within a potential geothermal system somewhere down below the surface, just waiting to be harvested and utilized directly and/or indirectly. This condition constrains the developmental process of a geothermal power plant in that the plant can only be built near the geothermal resource.

The first geothermal power plant began when a $\frac{3}{4}$ HP steam engine was used to drive a small generator in the Tuscany village of Larderello, Italy in 1904 and 10 years later the first 250 kW commercial unit ran in 1914 (Elliot et al., 1997). Geothermal power plants require high temperature geothermal resources to operate. This high temperature resource may come from dry steam wells, two phase wells or hot water wells. There are three types of geothermal power plants:

- **Dry steam plant**
Geothermal area either with a dry steam or vapour dominated reservoir characteristics; produces dry, saturated, or slightly superheated steam with very little water content. Even though this dry steam could be directly piped into a power plant and feed the turbine, a cyclone separator is still needed to remove any rock bits from the reservoir and to clean the steam of any unwanted material. Moisture removal is conducted at the entrance of the power house since the condensation process is applied along the transmission line.
- **Flash steam plant**
Flash steam plants are the most commonly used for electric power generation because most geothermal reservoirs are formed by liquid dominated hydrothermal systems. There is no significant difference from a dry steam plant except for the presence of waste liquid from the separator that requires handling. This type of plant utilizes two phase or liquid dominated geothermal fluid ($\sim 180^\circ\text{C}$) from a hot water reservoir. The fluid mixture has to be separated first and then the extracted steam drives the turbine while the liquid phase is disposed of out of the separator as brine water. The liquid from the separator may then be injected back into the injection well, sent to a heat exchange system for various direct heat applications, or flashed again to a lower pressure separator in order to produce extra steam for a low pressure turbine.
- **Binary steam plant**
One working method for utilizing low temperature geothermal fluid (85°C - 150°C) for electric generation uses a binary cycle method. Energy from a geothermal fluid is transferred to a low boiling synthetic working fluid such as propane, isopentane or ammonia through a heat exchanger or boiler mechanism. The heated working fluid flashes into vapour and drives the turbine. The vapour is then condensed and ready for the next heating cycle, creating a closed-loop system. A variant of the binary cycle technology, known as the Kalina Thermodynamic Cycle, potentially yields higher thermal efficiency compared to the ORC (Gupta & Roy, 2007). The Kalina cycle uses two-component vapour containing typically 70% ammonia and 30% water as the working fluid.

2.2.1 Single flash cycle

A single flash power plant is often considered for the first plant system installed in a newly developed geothermal area, especially in liquid dominated geothermal fields. Power generation in a single flash cycle involves a man-made flashing mechanism done by a cyclone separator; as depicted by its name, there is only one flashing process during the cycle. Flashing is important to keep the liquid portion out of the steam phase where a high quality of steam is needed by the steam turbine.

Geothermal fluid from the well is directed to a cyclone separator and tapped in-between to a silencer for emergency fluid venting. Separated steam from the cyclone separator is then throttled to a steam turbine and the liquid phase is sent to the injection well. The steam condensation process could be done either in a surface type condenser or a direct contact condenser. As seen in Figure 2, a surface type condenser is used where the geothermal steam passes through the shell side of a shell and tube heat exchanger and the cooling water passes through the tube side. Since geothermal fluid contains various amounts of non condensable gasses such as carbon dioxide, these gasses tend to accumulate within the condenser which could raise the pressure in the condenser and lower the turbine power output as a final effect.

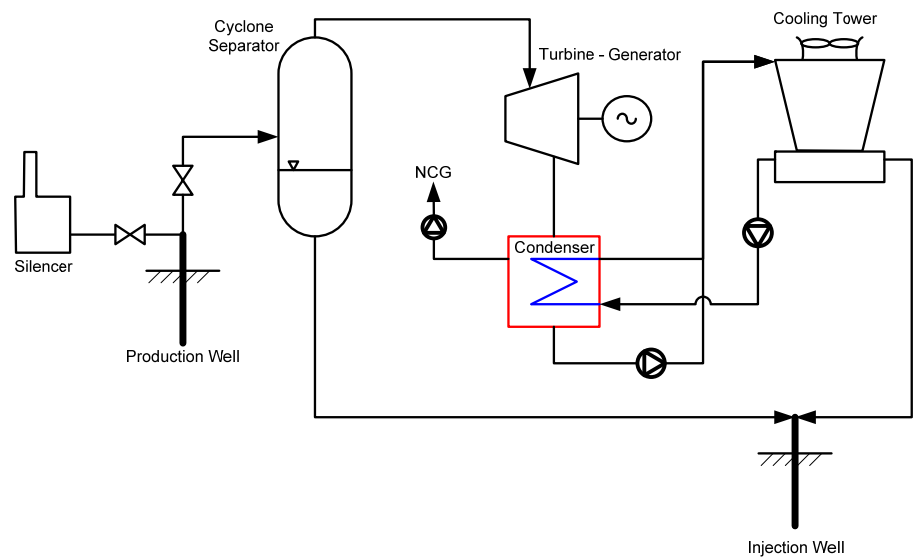


FIGURE 2: Simplified layout of single flash geothermal power plant

Heat exchange within the condenser is achieved by cooling water which is re-circulated through a cooling tower that removes heat from the cooling water and makes it ready for another condensing process. Small amounts of cooling water are lost to the environment during the process in the cooling tower. However, this could be compensated for by condensate that is mixed together with the heated cooling water before entering the cooling tower. Some excess liquids from the cooling tower could be pumped to the injection well.

2.2.2 Double flash cycle

The double flash steam plant (Figure 3) is an improvement on the single flash design in that it can produce 15-25% more power output for the same geothermal fluid conditions (DiPippo, 2007). The plant is more complex, more costly and requires more maintenance, but the extra power output often justifies the installation of such plants. As an improvement on a single flash cycle, a double flash system employs two stages of a steam flash mechanism from two different pressures of the cyclone separator. What makes this cycle different from a single flash cycle is the secondary flash of brine or liquid phase from the primary separator.

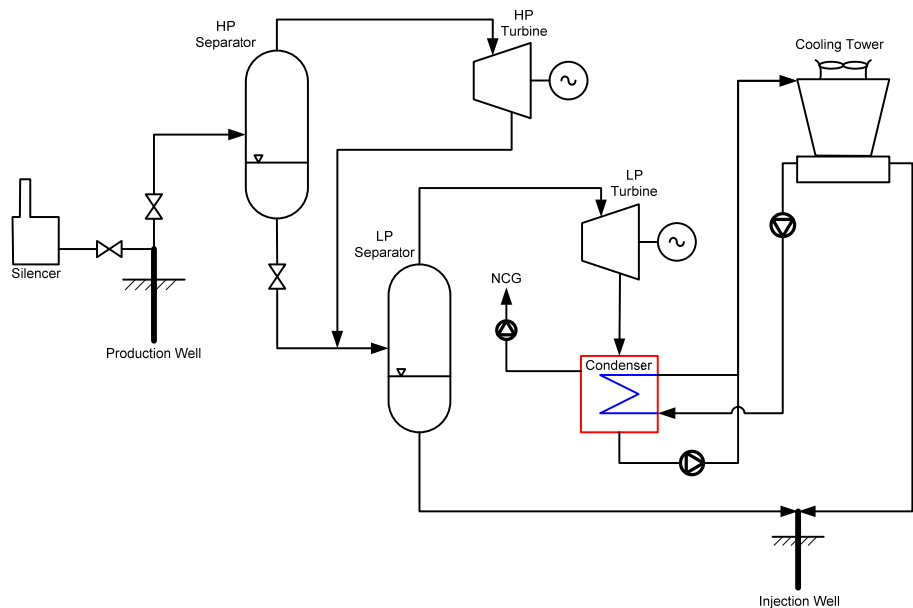


FIGURE 3: Simplified layout of double flash geothermal power plant

Brine water from a primary or higher pressure separator is led to a secondary or lower pressure separator producing low pressure steam. This low pressure steam drives a low turbine together with the exhaust steam from a high pressure turbine. Since the exhaust steam from a higher pressure turbine has high moisture content, it is necessary to clean it first in a special demister unit or by just mixing it with brine water from the primary separator. In this system, there will be two different pressures for each separator and turbine.

Employing additional flash processes, the waste brine amount in a double flash cycle is less than in a single flash cycle. Since the chemical content stays the same, the final brine water from the secondary separator has a higher chemical concentration than single flash can produce for similar characteristics of a geothermal fluid. Higher chemical concentrations lead to higher solubility temperature, thus, the processes should be designed properly to avoid chemical precipitation such as silica scaling.

2.2.3 Organic Rankine cycle

An organic Rankine cycle uses a secondary liquid for delivering energy from geothermal fluid to the application. The working fluid receives heat from the geothermal fluid through a heat exchanging process. By receiving the heat from geothermal fluid, the working fluid starts to vaporize and is then ready for the next power generation cycle such as drives the turbine and condensation process where the condensed working fluid is prepared for the next evaporation cycle. Thus, it forms a closed loop working fluid system. The first geothermal binary power plant was put into operation at Paratunka, near the city of Petropavlovsk on Russia's Kamchatka peninsula in 1967.

Organic Rankine is a promising technology when low temperature geothermal resource cannot drive the steam turbine directly or when geothermal fluid is too contaminated with dissolved gasses or corrosive minerals which can either jeopardize the turbine or become a problem in the flash cycle. Nowadays, the addition of an organic Rankine cycle as a bottoming unit in a flash steam plant to utilize low grade thermal energy from waste brine water is looked upon favourably.

Since the organic Rankine utilizes the low temperature of geothermal fluid, minimal geothermal fluid along the outlet of the evaporator and reinjection well should be maintained at a temperature above where silica scaling and other chemical problems begin. Pressurized geothermal fluid is an alternative that could overcome this problem.

A simplified layout of an organic Rankine cycle is illustrated in Figure 4, although it could be simplified more by removing the recuperation unit from the system. The recuperator is an additional unit that can increase the efficiency of a Rankine cycle by accommodating an appropriate heat exchange internally.

There are many choices for the working fluid of an organic Rankine cycle. The selection of a working fluid for a geothermal organic Rankine plant is based on the characteristics of the geothermal fluid, especially the temperature. The most

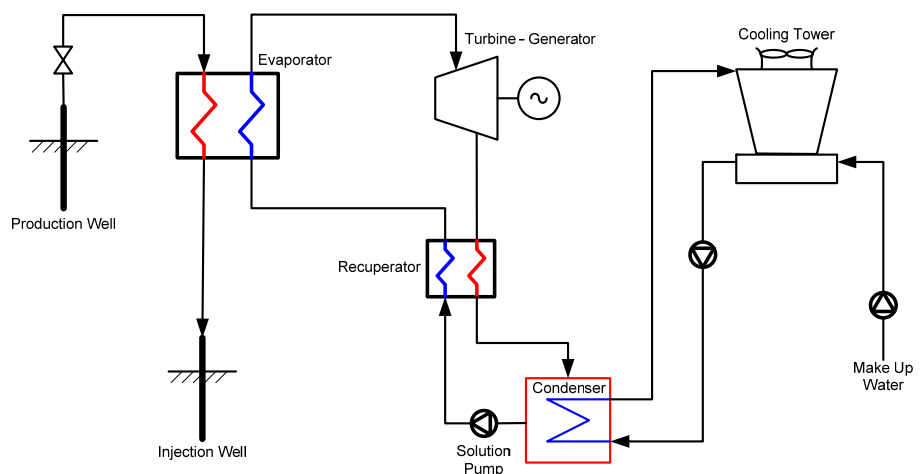


FIGURE 4: Simplified layout of organic Rankine cycle with recuperation unit

common and widely used working fluid is a hydrocarbon based fluid such as isobutane, isopentane or propane. A good design and selection of a working fluid gives optimum efficiency, both technically and economically for a given geothermal fluid condition.

TABLE 1: Thermodynamic properties of some candidate working fluids for binary plants (DiPippo, 2008)

Working fluid	Formula	Critical temperature [°C]	Critical pressure [kPa]
Ammonia	NH ₃	133.65	11,627
Isobutane	i-C ₄ H ₁₀	135.92	3,685
Isopentane	i-C ₅ H ₁₂	187.80	3,409
n-Butane	C ₄ H ₁₀	150.80	3,718
n-Pentane	C ₅ H ₁₂	193.90	3,240
Propane	C ₃ H ₈	96.95	4,236
Water	H ₂ O	374.14	22,089

3. REFRIGERATION SYSTEM

Refrigeration is a process for removing heat from an object, mainly in a confined space, and rejecting the unwanted heat into a specific preferable environment; in other words, the refrigeration process is a method for lowering the temperature of an object. There are two common refrigeration systems which are widely used: Absorption Refrigeration System (ARS) and Compression Refrigeration System.

A compression refrigeration system utilizes a mechanical compressor, i.e. electric motor, to mechanically drive the heat transfer from a low temperature to a high temperature (Figure 5). Conversely, in an absorption refrigeration system (Figure 6), this mechanical compressor is replaced by two heat exchange units, a generator/desorber and an absorber, which create a heat driven heat transfer from a low temperature to a high temperature. Even though these two units replace the function of a mechanical compressor, electric pump still can be found in most absorption refrigeration system as a common and simple way to circulate the working fluid from the low pressure level to the high pressure level. However, the electric pump only consumes a small amount of energy compared to the overall system, and is considered negligible.

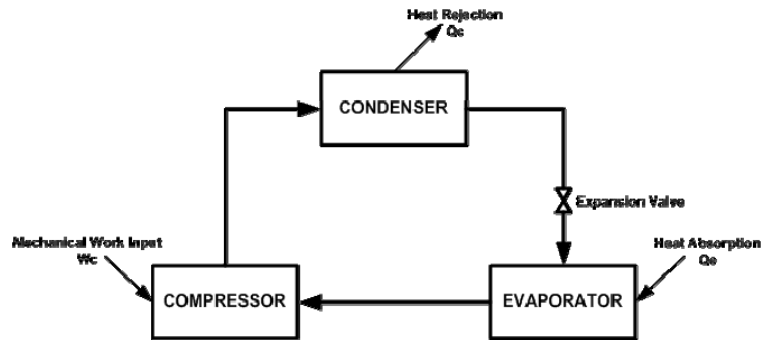


FIGURE 5: A simple compression refrigeration system

A single substance of working fluid is generally used for the entire heat transfer process within a compression system, but this cannot be achieved in an absorption system. The working fluid in an absorption system consists of two or more substances which will act as the absorbent and refrigerant. The refrigerant actually is the real working fluid for the refrigeration process while the absorbent will treat the refrigerant to a specific condition for a complete cycle continuation.

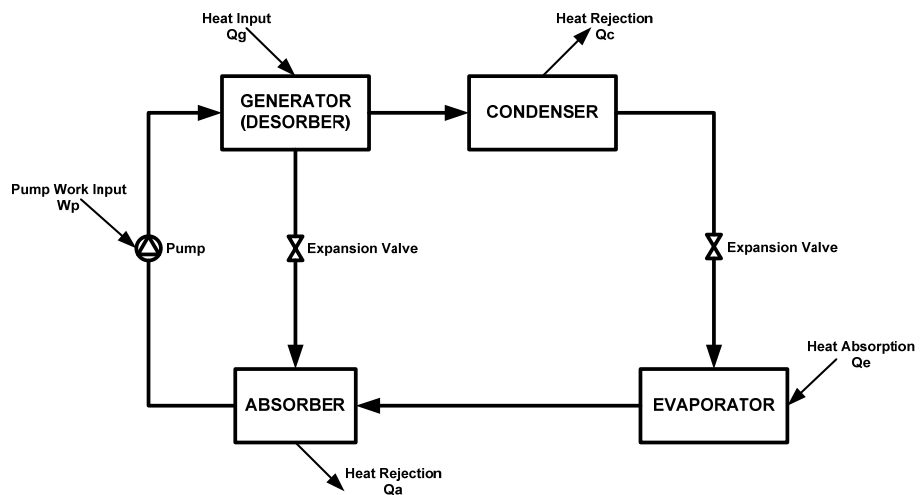


FIGURE 6: A simple absorption refrigeration system

Most commercial chillers in the world are mechanical chillers, meaning that an electrically-driven mechanical compressor is used. The most common types are reciprocating, centrifugal and screw compressors (Gordon & Ng, 2001). The absorption refrigeration cycle has recently attracted much research attention because of the possibility of using waste thermal energy or renewable energies as the power source, thus reducing the demand for electricity supply (Sun, 2006). Absorption cycles are used in applications where one or more of the exchanges of heat with the surrounding is a useful product, for example refrigeration, air conditioning and heat pumping. The two great advantages of the absorption cycles compared to other cycles with similar production are (ASHRAE, 2005):

- No large, rotating mechanical equipment is required;
- Any source of heat can be used, including low temperature sources (e.g. waste heat)

3.1 Absorption refrigeration system

An absorption refrigeration system is a heat activated thermal cycle; it exchanges the thermal energy with its surroundings. It operates often (always in a LiBr system) at lower pressure than the atmospheric pressure where this pressure is regulated by the vapour pressure of the working fluid. The vapour pressure of the working fluid is obviously strongly related to the temperature of the working fluid. An absorption system could be, at its simplest, a single effect or more advanced multiple effect absorption cycle. A single effect can be considered to occupy two pressure levels where the pressure difference only occurs in the flow restrictors and solution pump, neglecting the pressure drop along the circuit and changes in elevation.

A single effect refrigeration system basically consists of one solution pump, two flow restrictors and five heat exchangers where four of them will transfer the heat from the external source while the rest will work internally within the system as a solution heat exchanger. It is optional to install the solution heat exchanger in a basic single effect absorption refrigeration system, but in order to increase the refrigeration performance such a unit should be attached.

A specific format of an absorption refrigeration system's components can be drawn on a Duhring plot which will describe the cycle based on the temperature and pressure level of each component and their position within the system, together with their energy transfer between the system and the environment (Figure 7). As a basic representation of a specific heat transfer process, a Duhring chart can only schematically show the saturated states while the superheated and sub-cooled states cannot be accurately presented. The arrows that point out and into the cycle indicate the energy flow from the system out to the external environment and the energy flow that is supplied to the system, respectively. Heat rejection is employed by the absorber and condenser while the heat is injected into the system through the desorber and the evaporator.

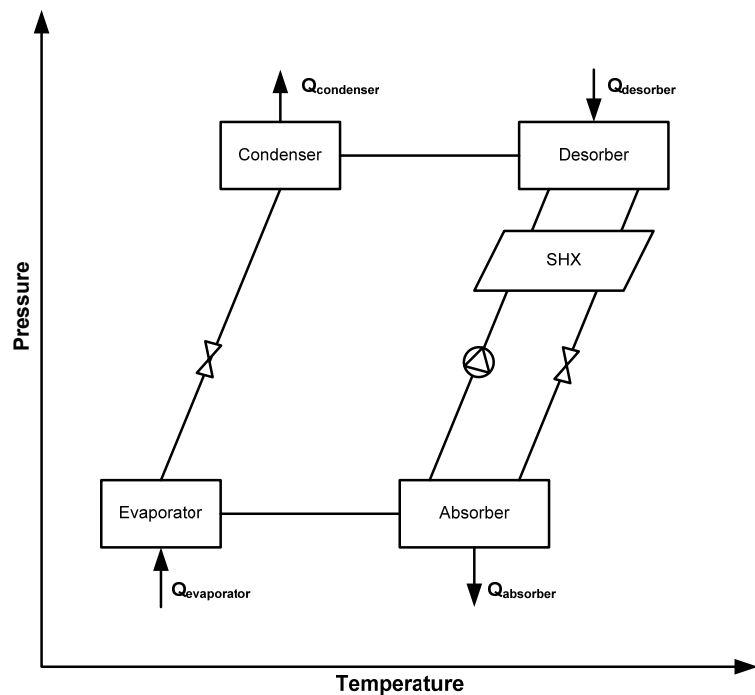


FIGURE 7: Duhring plot for single effect absorption system

Working fluid from the outlet of the absorber is pumped by the solution pump to the higher pressure level. In the desorber the refrigerant is then extracted from the working fluid solution by the addition of extra heat from an external heat source into the desorber and the rest of the solution in liquid state is drained back to the absorber as absorbent, ready to absorb the refrigerant vapour from the evaporator. Heat rejection and the condensation process of the refrigerant vapour occur inside the condenser giving a liquid phase of the refrigerant. The liquid then passes through an expansion valve, which lowers the pressure environment and produces a low temperature refrigerant liquid that is ready to be used for refrigerating purposes. The mixing of the absorbent and the refrigerant will bring the solution back into the initial liquid state condition and makes it possible to be pumped by the solution pump to the next cycle.

The need for two or more substances that should work together as a single solution of working fluid produced several variants of refrigerant-absorbent pairs in the ARS industry. The refrigerant should be more volatile than the absorbent so that the two can be separated easily. Water is usually used as the refrigerant for the solid absorbents (Gunther, 1957). There are several common combinations of absorbent-refrigerants:

- Water and Ammonia
- Lithium Nitrate and Ammonia
- Lithium Bromide and Water
- Lithium Chloride and Water

A recent developmental process of refrigerant-absorbent pairing improved the performance of the absorption system, for example:

- Lithium Bromide and (Water-Ammonia)
- Glycerol and Water
- (Lithium Nitrate-Potassium Nitrate-Sodium Nitrate) and Water

Lithium Bromide-Water and Water-Ammonia as conventional fluids still have desirable properties compared to other working fluid variants, especially for the high number of latent heat so can minimize the need of refrigerant flow rate. The Lithium Bromide-Water combination is limited to temperatures above the freezing point of water while the Water-Ammonia combination is favourable for sub-zero refrigerant temperatures.

3.1.1 Absorber

The absorber is a chamber where the absorbent and the refrigerant vapour are mixed together. It is equipped with a heat rejection system, i.e. bundles of tubes as in the condenser, and operates under a low pressure level which corresponds to the evaporator temperature. The absorption process can only occur if the absorber is at a sensible low temperature level, hence the heat rejection system needs to be attached. The mixing process of the absorbent and the refrigerant vapour generate latent heat of condensation and raise the solution temperature. Simultaneous with the developmental processing of latent heat, heat transfer with cooling water will then lower the absorber temperature and, together with the solution temperature, creates a well blended solution that will be ready for the next cycle. A lower absorber temperature means more refrigerating capacity due to a higher refrigerant's flow rate from the evaporator.

The energy balance during the mixing of the refrigerant and the absorbent is equal to the heat rejection process that is shown in the equation below, with all notations referring to Figure 8.

$$\dot{m}_6 \cdot h_6 + \dot{m}_{11} \cdot h_{11} - \dot{m}_1 \cdot h_1 = \dot{m}_{22} (h_{23} - h_{22}) \quad (1)$$

Mass flow equilibrium between the refrigerant and the absorbent that flows in and out of the absorber is a function of the concentration of lithium bromide or ammonia for each type of ARS system.

$$\dot{m}_1 \cdot x_1 = \dot{m}_6 \cdot x_6 + \dot{m}_{11} \cdot x_{11} \quad (2)$$

For a pure refrigerant species e.g. there is no lithium bromide or ammonia fraction in the refrigerant, the formula can be simplified as:

$$\dot{m}_1 \cdot x_1 = \dot{m}_6 \cdot x_6 \quad (3)$$

The log mean temperature difference for the absorber which is used in the calculation of absorber area, can be obtained from equation below:

$$LMTD_a = \frac{(T_6 - T_{23}) - (T_1 - T_{22})}{\ln\left(\frac{T_6 - T_{23}}{T_1 - T_{22}}\right)} \quad (4)$$

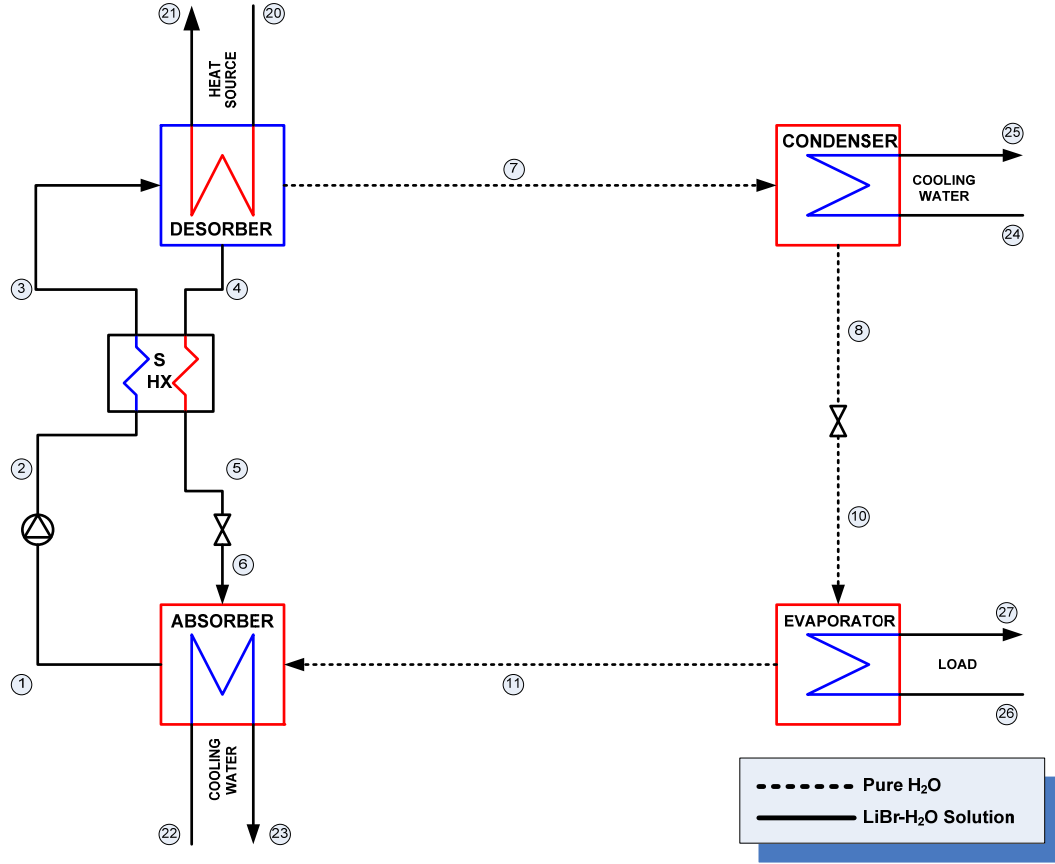


FIGURE 8: Single effect LiBr-H₂O absorption refrigeration system

3.1.2 Generator/desorber

The desorber operates under high pressure which is controlled either by the temperature of the incoming heat to the desorber or the condensation temperature required by the cooling water entering the condenser. The desorption process generates vapour and extracts the refrigerant from the working fluid by the addition of the external heat from the heat source; it could be desorption of water out of a lithium bromide-water solution or ammonia out of a water-ammonia solution. The refrigerant vapour travels to the condenser while the liquid absorbent is gravitationally settled at the bottom of the desorber; the pressure difference between the desorber and the absorber then causes it to flow out to the absorber through an expansion valve.

A lithium bromide-water system has lower temperature requirements for a refrigerant desorption process (75-120°C) than the water-ammonia system (125-170°C) (Florides et al., 2003). Changes in fraction during the extraction process of a refrigerant is fully controlled by the amount of heat supplied to the desorption process and vice versa, based on the formula in Equation (6). A strong lithium bromide solution and a weak ammonia solution is produced during desorption process for both lithium bromide and ammonia systems, respectively. These strong lithium bromide and weak ammonia solutions act as the absorbent that will absorb the refrigerant in the absorber. The fraction of each fluid stream regulates the mass flow equilibrium across the desorption process.

$$\dot{m}_3 \cdot x_3 = \dot{m}_4 \cdot x_4 + \dot{m}_7 \cdot x_7 \quad (5)$$

Energy balance:

$$\dot{m}_4 \cdot h_4 + \dot{m}_7 \cdot h_7 - \dot{m}_3 \cdot h_3 = \dot{m}_{20}(h_{20} - h_{21}) \quad (6)$$

Log mean temperature difference:

$$LMTD_d = \frac{(T_{20} - T_4) - (T_{21} - T_3)}{\ln\left(\frac{T_{20} - T_4}{T_{21} - T_3}\right)} \quad (7)$$

3.1.3 Condenser

A liquid state of a refrigerant is a must in order for the refrigeration process to run. Hence, the vapour phase of a refrigerant from the desorber is altered to a liquid by the condenser. The condensing process of a high pressure refrigerant vapour is done by rejecting the vapour's latent heat to the sink, following a regular heat balance formulation.

$$\dot{m}_7(h_7 - h_8) = \dot{m}_{24}(h_{25} - h_{24}) \quad (8)$$

$$LMTD_c = \frac{(T_7 - T_{25}) - (T_8 - T_{24})}{\ln\left(\frac{T_7 - T_{25}}{T_8 - T_{24}}\right)} \quad (9)$$

The sub-cooled liquid from the condenser is then passed through an expansion valve which lowers the pressure level; a consequence of this process is that some low quantity may flash into vapour. However, the refrigerant can still take latent heat from the environment.

3.1.4 Evaporator

The temperature of evaporation regulates the lower pressure level of the absorption system. A low pressure of two phase refrigerant from the flow restrictor continues to evaporate due to the addition of latent heat from the refrigeration environment. A complete evaporation process will convert the two phase refrigerant into vapour. Energy balance for the evaporator is:

$$\dot{m}_{10}(h_{11} - h_{10}) = \dot{m}_{26}(h_{26} - h_{27}) \quad (10)$$

Log mean temperature difference:

$$LMTD_e = \frac{(T_{26} - T_{11}) - (T_{27} - T_{10})}{\ln\left(\frac{T_{26} - T_{11}}{T_{27} - T_{10}}\right)} \quad (11)$$

3.1.5 Expansion valve

An expansion valve is a component that reduces the pressure and splits the two different pressure levels. In a simple model of a single effect absorption refrigeration system, the pressure change is assumed only to occur at the expansion valve and the solution pump. There is no heat added or removed from the working fluid at the expansion valve. The enthalpy of the working fluid remains the same on both sides. The pressure change process between the two end points of the expansion valve, while there is no mass flow change and the process is assumed as an adiabatic process, can change the volume if the fluid generates a small amount of steam phase via flashing.

The presence of the Solution Heat Exchanger (SHX) and Refrigerant Heat Exchanger (RHX) will drive the expansion valve's input fluid close to a sub-cooled state, and at the end will affect the amount of the steam flash out of the expansion valve.

Another thermodynamic changing process across the expansion valve is the possibility of a lower temperature at the end of the flashing process as some amount of energy must be taken from the fluid phase in order to drive the phase change. Thereby, the amount of steam flash will affect the magnitude of the temperature drop across the expansion valve.

3.1.6 Solution heat exchanger

A solution heat exchanger is a heat exchange unit with the purpose of pre-heating the solution before it enters the desorber and removing unwanted heat from the absorbent. The heat exchange process within the solution heat exchanger reduces the amount of heat required from the heat source in the desorber and also reduces the quantity of heat to be rejected by the heat sink (cooling water) in the absorber as well.

The heat exchange process occurs between the low temperature of the working fluid and the high temperature of the absorbent which will benefit both. The temperature of the absorbent that leaves the hot stream side has to be calculated first using Equation (12) in order to complete the variable needed for the energy balance calculation in Equation (13).

$$T_5 = T_2 \times \eta_{shx} + (1 - \eta_{shx}) \times T_4 \quad (12)$$

$$\dot{m}_2(h_3 - h_2) = \dot{m}_4(h_4 - h_5) \quad (13)$$

The existence of a solution heat exchanger in a refrigeration process increases the overall refrigeration system performance as shown in Figure 9. The results were applied for 100 kW refrigeration capacity and 5°C evaporator temperature while the weak-strong solution concentration difference was set to 7 for the lithium bromide and 0.1 for ammonia. The increment of *COP* is almost in linear correlation with the effectiveness as it changes from 0 (without a solution heat exchanger) to 1 (ideal heat exchange).

This sensibility is applied for both refrigeration systems in Figures 8 and 13 with the given parameters. The efficiency of a lithium bromide machine increases from 0.62 to 0.82 in line with the rise in effectiveness of the solution heat exchanger from 0 to 1, while the ammonia machine goes from 0.25 to 0.55.

Log mean temperature difference for the solution heat exchanger model in Figure 8 is:

$$LMTD_{shx} = \frac{(T_4 - T_3) - (T_5 - T_2)}{\ln\left(\frac{T_4 - T_3}{T_5 - T_2}\right)} \quad (14)$$

3.1.7 Solution pump

Although the main distinction between compression and absorption refrigeration is the replacement of the mechanically driven system by a heat driven system, the presence of a mechanically driven component is still needed in an absorption system. A solution pump will mainly circulate and lift the solution from the lower pressure level side to the higher pressure level side of the system. To maintain this pressure difference, a centrifugal type pump is preferable. Assuming the solution is an incompressible liquid, in other words the specific volume of the liquid (v) will not change during the pumping process, the power requirement to lift the solution with mass flow \dot{m} from pressure level P_1 to P_2 and certain pump efficiency is:

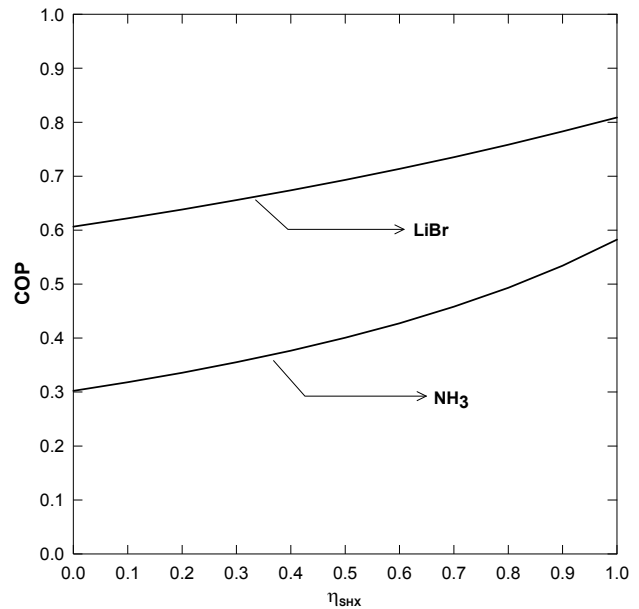


FIGURE 9: A typical effect of a solution heat exchanger's effectiveness on COP of refrigeration

$$W_{pump} = \frac{\dot{m}_1 \cdot v_1 \cdot (P_2 - P_1)}{\eta_{pump}} \quad (15)$$

The pumping process is negligible; it only consumes a small amount of energy compared to the overall system heat transfer process. Although the existence of the solution pump can be ignored thermodynamically, practical experience shows that the pump is a critical component that must be carefully engineered (Herold, Radermacher, & Klein, 1996), especially during the consideration processes of:

- Pump seals to avoid air leakage
- Pump cost
- Sufficient net positive suction head to avoid cavitations in the suction line

Taking the solution pump's work into the energy balance calculation across the pump, where the pumping process is an isentropic process will slightly increase the enthalpy of the solution at the discharge point. Hence, the energy balance across the solution pump can be expressed as:

$$\dot{m}_1 \cdot h_1 + W_{pump} = \dot{m}_2 \cdot h_2 \quad (16)$$

3.2 LiBr-H₂O absorption system

Lithium bromide aqueous solution is one of many other solutions widely used in the operation of the absorption heat pumps that are used for (heating and) cooling purposes. It has been used since the 1950s when the technology was pioneered by several manufacturers in the U.S. (Herold et al., 1996) where water acts as the refrigerant which absorbs and removes heat from the specific environment while lithium bromide becomes the absorbent that absorbs the water vapour into a solution and makes it possible to be circulated by a solution pump.

As an absorbent, Lithium bromide is advantageous because it is essentially non-volatile, resulting in cycle designs that avoid the need of rectifiers. Water is advantageous as the refrigerant because it does not crystallize; its limitation is that it will make the system work only for refrigeration temperatures above 0°C or even 5°C, due to the freezing point of water.

Lithium bromide is a lithium salt substance and indeed it is solid under normal conditions. However lithium bromide salt is highly soluble in fluids. It dissolves in water and forms a lower equilibrium vapour pressure of solution than pure water at the same operating temperature. As a comparison at the same 50°C reference temperature, a 60% Lithium Bromide has 6.47 kPa vapour pressure and pure water has 12.35 kPa. This condition could be found between the evaporator and absorber which would drive the refrigerant naturally from the evaporator side (pure water condition) to the inlet of the absorber (Lithium Bromide-water solution). A complete equilibrium chart for an aqueous lithium bromide solution for various solution concentrations is presented in Figure 10.

There are five assumptions for the thermodynamic states occupied by the cycle in Figure 8: saturated liquid (points 1, 4 and 8); saturated vapour (point 11); superheated vapour (point 7); sub-cooled liquid (points 2, 3 and 5); and two-phase solution (points 6 and 10). Point 6 can often also be saturated or nearly saturated liquid. These assumptions are still valid in order to achieve a simple modelling process and do not introduce a large error (Herold et al., 1996) since in the real machine the saturated condition will not be exactly saturated and the liquid stream would be sub-cooled while the vapour stream would be superheated.

For the temperature range and typical single effect application, carbon steel and copper are the preferred construction materials. Lithium bromide absorption machines have been proven to have a life expectancy of approximately 20 years; afterwards significant corrosion can be observed (Herold et al., 1996).

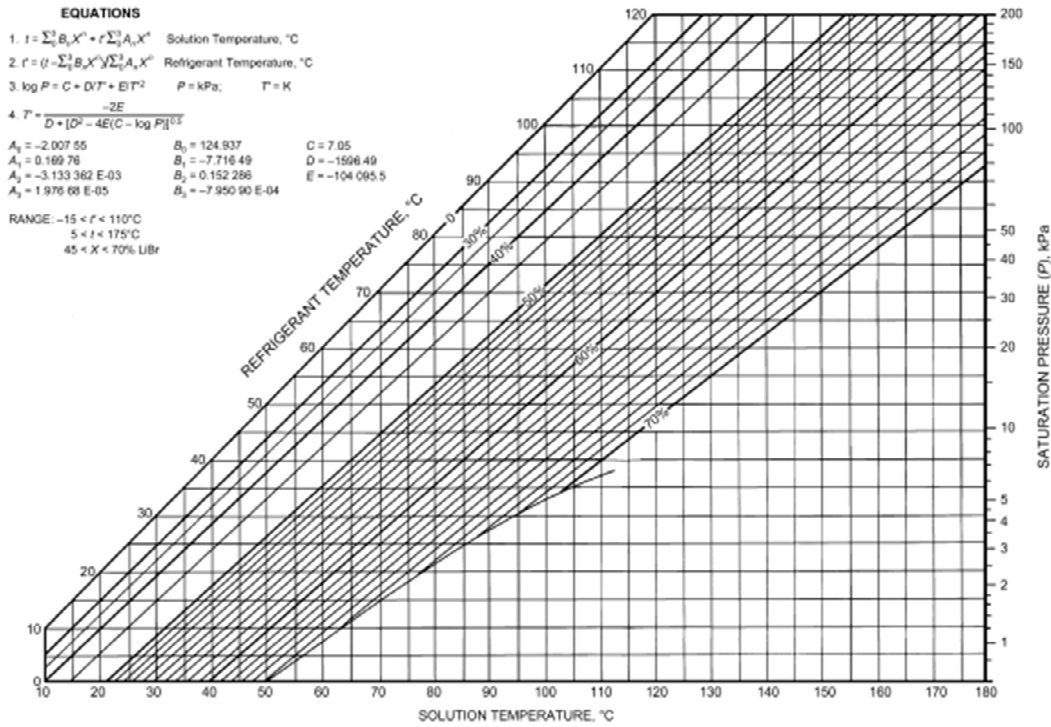


FIGURE 10: Equilibrium chart for aqueous lithium bromide solutions (ASHRAE, 2005)

3.3 Crystallization problem

Aqueous Lithium Bromide is a salt solution substance where the salt component will start to precipitate when the mass fraction of salt exceeds the maximum allowable of solution solubility. Since the temperature and the mass fraction of the solution impact the solution solubility more than the pressure, these two components will affect the crystallization process significantly.

The boiled refrigerant from the desorber is purely water since the possibilities for lithium bromide salt escaping from the solution are very low because the normal boiling point of solid lithium bromide salt is 1.28°C (Herold et al., 1996). However, a periodic salt tracing is recommended to detect and prevent corrosion due to the presence of salt precipitation along the system. The crystallization problem appears when the machine is off and the flow is stopped due to a significant temperature drop; during the operating stage, crystallization tends to occur at the outlet of the solution heat exchanger where temperatures are relatively low and mass fractions are high.

Aqueous lithium bromide solution solubility is a strong function of its mass fraction (Herold et al., 1996) and based on Figure 11, it is important to keep the

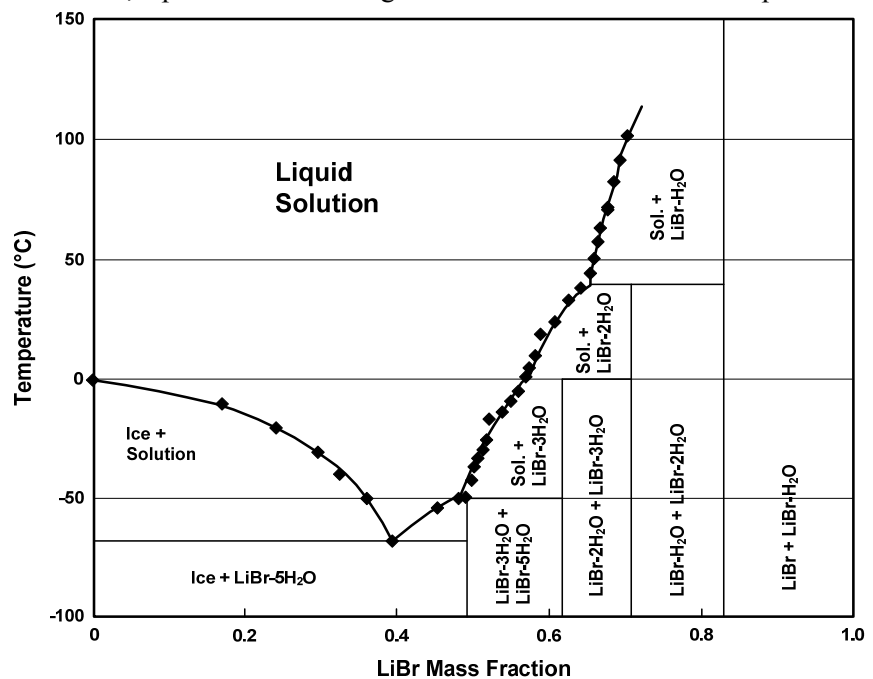


FIGURE 11: Aqueous lithium bromide phase diagram (Herold et al., 1996)

solution temperature above its solubility temperature limit in order to prevent crystallization. A complete mixing process between refrigerant and absorbent in the absorber is one of the main keys to preventing crystallization because the salt fraction is completely mixed with the refrigerant preventing the saturation of liquid solubility. A complete mix of refrigerant and absorbent is controlled by the heat rejection process in the absorber so the absorber temperature is maintained at the design condition. The Duhring plot represents the overall cycle solution. It is a helpful tool for analyzing the crystallization problem within the system.

3.4 H₂O-NH₃ absorption system

Water-Ammonia is an absorption fluid that has been used since the late 1800s at which time it was used for ice production prior to the introduction of vapour compression technology (Herold et al., 1996). Ammonia is highly soluble in water where the solubility increases as the water temperature decreases at constant pressure (Figure 12). In this system, ammonia will act as the refrigerant which will take the heat from the specific environment while the water becomes the absorbent that absorbs the ammonia vapour into a solution and makes it possible to be circulated by the pump. The vapour pressure of a water-ammonia solution is less than that of pure ammonia, at the same temperature. The low volatility ratio between ammonia and water requires a high operating pressure compared to the lithium bromide system.

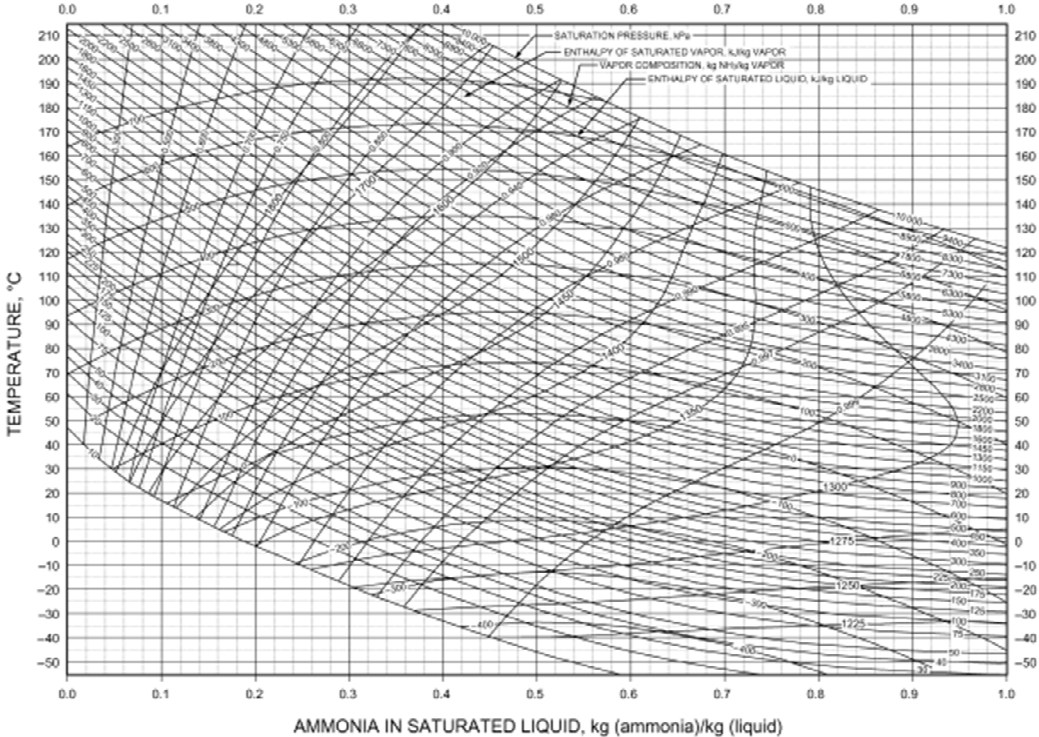


FIGURE 12: Enthalpy-concentration diagram for water-ammonia solutions (ASHRAE, 2005)

Utilizing ammonia which has a lower freezing temperature (-77.7°C) than water as the refrigerant will give the advantage of working at a much lower refrigeration temperature, although its toxicity level limits the use of ammonia to a well ventilated area or outdoors. The most common material for the construction of a water-ammonia system is steel or stainless steel.

A water-ammonia absorption cycle (Figure 13) is similar to a lithium bromide-water cycle except for some important differences in working fluid properties such as: ammonia has a lower latent heat than water; the volatility of the absorbent; and the different pressure and range of solubility. The latent heat of ammonia is only about half that of water, so, for the same duty, the refrigerant and absorbent mass circulation rates are roughly double that of water-lithium bromide (ASHRAE, 2005).

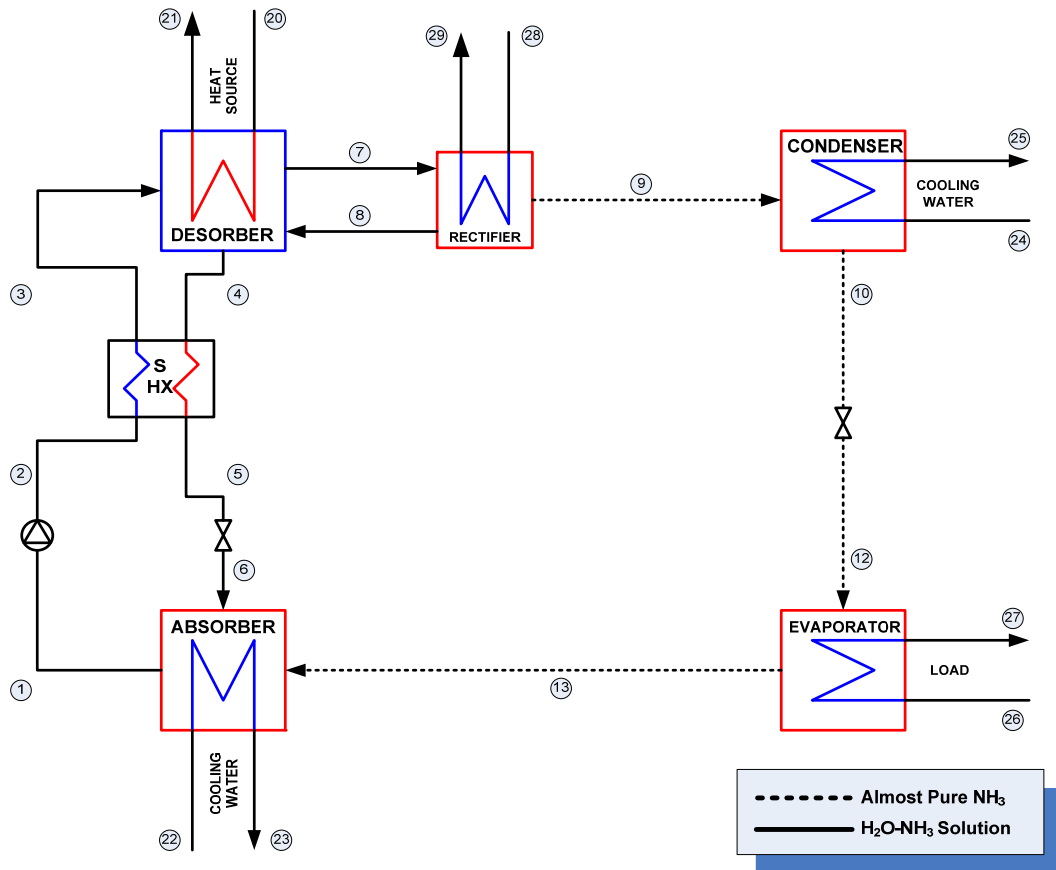


FIGURE 13: Single effect H₂O-NH₃ absorption refrigeration system

In normal conditions, the boiling point of ammonia is -33.35°C , low enough compared to water. But since water has the un-negligible vapour pressure, the refrigerant ammonia vapour that is generated by the desorber still contains a certain amount of water fraction. The presence of water in an ammonia refrigerant has to be minimized due to the chance of freezing when the system is employed for the refrigeration process below 0°C and water tends to accumulate and remain in a pool type of evaporator, lowering the evaporator pressure and affecting the system's performance. There are several common methods to gain purity of ammonia as a refrigerant:

1. Rectification

A rectifier has the same water cooled effect as a condenser but with a relatively small capacity of condensation. The idea is to condense the available water fraction that is carried away together with the strong ammonia solution and send it back to the desorber as reflux. Ammonia-water vapour mixture is cooled slightly so that a small portion of the vapour condenses and returns to the desorber. The process of this water removal will then increase the purity of ammonia in the strong refrigerant solution.

2. Reflux cooling

Ammonia-water vapour mixture is in contact with a cooled surface in the reflux cooler. Let a portion of vapour, mainly water vapour, is condensed and returned as reflux to the desorber. Due to some water content being removed from the original vapour, the remaining ammonia-water vapour is enriched with ammonia.

The energy balance for the rectification process is:

$$\dot{m}_7 \cdot h_7 - \dot{m}_8 \cdot h_8 - \dot{m}_9 \cdot h_9 = \dot{m}_{28}(h_{29} - h_{28}) \quad (17)$$

Log mean temperature difference:

$$LMTD_{rec} = \frac{(T_7 - T_{29}) - (T_9 - T_{28})}{\ln \left(\frac{T_7 - T_{29}}{T_9 - T_{28}} \right)} \quad (18)$$

3.5 System efficiency

Efficiency of an absorption refrigeration system can be easily expressed by a Coefficient of Performance (COP) which is defined as the ratio between the amount of heat/energy absorbed from the environment by the evaporator and the heat/energy supplied to the desorber to operate the cycle and work into the pump and fans if available. As the work supplied to the absorption system is very small compared to the amount of heat supplied to the desorber, generally the amount of work is often excluded from the calculation. For a compression refrigeration system, the heat source is determined by the mechanical or electrical energy needed to drive the compressor, fans or pumps. A refrigeration cycle is optimized when it can give more of a cooling effect for the same amount of heat that is supplied to the system in order to operate the cycle.

$$COP_{refrigeration} \approx \frac{Q_{evaporator}}{Q_{desorber} + W_{solution\ pump}} \quad (19)$$

In order to increase the overall refrigeration efficiency, a refrigerant heat exchanger could be installed where it will cause the heat exchange between the liquid from the condenser and the evaporator. This refrigerant internal heat exchange process alters the saturated liquid of a refrigerant to a sub-liquid state, thus, more heat could be removed by the refrigerant during the evaporation process. The efficiency of a refrigerant heat exchanger should be selected carefully since the temperature at the outlet of the cool stream side of the refrigerant heat exchanger obviously could not become higher than the temperature at the inlet of the hot stream side, thus limiting the maximum efficiency of the refrigerant heat exchanger. Referring to Figure 14, the efficiency of the refrigerant heat exchanger can be written as:

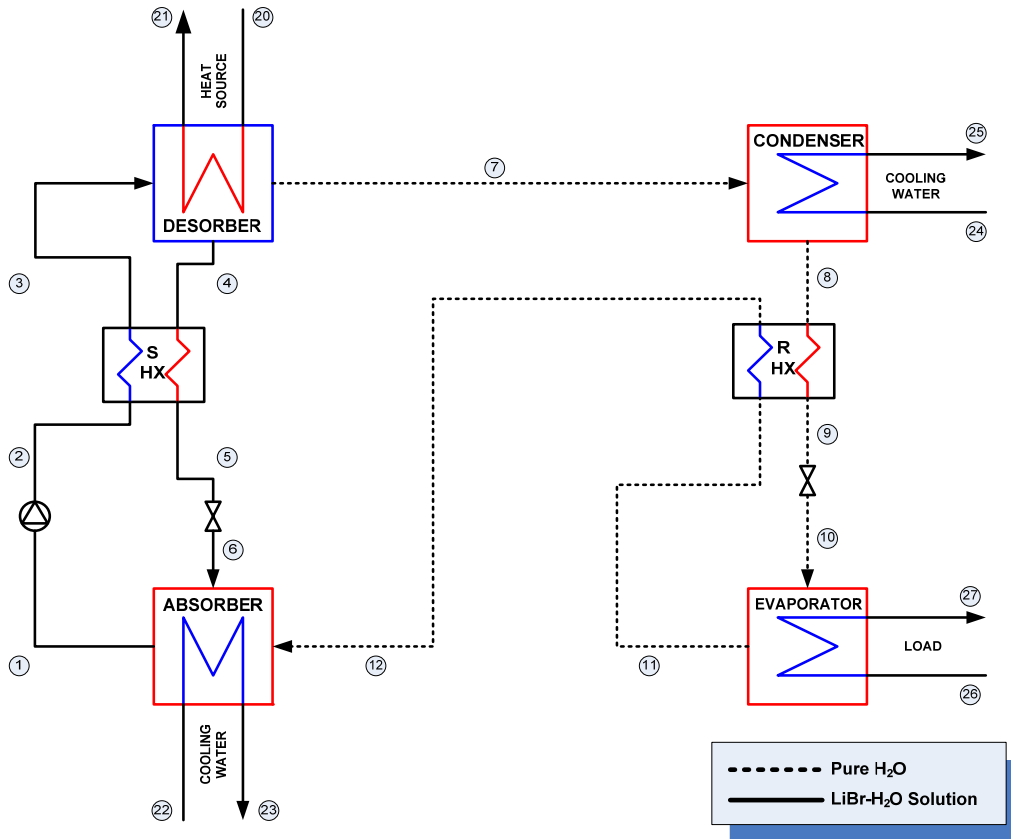


FIGURE 14: Single effect lithium bromide refrigeration with refrigerant heat exchanger

$$\eta_{rhx} = \frac{T_8 - T_9}{T_8 - T_{11}} \quad (20)$$

And the energy balance is:

$$\dot{m}_8(h_8 - h_9) = \dot{m}_{11}(h_{12} - h_{11}) \quad (21)$$

With log mean temperature difference:

$$LMTD_{rhx} = \frac{(T_8 - T_{12}) - (T_9 - T_{11})}{\ln\left(\frac{T_8 - T_{12}}{T_9 - T_{11}}\right)} \quad (22)$$

From Figure 15, the refrigerant heat exchanger raises the refrigeration efficiency more in the ammonia than in the lithium bromide system. The curves were extracted from the single effect absorption refrigeration system with and without the refrigerant heat exchanger unit. Evaporator was set to work on 100 kW refrigeration capacity and the solution heat exchanger had 60% efficiency. For the single effect absorption refrigeration system with the refrigerant heat exchanger, the efficiency followed the heat transfer process as the pinch temperature was set to 4°C.

If we review the process thoroughly in each system, the ammonia machine has a higher mass flow for the same refrigeration load compared to the lithium bromide machine. As the ammonia refrigerant exceeds the water refrigerant in mass flow, for similar temperature differences on the cold stream side of the refrigerant heat exchanger, the ammonia machine holds a higher heat exchange process than the lithium bromide. A higher amount of heat exchange between hot and cold streams leads to higher efficiency of the refrigerant heat exchanger and finally contributes to a higher overall refrigeration system efficiency.

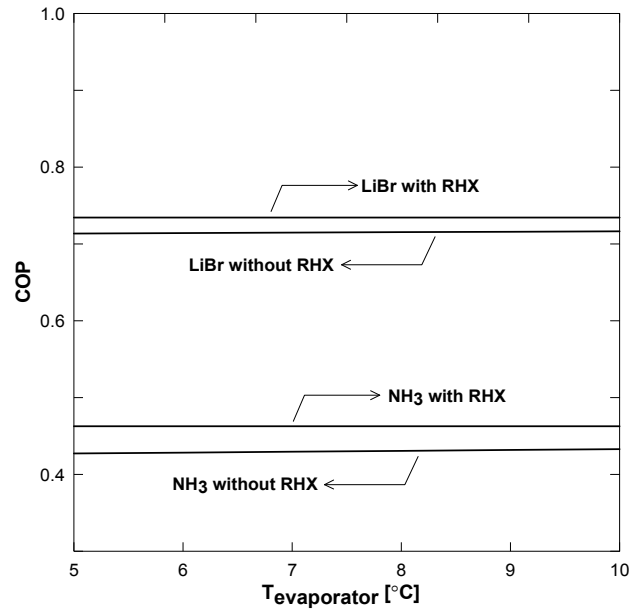


FIGURE 15: Typical curves showing the effect of refrigerant heat exchanger on COP for various evaporator temperatures

4. SYSTEM MODELLING

Two single effect absorption refrigeration technologies, Lithium bromide-Water and Water-Ammonia absorption refrigeration systems are going to be modelled. A single geothermal well will feed them directly as a heat source while the machines refrigerate a stream of water for a specific cooling load. Performance for each machine is observed and compared while the variables are maintained to achieve the best performance with the least heat exchanger area.

Three geothermal power systems are also modelled and then each of the lithium bromide and ammonia refrigeration cycles is attached to supply a lower temperature of cooling water to the power plant. By using this scenario, the ARS machine is powered by the waste fluid from the separation process. Where there is a lack of energy, the ARS machine is allowed to collect additional mass flow directly from the well.

Models are calculated and analyzed based on their steady state conditions, with the assumptions:

- Heat exchanger is well insulated from the surroundings; means there is only heat exchange between hot and cold fluid stream.
- Potential and kinetic energy change during the heat exchange and, at all fluid streams, are ignored.
- A simple non-condensable gas extraction process is attached at the power plant's condenser thus allowing low enough condensing pressure.

Modelling the Absorption Refrigeration System and the Geothermal Power Plant System is done by Engineering Equation Solver (EES), computer engineering software released by F-Chart Software. There are six EES fluid property routines that will be applied for modelling purposes (F-Chart Software, 2008):

- Steam_IAPWS routine implements high accuracy thermodynamic properties of water substance with the 1995 *Formulation for the Thermodynamic Properties of Ordinary Water Substance for General and Scientific Use*, issued by The International Association for the Properties of Water and Steam (IAPWS). This routine is available only in the Professional version of EES.
- Water or Steam routine provides steam properties, but they use less accurate correlations which require significantly less computational effort. This is thermodynamic properties of water substance that have been implemented using the thermodynamic property correlation of Harr, Gallagher, and Kell, *NBS/NRC Steam Tables*, Hemisphere Publishing Co, 1984.
- CO₂ routine provides ideal gas thermodynamic properties for carbon dioxide valid over the temperature range from 250 K to 3500 K, based on the constant pressure specific heat correlation from Van Wulen and Sonntag, *Fundamental of Classical Thermodynamic*, 3rd ed, John Willey and Sons, 1996.
- NH₃H₂O procedure provides the thermodynamic properties of ammonia-water mixtures in sub-cooled, saturated and superheated conditions. The correlations are taken from Ibrahim, O.M., Klein, S.A., *Thermodynamic Properties of Ammonia-Water Mixtures* ASHRAE Trans.,: Symposia, 21,2,1495 (1993).
- Isopentane routine provides high accuracy thermodynamic properties for isopentane (Molar Mass = 72.115 g/mole) using the Fundamental equation of State, as described by Reiner Tillner-Roth, *Fundamental equation of State*, Shaker, Verlag, Aachen, 1998.
- Lithium bromide correlation for enthalpy, temperature and pressure routines are taken from the *1989 ASHRAE Handbook of Fundamentals* while the specific volume routine was developed by Keith E. Herold at University of Maryland based on data from Uemura, T., Hasaba, S., Tech. Repr. Kansai Univ., 6, 31-35, 1964.

4.1 Refrigeration system

A single effect absorption refrigeration system complete with refrigerant heat exchanger is going to be modelled both for Lithium Bromide-Water and Water-Ammonia system. In this refrigeration scenario, the absorption machine is set to cool down a stream of water as the refrigeration load with 100 kW refrigeration/evaporator capacity. It was assumed that the absorption machine was fed by 150°C brine water from an 800 kPa separation process. The affect of solution concentration to refrigeration performance is held by tuning the strong and weak concentration differences in a certain range. A complete list of initial design parameters are described in Table 2. Other parameters will be freely configured to achieve a preferable machine performance. The more specific variables for each machine will be described in the next sub-chapter. Hence, based on a similar heat source and load, the performance of each system can be compared as well as the area needed for the heat exchange processes.

TABLE 2: Initial design parameters for single effect ARS scenario

T_{source}	150°C
P_{source}	800 kPa
\dot{m}_{source}	2 kg/s
$Q_{evaporator}$	100 kW
$T_{evaporator}$	5°C
η_{pump}	0.95
η_{shx}	0.60
$T_{pinch,RHX}$	4°C
$T_{cooling\ water}$	25°C

4.1.1 Single effect lithium bromide-water absorption system

The model of a single effect lithium bromide-water machine is simplified by assuming there are only two pressure levels that will be occupied within the cycle, neglecting the pressure losses along the connection pipe. It means a desorber and condenser as well as an evaporator and absorber are under the same pressure level. The higher pressure level is determined from the pressure of saturated liquid at the outlet of the condenser while the lower pressure level is determined from the refrigerant temperature at the outlet of the evaporator.

The first assumption that has to be stated is that the refrigerant temperature at the outlet of the condenser is assumed to follow the inlet temperature of the cooling water. Hence, the temperature of the saturated refrigerant liquid at the outlet of the condenser was set to 20°C higher than the inlet temperature of the cooling water.

The weak lithium bromide concentration at the outlet of the absorber was determined from solution temperature and pressure. Temperature at the outlet of the absorber was set to 32°C, maintaining a 7°C temperature difference from the temperature of the cooling water. The initial design conditions for a single effect lithium bromide with refrigerant heat exchanger are listed in Table 3.

TABLE 3: Design parameters for lithium bromide absorption system

T_8	$T_{24} + 20^\circ\text{C}$
T_{11}	[5-10]°C
$T_{pinch\ absorber}$	7°C
$T_{cooling\ water}$	25°C
$T_{crystallization\ margin}$	min 10°C

A sensible assumption was made for the refrigerant vapour at, and the saturated liquid at, the outlet of the desorber. The temperature of the saturated liquid at the outlet of the desorber was determined from the concentration of strong lithium bromide solution at the respective desorber pressure level. Refrigerant vapour leaves the desorber as a pure water vapour with the same temperature as the saturated temperature of the weak lithium bromide solution at the respective desorber pressure level. Thus, the refrigerant temperature becomes higher than water vapour saturation temperature at the same pressure level and then alters the refrigerant vapour to the superheated state.

The thermodynamic properties of mixtures of lithium bromide and water are implemented as an externally compiled EES routine where the EES LIBR external routine evaluates a particular range of temperature and fluid concentrations that have to be followed. The routine for enthalpy calculation is applicable for concentrations between 40% and 70% with temperatures between 60°F and 330°F. Temperature calculation is applicable for concentrations between 45% and 75%. The routine to obtain the pressure is applicable for concentrations between 45% and 75% and temperatures between 40°F

and 350°F. Using this information as a constraint in the modelling process, the water-lithium bromide solution concentration was kept in the range of 45%-70%.

Weak-strong lithium bromide concentration differences should be fine tuned in order to achieve a certain level of refrigeration efficiency with the least heat exchanger area. Crystallization temperature and previously set temperature margins constrain the weak-strong lithium bromide concentration difference parameter (Figure 16).

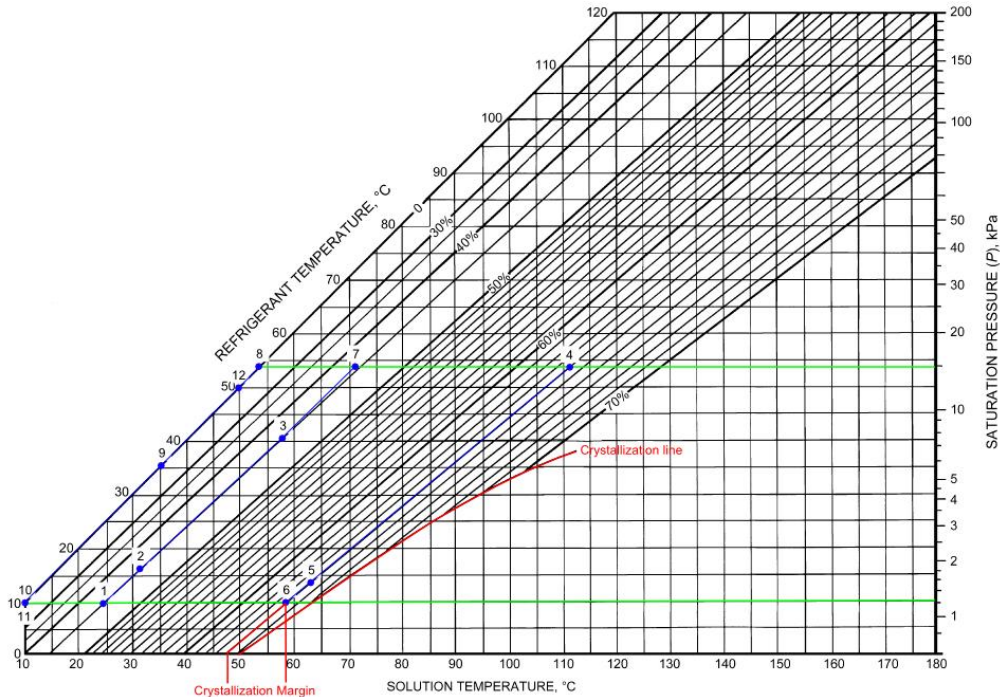


FIGURE 16: Duhring plot for LiBr crystallization control

The aqueous lithium bromide solutions had the closest margin to the crystallization line when it flowed from the expansion valve into the absorber (point 6, Figure 14). Hence, in order to prevent crystallization, the absorption parameters had to be designed appropriately. During the simulation process, the temperature margin between this critical point and the crystallization temperature was maintained at a minimum 10°C temperature difference.

4.1.2 Single effect water-ammonia absorption system

This model mostly operated for the same general design parameters as a single effect water-lithium bromide machine with the distinction in solution concentration and obviously the presence of an ammonia purification unit (Figure 17). Using a similar assumption as in the lithium bromide system, the saturated liquid temperature at the outlet of the condenser exceeded the inlet temperature of the cooling water by 20°C.

The higher pressure level was determined from the temperature of the condensed refrigerant together with its ammonia concentration at the outlet of the condenser while it was in its saturated liquid phase. The lower pressure level was determined from temperature, concentration and vapour quality of the refrigerant at the outlet of the evaporator where all of these parameters were given as input parameters. The desorber, rectifier and condenser operated at the higher pressure level while the evaporator and the absorber resided in the lower pressure level.

By having the pressure set and the already known refrigerant quality and refrigerant ammonia concentrations, the temperature and other parameters at the outlet of rectifier could be found easily. This method is applicable for finding the rest of the properties of the ammonia vapours at the outlet of the desorber.

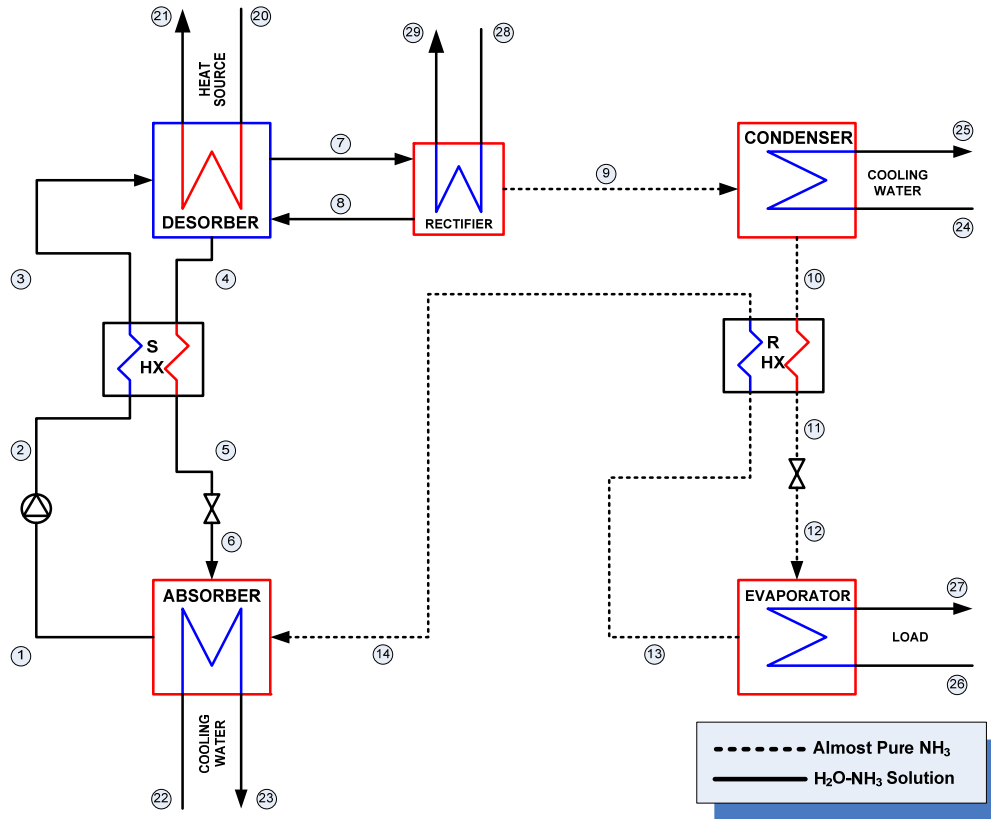


FIGURE 17: Single effect NH_3 refrigeration with refrigerant heat exchanger

A rectifier employs external cooling water to condense the water portion from ammonia refrigerant. It was assumed that the desorber produced ammonia refrigerant with an ammonia concentration of 94.44% and then the purities were increased by the rectifier up to 99.96%. These ammonia concentration parameters were adopted from Example 9.2 of Absorption Chillers and Heat Pump book (Herold, Radermacher, & Klein, 1996). The reflux liquid flowed back to the desorber at the same temperature as the vapour temperature at the outlet of the desorber.

Though the ammonia itself can operate at temperatures far below 0°C , here the ammonia vapour temperature at the outlet of the evaporator was kept at the same level as the temperature in the lithium bromide system. By having similar general parameters, both systems could be compared fairly. However, in order to see the effect in lowering the evaporator temperature below 0°C , a dedicated ammonia absorption refrigeration simulation could be observed separately. The initial design conditions for single effect ammonia with refrigerant heat exchanger are listed in Table 4.

TABLE 4: Design parameters for ammonia absorption system

x_7	0.9444
x_9	0.9996
T_{10}	$T_{24} + 20^\circ\text{C}$
T_{13}	$[5-10]^\circ\text{C}$
$T_{cooling\ water}$	25°C
$T_{pinch\ absorber}$	7°C

Similar to the lithium bromide machine, the weak-strong ammonia concentration differences should be fine tuned to adapt the refrigeration load and the available heat sources. By choosing the correct concentration difference, the ARS machine can operate with high refrigeration efficiency while keeping the heat exchanger area minimized.

4.1.3 Calculation of heat exchanger area

The requirement of the heat exchanger area for the absorption system was calculated using the log mean temperature difference method. Since the rate of heat transferred is a linear function of the overall coefficient of heat transfer, the heat transfer area of the heat exchanger and the log mean temperature difference, for the heat transfer process could be derived from Equation (23).

$$Q = U \cdot A \cdot LTMD \quad (23)$$

TABLE 5: U value for several heat exchange situations (DiPippo, 2007)

Fluids	Overall Heat Transfer Coefficient [W/m ² .K]
Ammonia (Condensing) – Water	850 – 1,400
Refrigerant (Condensing) – Water	450 – 850
Refrigerant (Evaporating) – Water	170 – 850
Refrigerant (Evaporating) – Brine	170 – 850
Steam – Water	1,000 – 3,400
Steam (Condensing) – Water	1,000 – 6,000
Water – Water	1,020 – 1,140

The overall heat transfer coefficient really depends on the construction of the heat exchangers and the fluid properties, thus, an accurate coefficient could be obtained from the experiment. As a guideline for preliminary calculations, Table 5 can be used as a reference for the overall heat transfer coefficient. Hence, U values for each exchanger unit within the absorption system are determined and listed in Table 6.

TABLE 6: Design parameter of U value for each unit of heat exchanger

No	Heat Exchanger	HE Type	U [kW/m ² .C]	
			LiBr Model	NH ₃ Model
1	Absorber	Shell & Tube	0.85	0.85
2	Solution Heat Exchanger	Plate	1.10	1.10
3	Desorber	Shell & Tube	0.85	0.85
4	Rectifier	Shell & Plate	-	1.00
5	Condenser	Shell & Tube	1.40	1.40
6	Refrigerant Heat Exchanger	Plate	1.10	1.10
7	Evaporator	Shell & Tube FF	1.50	1.50

4.2 Combination of power generation and refrigeration systems

The availability and the quality of the cooling water affect the power generation capacity of the geothermal power plant. A lower temperature of cooling water assists the condenser in lowering the pressure in condensation. Based on this causality, an integrated model of a geothermal power plant and a single effect absorption refrigeration system were set to work together and the performance was analysed. General parameters for the integrated power and absorption system are found in Table 7.

The basic idea of this integrated system was to have a closed loop of a cooling water circulation system where the absorption machine removed heat from the heated cooling water right after the steam condensation process, thus eliminating the need for an ordinary cooling tower. However, as a preliminary observation, a power plant cooling system still employs a cooling tower as the primary cooling unit which cools down the heated cooling water from the condensation process. An absorption refrigeration system then once again lowered the cooling water temperature from the cooling tower right before it entered the condenser, ready to condense the steam. From this point of view, the absorption refrigeration system gave more cooling effect to the cooling water. With these two stages of cooling water treatment, the final temperature of the cooling water could be lower than the average environment and surrounding air temperature.

TABLE 7: General design parameters for integrated power and absorption system

h_{well}	1,400 kJ/kg
\dot{m}_{well}	10 kg/s
P_{well}	1,255 kPa
T_{well}	190°C
$P_{environment}$	101.3 kPa
$T_{environment}$	25°C
$\eta_{generator}$	0.85
$\eta_{turbine}$	0.85

A cooling tower removes and releases the heat from the heated cooling water to the surrounding air. Due to its dependencies on the surrounding air temperature, the product of a cooling tower could not have temperature below the average temperature of the surrounding air. In this integrated power and refrigeration system, the cooling tower was loaded by the heated cooling water both from the power plant and the absorption system. This increased the capacity of the cooling tower significantly.

The absorption system could be set to give various cooling effects to the cooling water before it reached the condenser to condense the steam. However, a minimum 4°C pinch between the chilled water outlet and refrigerant inlet should be maintained, means the maximum cooling effect is limited by the refrigerant temperature at the inlet of the evaporator. The refrigeration capacity would then depend on the mass flow of cooling water that was supplied for the plant condensation process. A simplified layout of an integrated power generation and absorption generation system is sketched in Figure 18. Energy for the absorption system mainly comes from brine water; in a case of a lack of energy supply, the absorption system is designed to tap the geothermal fluid directly from the well to cover the thermal energy shortage. The tapped mass flow is properly maintained to accommodate the need of thermal energy in the absorption system while keeping the electricity production at its peak condition.

The integrated system would utilize the heat from a liquid dominated geothermal well, as addressed before those most geothermal reservoirs are formed by liquid dominated hydrothermal systems. A 190°C geothermal fluid temperature is enough to operate flash steam plant and together with 1,400 kJ/kg enthalpy, the geothermal fluid has 29% steam fraction so it can be categorized as a liquid dominated geothermal resource. The system was set to run in tropical country which had 25°C ambient temperature.

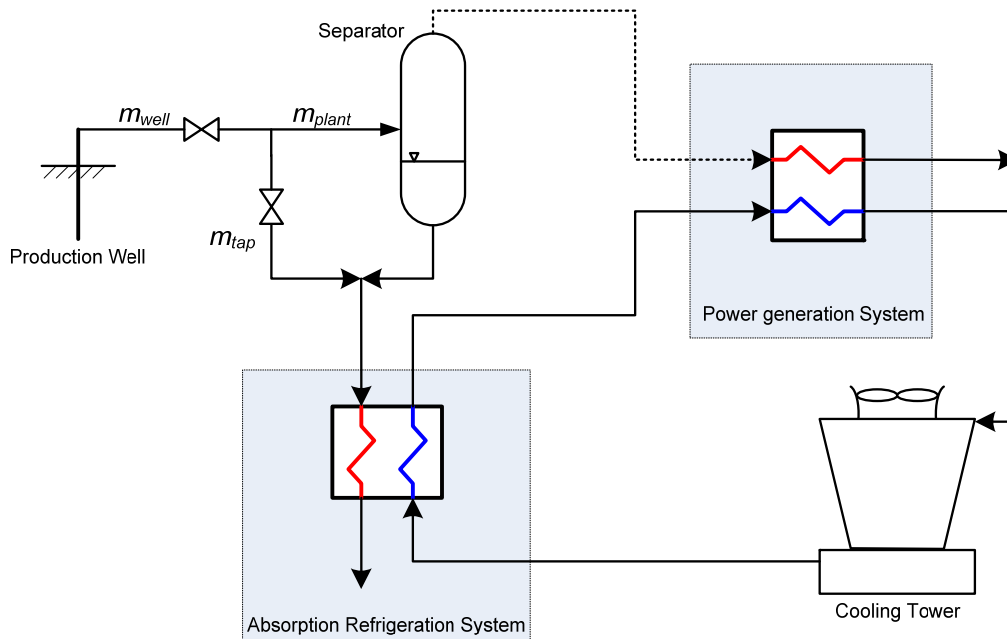


FIGURE 18: Basic design of integrated power generation and absorption refrigeration system

Minor modification was made for the single effect water-ammonia absorption machine where the heat exchange process within the rectifier was changed to an internal heat exchange process, utilizing the solution stream between the solution pump and solution heat exchanger, as shown in Figure 19.

4.2.1 Full resource utilization scenario

The objective of this scenario was to produce as much electricity as possible from the given 10kg/s geothermal fluid (\dot{m}_{well}). Such an amount of mass flow fed both power plant (\dot{m}_{plant}) and refrigeration system (\dot{m}_{tap}) and then the mass flow distribution had to be managed in order to achieve

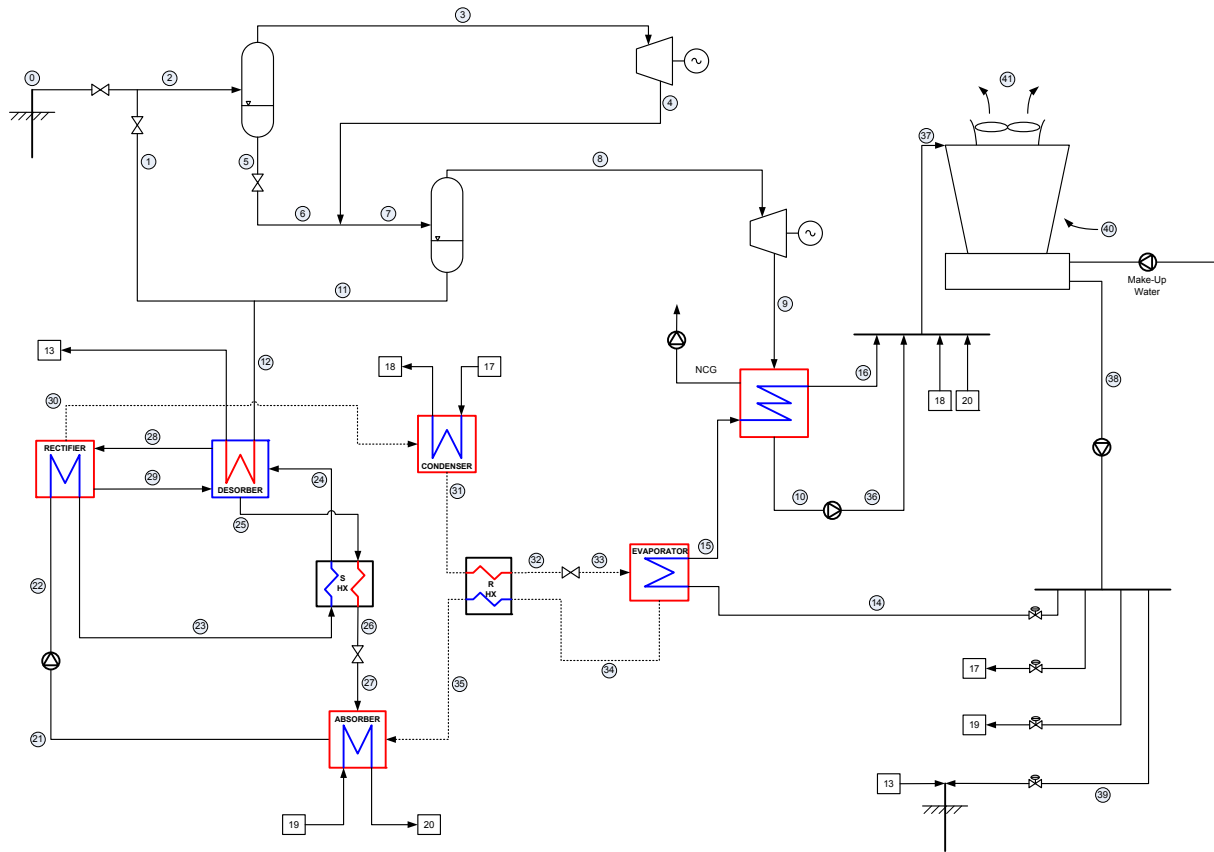


FIGURE 19: Model of double flash and water-ammonia absorption refrigeration system

the main objective. Refrigeration capacity depended on the power plant cooling demand. As the capacity of the power production increased, it pushed up the capacity of the refrigeration unit as well as the refrigeration energy demand.

Modelling of power generation and an absorption system in a full resource utilization scenario was done in two stages. First was the determination of maximum electrical power that could be generated by regular geothermal power generation systems such as single flash, double flash and organic Rankine systems without any absorption machine installed. Second was to determine the maximum electrical power generation that could be produced by an integrated power generation and absorption refrigeration system.

By splitting the stages into two, the effect of an absorption system to the output power of the power plant could be observed clearly, as well as whether it gave a positive or negative impact. To see the influence of the refrigeration system on overall plant system performance, the condenser pressure would follow the variations of cooling water temperature that came into the condenser. The power plant's condenser was simulated to have a temperature level 20°C higher than the cooling water inlet temperature and the cooling water temperature at the outlet of condenser increased as high as 12°C during the condensation process.

Models were developed for each of these cycles: single flash, double flash and isopentane organic Rankine cycle. The three models used the chilled water from each lithium bromide and ammonia absorption refrigeration system for the steam condensing process within the condenser. In all power generation systems, it was assumed that the turbine and the generator had 85% efficiency each. Specific conditions were set for the organic Rankine cycle where the minimum temperature difference between the inlet of the working fluid and the outlet of geothermal fluid at the boiler was 5°C.

Several cooling effect variations were simulated in this scenario. As the difference between the inlet and the outlet of chilled water at the evaporator increased, the absorption system needed more heat to provide the refrigeration demand. In this situation, the tapped mass flow (\dot{m}_{tap}) had to be increased to

accommodate the refrigeration demand but the consequent power plant capacity decreased because some of its original mass flow (\dot{m}_{plant}) had to be switched to the absorption system. Hence, the geothermal fluid mass flow could be changed appropriately in order to accommodate refrigeration heat demand.

4.2.2 1 MW power generation scenario

The objective of this scenario was to see the effect of the refrigeration unit on electricity generation capacity if geothermal fluid mass flow was made constant for both power and refrigeration systems. Capacity of the refrigeration unit was limited by the available heat source supplied.

This scenario was simulated to observe the real influence of an absorption refrigeration system on power generation capacity where both refrigeration and power generation systems operated with an appropriate supply of energy. The first step to simulate this scenario was to calculate the amount of geothermal fluid (\dot{m}_{plant}) that had to be delivered to each basic single flash, double flash and organic rankine geothermal power plant so they could generate 1 MW of electricity.

The known mass flow became a reference for the next scenario where the absorption machine was attached to the power plant system. An absorption refrigeration system could only use the waste heat source either from the power plant or un-utilized geothermal fluid. In this way, we had constant geothermal fluid supply for each power plant (\dot{m}_{plant}) and absorption machine unit (\dot{m}_{tap}). Both systems were set to operate at 25°C ambient temperature. The absorption refrigeration system was optimized to have a maximum extra power generation for each unit area of heat exchanger installed. The total area of the heat exchanger for the refrigeration system included the cumulative area of the desorber, condenser, refrigerant heat exchanger, evaporator, absorber and solution heat exchanger with the addition of a rectifier for the ammonia machine. The picture below shows one possible combination of a double flash power generation system and a single effect water-ammonia absorption refrigeration system. A complete combination of a power plant and an absorption refrigeration system are shown in 0.

4.3 Non condensable gases

Some non condensable gases such as carbon dioxide (CO₂) and hydrogen sulphide (H₂S) are carried by the geothermal fluid from the well(s) and might flow together with the steam and finally accumulate within the condenser. The accumulated gasses increase the condenser pressure as well as the condensing temperature which can reduce turbine power output significantly. The non condensable gas content may vary from one geothermal site to another; moreover, it fluctuates from time to time. Obviously, this condition works contrary to the objective of extra turbine power output by lowering the condenser pressure. Therefore, these non condensable gases somehow must be pumped out of the condenser using gas extraction equipment, i.e. steam jet ejectors, vacuum pumps or turbo compressor technology.

All power plants are modelled with a vacuum pump unit attached to the condenser to remove unwanted non condensable gas. Geothermal fluid that comes from the well is assumed to have 0.15% non condensable carbon dioxide content. As the non condensable gases are always mixed with the steam, some portion of the steam may still be released together with the non condensable gases from the condenser during the gas extraction process. Therefore, in order to minimize the amount of steam that will be pumped out during the gas extraction process, temperature at the gas extraction outlet should be lower than the average condenser temperature. Thus, most of the steam phase is condensed before passing the gas extraction process. Here, the saturated temperature for the gas extraction process was set to 4°C below the temperature of condensation.

5. RESULTS AND DISCUSSIONS

Modelling both absorption and power generation systems in EES makes the calculation and simulation processes easier. Though the capability of EES for automation and optimization is relatively good, since the aim of this study was not to develop a good and nice looking program, there were some parameters in the simulation process that had to be set and fine tuned manually. It means the optimization process was done manually by choosing and changing the main parameters, especially the weak-strong solutions concentration differences, evaporation temperature and temperature difference at the inlet and outlet of the evaporator.

5.1 Absorption refrigeration system

A series of calculations for different parameters were made to observe the effects of each absorption parameter on system performance for a given heat source and cooling load. The total heat exchanger area for the refrigeration machine was deemed another important factor that had to be monitored and considered side by side with the Coefficient of Performance during the simulation. The total area of the heat exchangers increased as the refrigeration capacity increased because the system deals with heat transfer processes more than a lower refrigeration capacity.

The total heat exchanger area for various refrigeration capacities and different temperatures at the evaporator is presented in Figure 20. The total area needed for a lithium bromide machine is profiled by a dashed line; the bold line represents the ammonia machine. The area of the heat exchanger tended to cluster in a narrow temperature range at a lower refrigeration capacity; the range started to widen as the refrigeration capacity rose.

The change in the evaporation temperature gave a slight line shift for lithium bromide but had a significant influence on the ammonia machine. Heat demand for the refrigeration process and the actual heat supplied to the desorber also had a big impact on the heat exchanger area. As the heat demand got closer to the maximum available heat supplied to the system, a larger heat exchanger area had to be built to run the process.

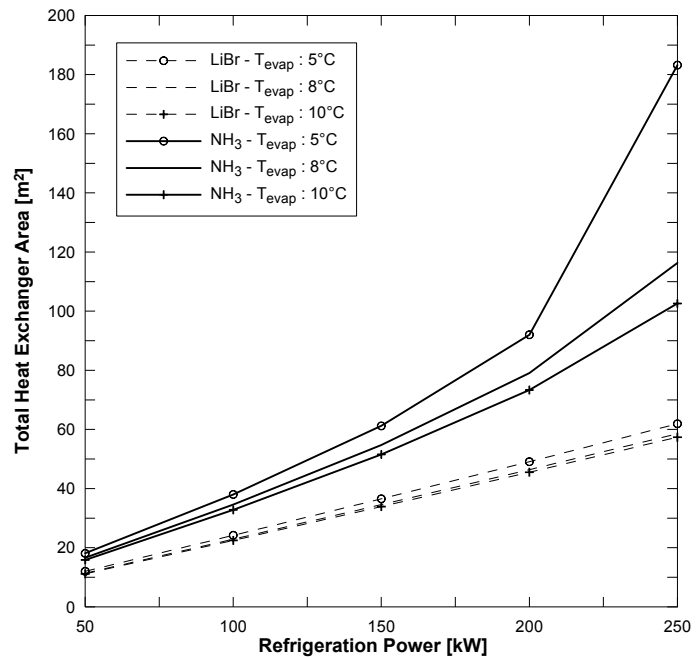


FIGURE 20: A typical total heat exchanger area for different refrigeration capacities and evaporator temperature

Evaporation temperature, together with evaporation capacity, controls the total heat demand necessary for the refrigeration system. The machines needed more heat to create a lower evaporation temperature than a higher evaporation temperature, clearly shown in Figure 20. Also observed was that for each cooling load, the concentration difference between strong and weak solutions could be fine tuned to find an optimized result for the total heat exchanger area.

5.1.1 Weak and strong solution concentration differences

It is noticeable that the concentration differences between the weak and strong solutions in the absorption refrigeration system are strongly related to the mass flow of the refrigerant as stated previously in Equations (2) and (5). The bigger the concentration difference, the more refrigerant was extracted from the solution and, at the same time, increased refrigeration capacity.

The typical relationship between the solution concentration difference, the coefficient of performance and the total heat exchanger area is shown in Figures 21 and 22 for ammonia and lithium bromide, respectively. The coefficient of performance tended to increase in line with the increment of solution concentration differences where the weak-strong solution concentrations reflected the amount of refrigerant which could be extracted from the original solution. As the refrigerant's mass flow increased, the absorption machine could be loaded with a higher cooling capacity. A constant energy demand and a higher cooling capacity led to a higher system performance.

At the same refrigeration capacity, changing the weak and strong concentration difference affected the total area needed for the overall refrigeration machine. In general, it tended to have a parabolic correlation with the increment of solution concentration differences. Since it was decided that the optimization of absorption refrigeration machines involved the total heat exchanger area, the minima of the parabola could be used as a good indicator when choosing the optimum absorption parameter. But in some cases the maximum concentration difference between the strong and weak solutions had to be bound by the limited heat supply, stopping the refrigerant extraction process. Thus, it is important to have a minimum area of a heat exchanger since it is strongly related to the investment costs even though the coefficient of performance increases as the difference widens.

The problem of crystallization is an important factor to monitor for a water-lithium bromide absorption machine because it might affect the operation and the lifetime of the absorption machine. Crystallization tends to occur between the expansion valve and the absorber where the pressure level is low enough and the solution temperature is close to the crystallization line. Referring to Figure 11, the fitted formulation for the lithium bromide phase diagram could be calculated (0) and later used in EES to monitor the crystallization temperature margin on various system parameters.

A higher concentration difference means the fraction of lithium bromide at the outlet of the desorber is higher than the lower concentration difference and more of the water fraction is extracted from the low weak solution as a refrigerant. Since the solubility limit is a strong function of mass fraction and temperature, the salt substance of aqueous lithium bromide solution tends to precipitate easily at a higher solution concentration. It is important to keep the solution temperature above and not allow it to go below the crystallization temperature line.

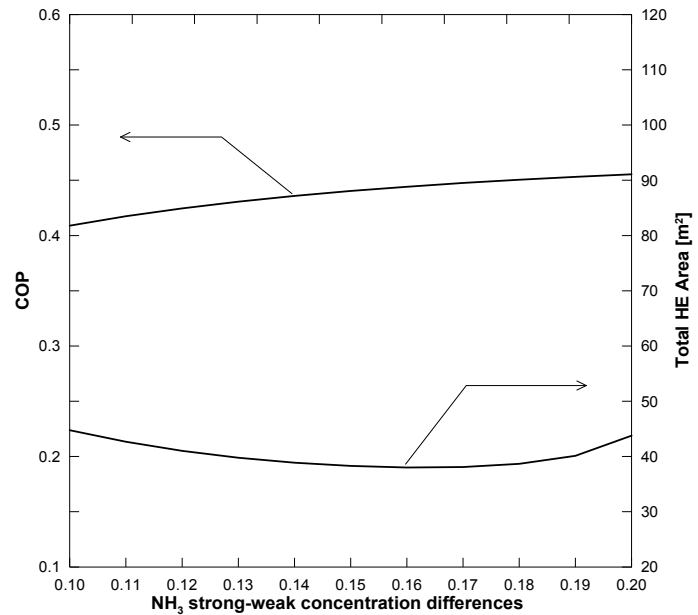


FIGURE 21: A typical effect of weak and strong NH_3 concentration differences on system performance

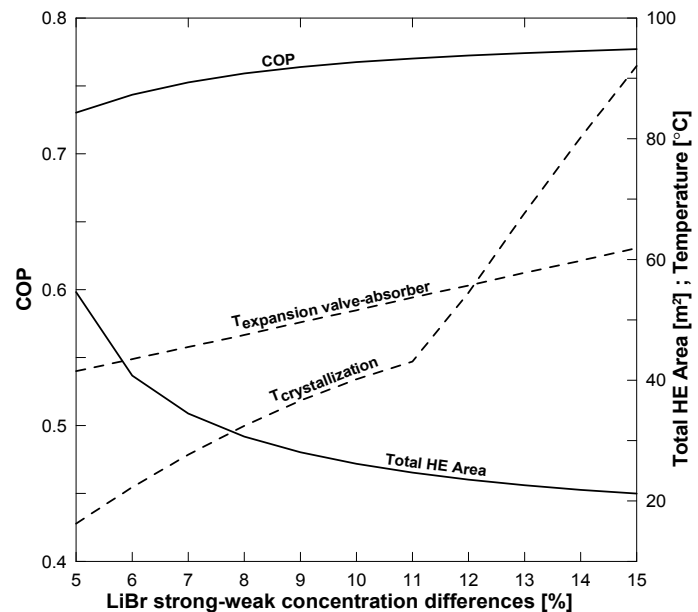


FIGURE 22: Effects of weak and strong LiBr concentration differences on system performance

As seen in Figure 22, temperature along the expansion valve and absorber was monitored since the crystallization process appears most at this part of the lithium bromide absorption machine. It is clear that the temperature at this section starts to cross the crystallization line as the concentration difference widens. The fact is that crystallization constrains the design parameter of a lithium bromide absorption machine even though higher refrigeration efficiency might be achieved beyond the crystallization line. Dashed lines show the temperature along the expansion valve and absorber and the temperature at which crystallization starts to occur. Both lines show a temperature increment as the concentration difference widens, but as the temperature of crystallization changes more quickly, the two lines start to cross at some point. Giving an adequate margin to this crystallization temperature helps to keep the machine free from crystallization although it reduces refrigeration efficiency and increases the total heat exchanger area needed. A sensible temperature margin has to be maintained in order to achieve safety conditions without sacrificing the optimum design further.

5.1.2 Solution temperature at the absorber's outlet

The temperature of either ammonia or lithium bromide at the outlet of the desorber affects the efficiency of an absorption refrigeration system differently. The absorption process of a refrigerant by the absorbent in the absorber unit requires low temperature in order for the absorption process to properly develop, thus a heat sink system is attached to remove the heat created during the absorption process. The final purpose of an absorption process is to produce a saturated solution liquid which then could be pumped and circulated more easily than a vapour mixture solution.

A lithium bromide solution concentration at this point is controlled by the pressure and the temperature at the outlet of the absorber. Since a $\text{NH}_3\text{H}_2\text{O}$ procedure was used, three parameters were needed to determine ammonia concentration at the outlet of the absorber; a combination of temperature, pressure and ammonia vapour fraction is one possible combination. At higher solution temperature for a constant pressure, the absorber needs more absorbent to completely absorb the same amount of refrigerant, proven during the simulation process with the presence of a higher amount of absorbent mass flow for a constant refrigerant mass flow. As the amount of mass flow increased, the heat exchange process within the absorber and desorber increased likewise as they both deal with the same solution mass flow. This condition makes the absorption machine require more heat to work properly. Extra heat for constant refrigeration capacity decreases the performance, as seen in Figure 23 for ammonia and Figure 24 for the lithium bromide machine.

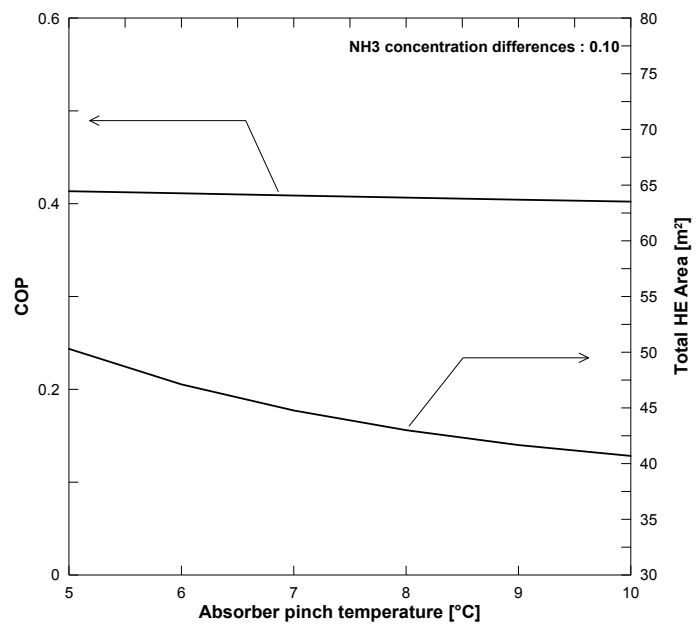


FIGURE 23: A typical system performance for various NH_3 strong solution temperatures at the outlet of the absorber

It is important to keep the temperature at the outlet of the absorber at the lower possible temperature. A low temperature at this point helps minimize the vapour fraction, particularly for the lithium bromide solution, which can keep the crystallization temperature low. The only advantage to having a high temperature at the outlet of the absorber is a reduced total area needed for the refrigeration system.

5.2 Electric power generation

The availability of low temperature cooling water could be considered the key factor in achieving a high performance of power generation, aside from the heat source quality and quantity. Recent technology makes it possible to build a low pressure machine close to full vacuum condition. A lower temperature of the cooling water can lead to a lower pressure of the power generation component, especially for the steam condenser. In order to observe the correlation between cooling water temperature, condenser pressure, condenser heat exchanger area and power generation capacity, a series of simulations were run for a single flash geothermal power plant with the results graphically shown in Figure 25. In order to harvest the optimum power, the separation pressure is set to follow the change of the condenser temperature. Condenser pressure and mechanical work of the turbine respond to the temperature of the cooling water conversely and the volume and size of the condenser increases as the condenser pressure decreases. The availability of low temperature cooling water helps to condense the steam in a lower pressure environment. A lower condenser pressure spans the enthalpy differences between the inlet and outlet of the turbine so more mechanical work can be produced.

In Figure 25, the condenser is set to a constant pinch temperature with the cooling water temperature at the inlet of the condenser. Based on the *UA* method, the area will be controlled by the log mean temperature difference and condenser capacity since the coefficient of heat transfer for the condenser stays the same.

5.2.1 Total electric power generation

All presented results in this sub-section are based on simulation of both the 4.2.1 Full resource utilization **scenario** and a 4.2.2 1 MW power generation **scenario**. By adding the absorption refrigeration system onto the power plant cooling system some extra power generation should be expected. For reference, the maximum power generation that could be generated by each regular geothermal power generation system, for the given geothermal resource and 1 MW power generation, is put as the base power of each scenario. Power generation from each integrated power and refrigeration system should refer to this base power to see whether the refrigeration system has a positive or negative impact on power generation capacity. Several refrigeration capacities and geothermal fluid mass flow managements were simulated for the 4.2.1 Full resource utilization **scenario** in order to find the maximum generation capacity, while in the 4.2.2 1 MW power

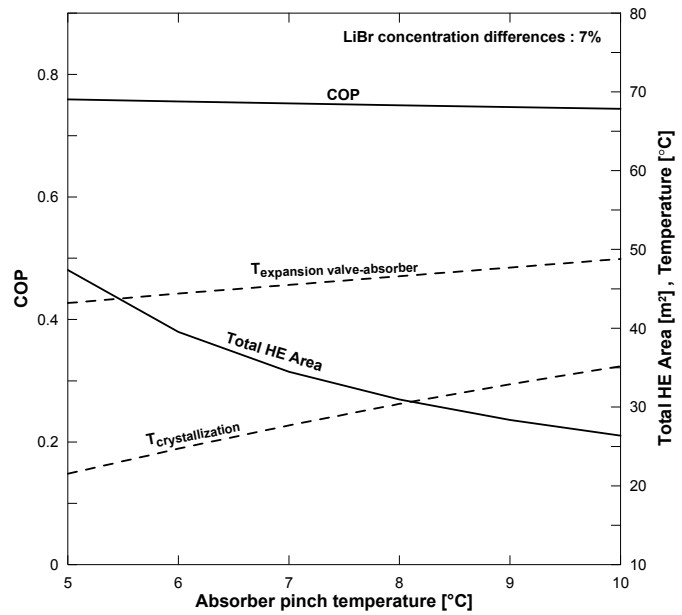


FIGURE 24: A typical system performance for various LiBr weak solution temperatures at the outlet of the absorber

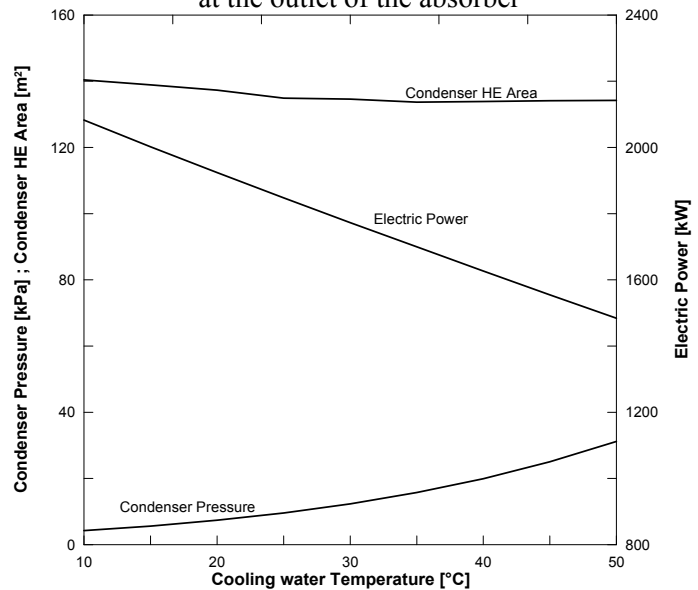


FIGURE 25: A typical relationship between cooling water temperature, condenser and generation capacity

generation scenario no mass flow change was allowed and the only parameter that could be fine tuned was the absorption machine parameters.

Each scenario was simulated for several evaporator temperatures and chilled water temperature differences at the inlet and outlet of the evaporator. All electric power generated by any integrated power and refrigeration system is in the form of net electric power; electric power from the generator was deducted to feed the refrigeration energy demand such as in the solution and cooling water pump.

Integrated single flash and single effect absorption refrigeration system

An integrated single flash geothermal power plant and single effect absorption refrigeration system generally had a positive effect on power generation capacity, both in the Full resource and the 1 MW scenarios. In the Full resource scenario, the lithium bromide machine still gave more refrigeration effect than ammonia for the same amount of waste heat from the separator. This situation is in line with the fact that a water-ammonia absorption refrigeration system needs more power than the lithium bromide-water for similar refrigeration capacity. As the temperature difference at the outlet of the evaporator went beyond 5°C, the lithium bromide machine started to require more heat source from the tapped system because the heat source supplied by the brine water was not enough; total power generation began to decrease continuously as the refrigeration capacity increased. As shown in Figure 26, these two scenarios affected the integrated power and refrigeration system differently, mainly caused by the available heat that could be utilized by the absorption system. In the 1 MW power generation scenario, there was still enough heat to run the ammonia ARS up to 7°C of chilled water temperature difference at 10°C evaporator temperature. Beyond this point, there was not enough heat to run the system. The lithium bromide ARS still ran and gave maximum power generation at a temperature difference of 16°C and 8°C evaporator temperature.

The power generation curve in the 1 MW scenario always showed an ascending linear curve as cooling water temperature difference increased because during simulation the geothermal fluid mass flow for both systems was kept constant.

A combination of single flash and lithium bromide ARS gave the maximum positive power gain up to 62 kW in the Full resource scenario and 131 kW in the 1 MW scenario. This extra power capacity will be examined later to see if the feasibility of such a power gain requires extra investment costs.

Integrated double flash and single effect absorption refrigeration system

An integrated double flash geothermal power plant and single effect absorption refrigeration system acted similarly to a single flash, the only distinction being in the amount of waste heat from the separation process that could be utilized by the absorption machine. As a double flash power generation system has higher efficiency and extracts more energy than a single flash system, the amount of waste heat from the separation process was far reduced. Two identical power generation curves were performed by these two different power generation systems. The ability of the refrigeration system operating at a higher refrigeration capacity was limited in the double flash system, as shown in Figures 26 and 27 for a single flash and a double flash system, respectively.

In the Full resource scenario, the double flash and ammonia machine did not give any positive generation capacity at all because power gained by the lower condenser pressure could not compensate for the power loss due to the mass flow change. Combination with a lithium bromide machine gave a positive effect even though it was lower than the single flash and lithium bromide systems.

In the 1 MW scenario, the fact is that the double flash system needed less mass flow to generate 1 MW of electricity than the single flash system. This is an advantage for the absorption refrigeration system because it received more heat source than in the integrated single flash system. That is why the refrigeration system in a double flash system can work at a higher cooling capacity than a single flash system. One special condition was applied for the lithium bromide machine: the heat supply was sufficient to run the system, but the cooling water temperature difference could not go lower because it was bound by the pinch temperature between the outlet of chilled water and the evaporator temperature. Thus, by having 29°C cooling temperature inlet, 5°C evaporator temperature and 4°C

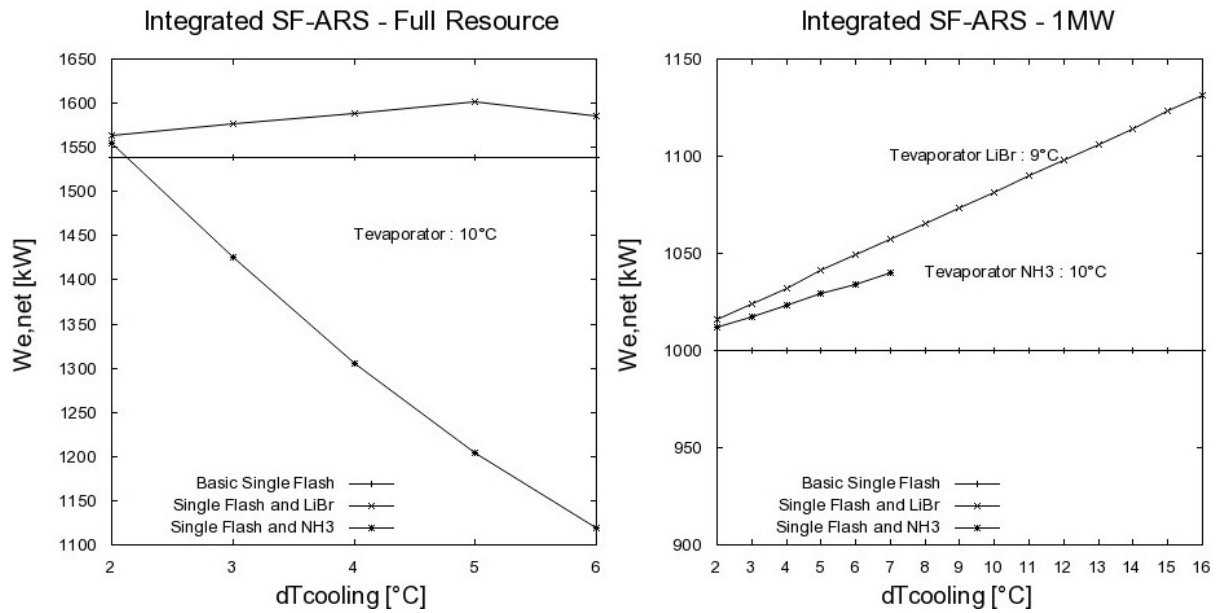


FIGURE 26: Integrated single flash-single effect absorption refrigeration system electric generation capacity for full resource (left) and 1 MW (right) scenario

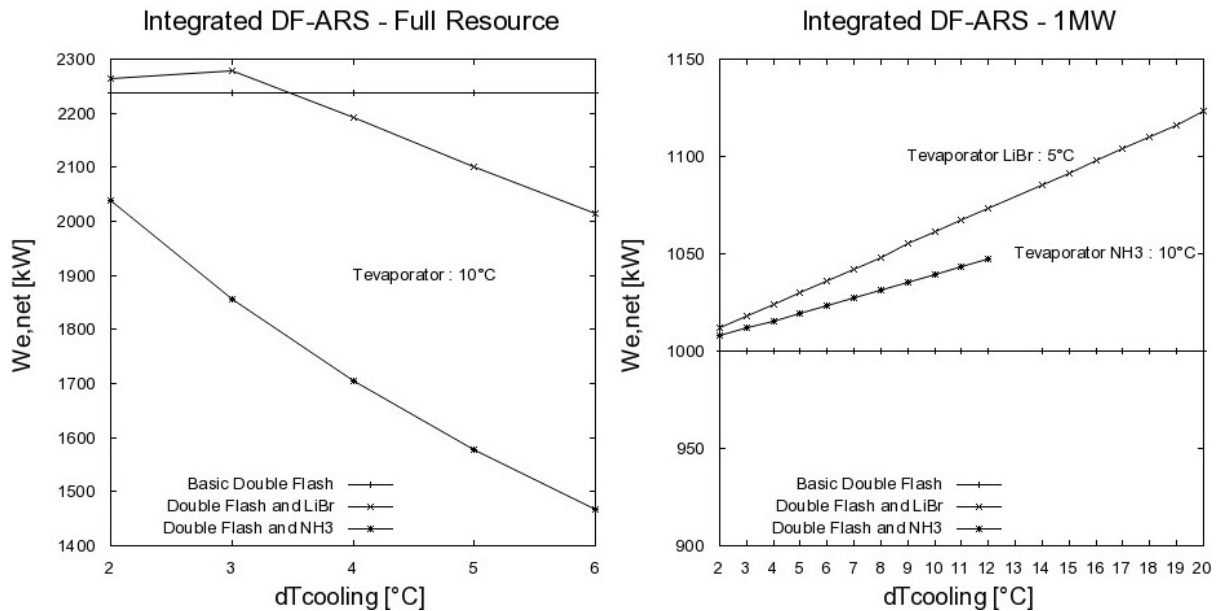


FIGURE 27: Integrated double flash-single effect absorption refrigeration system electric generation capacity for full resource (left) and 1 MW (right) scenario

pinch, the cooling temperature at the inlet and outlet of the evaporator could only have a difference of up to 20°C.

A combination of double flash and lithium bromide ARS gave the maximum positive power gain up to 40 kW in the Full resource scenario and 123 kW in the 1 MW scenario. This extra power capacity together with the previous results are going to be examined later to see if the feasibility of such a power gain requires extra investment costs.

Integrated ORC and single effect absorption refrigeration system

An integrated organic Rankine cycle geothermal power plant and single effect absorption refrigeration system seems to be the worst combination when compared to both previous integrated systems. As the Rankine cycle only disposed of a small amount of waste heat from its boiler/evaporation unit, this combination had a negative effect for both lithium bromide and ammonia absorption systems when operated in a Full resource scenario. In the 1 MW scenario, to produce 1 MW of electricity, an ORC

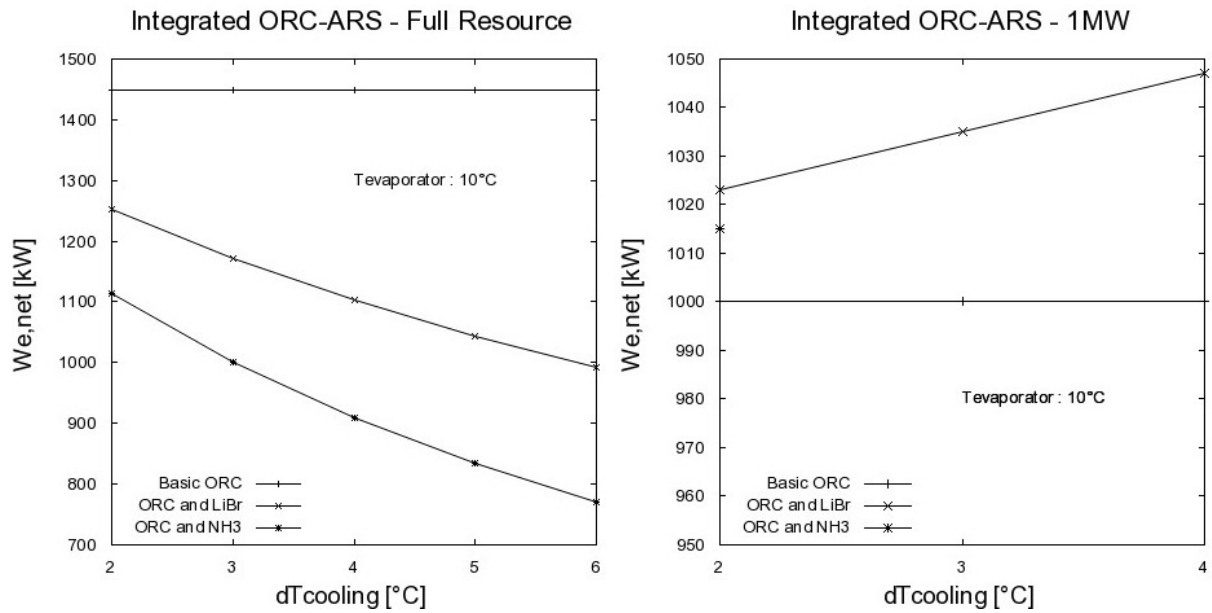


FIGURE 28: Integrated organic Rankine cycle-single effect absorption refrigeration system electric generation capacity for full resource (left) and 1 MW (right) scenario

plant required more mass flow than either single or double flash plants and reduced the amount of tapped mass flow which could be used to run the absorption machine (Figure 28).

A lithium bromide machine in an ORC system could only lower the cooling water to 4°C while the ammonia machine stuck on a 2°C temperature difference. A combination of an organic Rankine cycle and lithium bromide ARS gave no positive power gain in a full resource scenario and 47 kW in a 1 MW scenario.

Summary

A combination of a geothermal power plant unit and absorption refrigeration unit mostly has a positive effect on extra power generation, especially if a vast un-utilized heat source is available. Based on an evaporator temperature range of 5-10°C, the maximum production capacity in a Full resource scenario is given at the higher boundary of the evaporator temperature which is 10°C, because putting the evaporator at a lower temperature means the refrigeration system would require more energy. The advantage to having such a low evaporator temperature is that the evaporator has more of a chance to produce a lower temperature of chilled water. It only can be achieved if there is enough energy to operate the absorption system at such an evaporator temperature. This is well proven in the 1 MW scenario where the maximum generation capacity was achieved at an evaporator temperature of 9°C for single flash with a lithium bromide machine and 5°C for double flash with a lithium bromide machine.

In a double flash system, though, the amount of un-utilized mass flow is higher and the refrigeration system can go with a lower evaporation temperature than in a single flash system, but since the affect of cooling water is only applied on the lower pressure side of a generation system, the extra power gain that can be produced by a double flash system is still below that of the single flash system.

As listed in Figure 29 and Table 8, the highest net power gain of both scenarios is given by the integrated single flash and lithium bromide system. Net power generation profiles on various $T_{evaporator}$ and $\Delta T_{cooling}$ at the outlet of the evaporator are fully listed in 0.

Based on Figure 30, in the Full resource scenario, a lithium bromide machine still can utilize the heat from the power plant separation process with a cooling temperature of up to 5°C and variations of the evaporator temperatures almost give the same net power generation. Beyond a 5°C cooling temperature, the refrigeration machine starts to take some portions of mass flow from the system. It reduces the power output and the magnitude of power loss depends on the amount of mass flow that

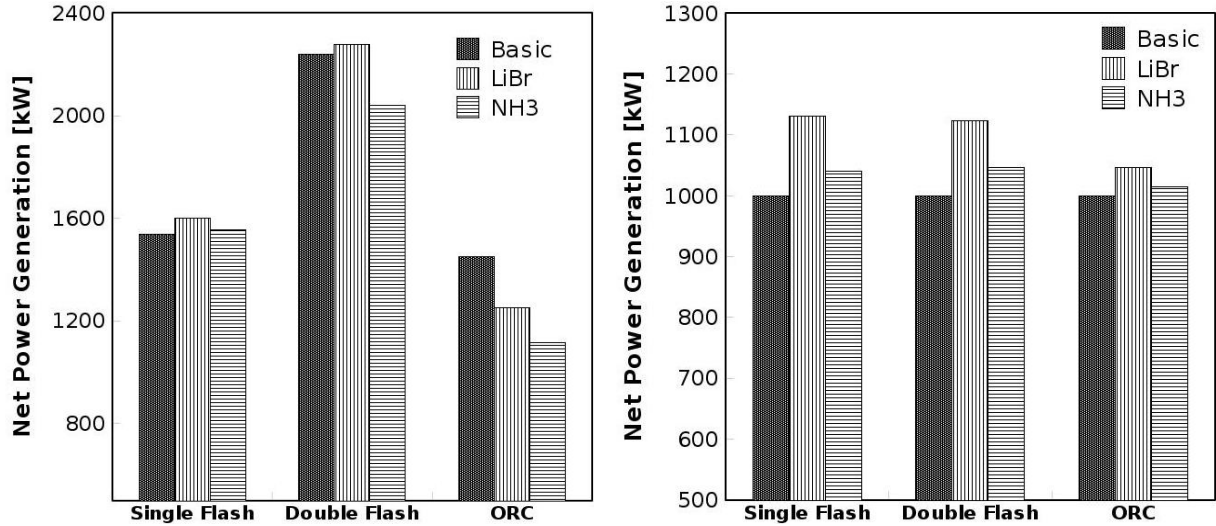


FIGURE 29: Maximum possible net power output for each combination of power and refrigeration system on full resource scenario (right) and 1 MW scenario (left)

has been taken from the power generation system. Thus, net power output is different for various evaporator temperatures even though the cooling effect is kept at 6°C. This is obvious as a refrigeration machine with lower evaporator temperature requires more heat and then decreases the net power output from the power generation system.

TABLE 8: Maximum possible net power output for each combinations of power plant and refrigeration

Combination	Full Resource Scenario			1 MW Scenario		
	$W_{e,ref}$ [kW]	$W_{e,net}$ [kW]	ΔW_e [kW]	$W_{e,ref}$ [kW]	$W_{e,net}$ [kW]	ΔW_e [kW]
Single Flash with LiBr	1,539	1,601	62	1,000	1,131	131
Single Flash with NH ₃	1,539	1,554	15	1,000	1,040	40
Double Flash with LiBr	2,238	2,278	40	1,000	1,123	123
Double Flash with NH ₃	2,238	2,039	-199	1,000	1,047	47
ORC with LiBr	1,449	1,252	-197	1,000	1,047	47
ORC with NH ₃	1,449	1,114	-335	1,000	1,015	15

A 1MW scenario gives relatively constant net power output on various evaporator and cooling temperatures but the maximum power generation can only be achieved at 7, 8 and 9°C evaporator temperature with 16°C cooling temperature. This situation is not well presented by Figure 30 (left) due to all the curves being stacked together. At evaporator temperature of 10°C, the cooling temperature cannot go beyond 15°C due to pinch restrictions even though the heat source still can go for higher refrigeration capacity. Changing the evaporator temperature to 9°C makes it possible for the cooling temperature to go up to 16°C and indeed gives more power output. Again the evaporator temperature was changed to 8°C but the refrigeration machine could not successfully operate at 17°C cooling temperature due to the lack of energy; the cooling temperature stuck at 16°C as before. As the evaporator temperature got lower, the cooling temperature had to be lowered in order to make the refrigeration machine operate.

There are some combinations of evaporator and cooling temperature that give similar power output with differing total areas of the heat exchanger. Hence, it is reasonable to compare the power gain over the area of heat exchanger needed by the refrigeration system. Figure 31 shows the ratio between extra power produced by the generation system and the total area of the heat exchanger necessary for such extra power.

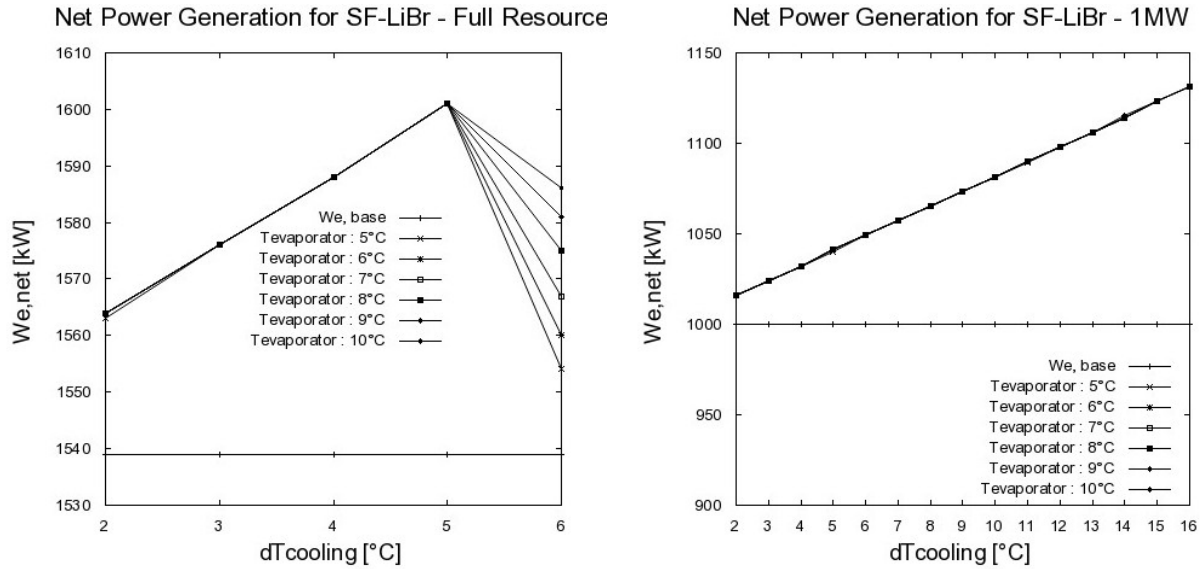


FIGURE 30: Net power generation on various evaporator temperature and chilled water temperature for full resource (left) and 1 MW (right) scenario

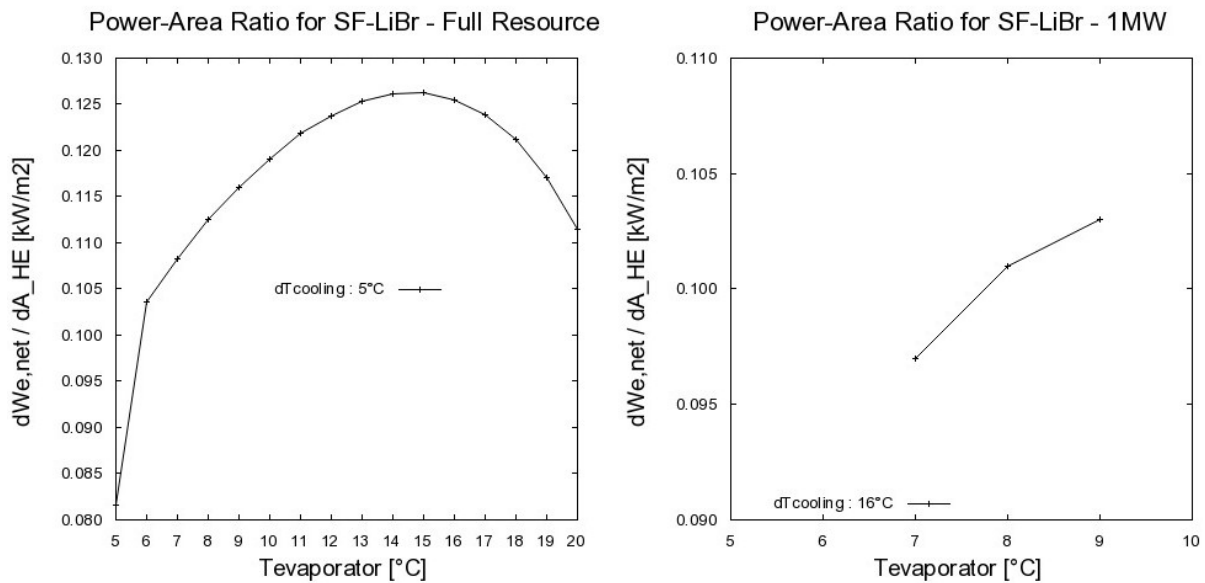


FIGURE 31: Net power-area ratio of integrated single flash and lithium bromide-water ARS for full resource (left) and 1 MW (right) scenario

The net power-area ratio curve describes how much net electric power gain is achieved for each area of exchanger installed, thus the highest ratio is preferable. In the Full resource scenario, the temperature of the evaporator was extended up to 20°C in order to see a Full ratio profile of the net power output over the heat exchanger area. As observed in previous sections, the absorption refrigeration machine has a minimum total area of heat exchanger by setting the correct parameter of weak-strong solution concentration difference and temperature at the outlet of the evaporator. The Full resource curve indicates the optimum parameter for a lithium bromide absorption machine can be achieved by having the evaporator and cooling temperature at 15°C and 5°C, respectively.

In the 1 MW scenario, the maximum net power output was produced at 16°C cooling temperature and a range of evaporator temperatures of 7-9°C. Temperature at the outlet of the evaporator could not go beyond 9°C due to evaporator pinch temperature restrictions, making the optimum parameter for this scenario 9°C evaporator temperature and 16°C cooling temperature. Obviously the temperature at the

outlet of the evaporator can be set at a higher level by lowering the cooling temperature, but by doing this net power output must be sacrificed.

The main setting parameters and the area of each component for an integrated single flash and lithium bromide-water absorption refrigeration system are listed in Table 9.

5.2.2 Power plant condenser pressure

A lower condenser pressure can be achieved by employing a lower cooling water temperature

in the condenser. However, there are some potential obstacles to be faced such as non condensable gas content and steam quality during the steam expansion process.

Non condensable gases (NCGs)

The presence of non-condensable gases in geothermal fluid controls how low the condenser pressure can go. The higher the non-condensable gas content, the more work is needed to remove the accumulated gases from the condenser. A large quantity of non condensable gases and very low condenser pressure limit the gas extraction equipment because it deals with a high gas specific volume and huge equipment.

Referring to the optimum simulation results, the average condenser temperature for the Full resource and 1 MW scenario is 44°C and 33°C, respectively. The condenser pressure can be obtained from the condenser temperature: at 44°C the condenser pressure is about 9.113 kPa and 5.035 kPa for 33°C. Though the condenser pressure is very low, it is still affordable since the non condensable gas content is very low. Complete results for the gas extraction process are listed in Table 10.

Steam quality at the outlet of the turbine

As the pressure at the condenser (at the outlet of the turbine) is shifted to a lower level, the steam quality after the expansion process decreases and more water droplets are created within the steam mixture. The presence of water droplets can harm the turbine blade. Depending on the turbine design, there is a limit for the minimum allowed steam quality at the outlet of the turbine.

A view of the thermodynamic steam expansion process across the turbine is drawn in Figure 32. The vertical line represents the isentropic process when the steam vapour flows across the turbine. Saturated vapour at 100 kPa pressure lowered to 20 kPa condenser pressure creates x_1 steam quality, and when the pressure goes down to 10 kPa the steam quality becomes x_2 . It is obvious that the quality of x_2 is lower than x_1 .

The last two simulation results indicate that the steam quality at the outlet of a single flash turbine is around 0.83 and 0.82 for each Full resource and 1 MW scenario. In the 1 MW scenario, the quality is

TABLE 9: ARS main parameters and the final results for both full resource and 1MW scenario

Component	SF w/ LiBr Full Resource	SF w/ LiBr 1 MW
Electric gain[kW]	62	131
Evaporator capacity [kW]	2,134	4,414
$T_{evaporator}$ [°C]	15	9
$\Delta T_{cooling}$ [°C]	5	16
ARS cooling water [kg/s]	76.14	161.48
Absorber [m ²]	218.20	608.60
SHX [m ²]	5.08	16.66
Desorber [m ²]	74.21	224.90
Condenser [m ²]	63.32	116.90
RHX [m ²]	4.56	10.26
Evaporator [m ²]	125.70	296.00
Total HE Area [m ²]	491	1,273

TABLE 10: Gas extraction process data

	Full Resource Scenario	1 MW Scenario
$T_{condenser}$ [°C]	44	33
$P_{condenser}$ [kPa]	9.113	5.035
$T_{sat,NCG}$ [°C]	40	29
\dot{m}_{NCG} [kg/s]	0.04	0.03
$W_{pump,NCG}$ [kW]	0.752	0.433

lower than for the Full resource scenario due to the lower condenser pressure. These steam qualities are fairly safe for the low capacity power plant that is simulated in this report. Again, depending on generation capacity and turbine specification, the steam quality at the outlet of the turbine may range from 0.80 up to 0.88 for a large geothermal power plant. Obviously this is not a fixed allowed range of quality at the outlet of the turbine. The steam

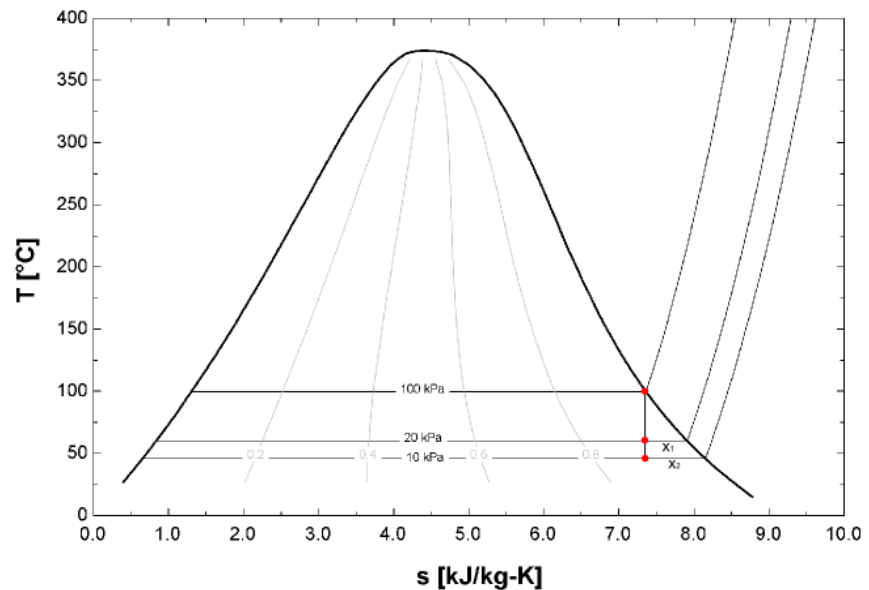


FIGURE 32: A temperature-entropy diagram for the steam

quality at the outlet of the turbine is possible to go beyond 90%, but the consequent turbine power decreased while the steam still has energy to generate mechanical power.

5.2.3 ARS investment cost

Once the area of each heat exchanger component for the absorption machine is known, the investment cost for each of them can be roughly calculated. Material that is used to construct the heat exchanger becomes the main factor that affects the heat transfer coefficient and the investment cost, but selecting the correct material for such working fluid is the most important thing compared to the investment cost because it will affect the life expectancy and maintenance complexity of the absorption machine.

Carbon steel and copper are the preferred materials for the single effect aqueous lithium bromide absorption system environment, even though the presence of oxygen in aqueous lithium bromide makes it aggressive to many metals including carbon steel and copper. Since the presence of oxygen is very little in an absorption machine, the aggressiveness and corrosion rates are much slower (Herold et al., 1996) and preventive action should be taken to minimize the effects. Steel and stainless steel are the most common materials to put in an ammonia-water environment because ammonia is a very good solvent for copper. A corrosion inhibitor is still needed when steel is considered as the heat exchanger material.

The general cost estimations for the heat exchanger components refer to Matche's (2009) website (Matche's Process Equipment Cost Estimates) where the price is based on F.O.B. Gulf Coast USA year 2007. Total investment cost for each system was calculated based on heat exchanger and pump initial cost (Bejan et al., 1996) as listed in Table 11.

A comparison of the total investment cost for both scenarios was calculated to see how much extra investment cost would need to be invested to gain 1 kW of electric power; results are listed in Table 12. The higher investment cost in the 1 MW scenario than in the Full resource scenario can be covered by the extra amount of electricity gained by the ARS system. Hence, applying an integrated single flash and lithium bromide-water absorption refrigeration system in 1 MW scenario gives the lowest investment cost for each kilowatt of electricity gained.

A total investment cost of \$ 2,089,816 to gain an extra 131 kW of electricity does not seem to be economically feasible. A rough optimistic calculation could be made to determine how many years it would take for the given investment cost to be returned. Assuming 0.04 \$/kWh as the price of electricity and neglecting such operational, maintenance costs and the interest to gain the income and make the return time faster, it would require ca. 45 years to take the investment cost of the absorption

machine back and even longer if operational costs, maintenance costs and t interest are included, too long when compared to the 20-25 years of life expectancy for a geothermal power plant.

TABLE 11: Estimation of total capital investment for single effect lithium bromide-water ARS

Cost components	SF w/ LiBr – full resource	SF w/ LiBr – 1 MW
I. Fixed capital investment (FCI)		
A. Direct cost (DC)		
1. Onsite cost (ONSC) and purchased equipment cost (PEC)		
a. Heat exchanger	\$ 322,500.0	\$ 570,600.0
b. Pumps	\$ 4,100.0	\$ 4,100.0
c. Piping system [5% of (a+b)]	\$ 16,330.0	\$ 28,735.0
d. Electrical control & monitoring system [30% of (a+b+c)]	\$ 102,879.0	\$ 181,030.5
Total onsite cost	\$ 445,809.0	\$ 784,465.5
2. Offsite cost (OFSC)		
a. Civil, structural & architectural work [20% of ONSC]	\$ 89,161.8	\$ 156,893.1
b. Service facilities (hot source & cold sink connection) [25% of ONSC]	\$ 111,452.3	\$ 196,116.4
c. Contingencies [15% of ONSC]	\$ 66,871.4	\$ 117,669.8
Total offsite cost	\$ 267,485.4	\$ 470,679.3
Total direct cost	\$ 713,294.4	\$ 1,255,144.8
B. Indirect cost (IDC)		
1. Engineering & supervision [15% of DC]	\$ 106,994.2	\$ 188,271.7
2. Construction cost incl. contractor's profit [15% of DC]	\$ 106,994.2	\$ 188,271.7
3. Contingencies [20% of DC]	\$ 142,658.9	\$ 251,029.0
Total indirect cost	\$ 356,647.2	\$ 627,572.4
Total fixed capital investment	\$ 1,069,941.6	\$ 1,882,717.2
II. Other outlays		
Total other outlays	\$ 117,693.6	\$ 207,098.9
Total capital investment of ARS machine	\$ 1,187,635.2	\$ 2,089,816.1

TABLE 12: Estimation of ARS investment cost for 1MW power generation scenario

	SF w/ LiBr Full Resource	SF w/ LiBr 1 MW
Electric gain [kW]	62	131
ARS investment cost [USD]	1,187,635	2,089,816
ARS investment cost [USD/kW]	19,155	15,952

6. CONCLUSIONS

Latent heat of the refrigerant and the heat requirement to increase the solution temperature are the main key factors that affect the performance of a refrigerant. Because of refrigerant properties, refrigeration performance of a single effect lithium bromide-water system is higher than a single effect water-ammonia system based on the same cooling load. It was revealed during the Full resource utilization scenario that the absorption refrigeration system should be properly designed to achieve its peak performance since different amounts of heat source and cooling load affects refrigeration parameters. Fine tuning the weak-strong concentration difference can lead to minimum total area of heat exchanger and indeed increase the economy of an absorption refrigeration machine.

As the product of an absorption refrigeration system is flowing water, the need to build a low temperature refrigeration system is not necessary. The advantage of a water-ammonia absorption system which can work far below 0°C is not applicable. Lithium bromide-water ARS and water-ammonia ARS have different refrigeration markets, determined by the temperature of the refrigeration demand.

Non condensable gas content that comes with the geothermal fluid controls how low the condenser pressure can go even though the gas extraction equipment generally can handle this problem. However, the very low condenser pressure and large amount of gas that must be handled limit the gas extraction size and performance. Steam quality at the outlet of the turbine also has to be considered since any effort in lowering the condenser pressure can make the steam quality decrease. Of course this condition is well coped with by creating a superheated steam at the inlet of the turbine so the isentropic line is shifted to the higher steam quality.

An integrated power and absorption system still cannot fulfil today's feasibility requirements. A power plant cooling system needs a high-cooling rate, meaning that the evaporator has to lower the cooling water temperature very quickly. Such a cooling rate requires a large refrigeration capacity and makes the total investment cost skyrocket. Return time for the investment cost is more than the normal life expectancy for a geothermal power plant which is generally in the range of 20-25 years. The development of absorption technology in the future, especially the technology to reduce investment costs and increase the performance of the working fluid could change this paradigm and provide a good market for an integrated power and absorption system. The possibilities of a higher power price and lower steel price in the future more or less should give a positive contribution to the development of this integrated power and refrigeration system.

7. RECOMMENDATION FOR FUTURE WORK

Adding more variables into the optimization process is one possibility in order to achieve a higher system performance. Well head and separation pressure was set to be constant during the simulation. By changing these two parameters, especially if different mass flow is applied, the system performance can be further optimized.

An advance absorption refrigeration cost analysis can be considered to reduce the total investment cost. As brought in this report, the total investment cost was calculated as if the absorption machine was built on a new site. Some of cost components can be neglected i.e. civil, structural and architectural work, if the absorption machine is going to be built on an existing plant site. Comparing the price of electricity for different places also can give different perspectives on the feasibility since different places have different electricity price as well as a different approach on cost estimating gives different feasibility.

The idea of replacing the cooling tower with the absorption refrigeration system needs to be analyzed more in order to make it feasible for application. In a stand-alone ARS system without the help of a cooling tower, the ARS operates at higher refrigeration capacity because it also has to cool down extra cooling water for self cooling purposes.

An overview of system performance based on exergetic efficiency also can be analysed, which measures the potential work and final work output relative to environmental condition. Putting a thermo-economic optimization on both power and refrigeration system can be considered as a good step for the future work.

As the simulation deals with more variables and to achieve an easy and convenient way for doing the optimization, selecting the correct tool is important. Re-writing the code in Matlab as the basic engine and Refprop as the thermodynamic database can be a good choice for running the optimization in the future.

REFERENCES

- ASHRAE, 2005: *ASHRAE handbook: Fundamental*. ASHRAE, Atlanta.
- Bejan, A., Tsatsaronis, G., and Moran, M., 1996: *Thermal design and optimization*. Wiley, New Jersey, 560 pp.
- DiPippo, R., 2008: *Geothermal power plants: Principles, applications, case studies, and environmental impact* (2nd ed.). Butterworth-Heinemann. Elsevier, Oxford, 517 pp.
- Elliot, T.C., Chen, K., and Swanekamp, R.C., 1997: *Standard handbook of powerplant engineering* (2nd edition). Mc Graw-Hill, New York, 1248 pp.
- F-Chart Software, 2008: *Engineering Equation Solver*. F-Chart Software internet website, <http://www.fchart.com/ees/ees.shtml>.
- Florides, G.A., Kalogirou, S.A., Tassou, S.A., and Wrobel, L.C., 2003: Design and construction of a LiBr-water absorption machine. *Energy conversion management*, 44, 2483-2508.
- Gordon, J.M., and Kim Choon Ng, 2000: *Cool thermodynamic*. Cambridge International Science Publishing, Cambridge, 260 pp.
- Gunther, R.C., 1957: *Refrigeration, air conditioning and cold storage* (2nd edition). Chilton Company, Philadelphia, 1232 pp.
- Gupta, H., and Roy, S., 2006: *Geothermal energy: An alternative resource for the 21st century*. Elsevier Scientific Publishing Company, Amsterdam, 279 pp.
- Herold, K.E., Radermacher, R., and Klein, S.A., 1996: *Absorption chillers and heat pumps*. CRC Press Inc., Boca Raton, 329 pp.
- Kim, D.S., 2007: *Solar absorption cooling*. Dissertation, Delft University of Technology.
- Matche, 2009: *Matches' process equipment cost estimates*. Matche's Home Page: <http://www.matche.com/EquipCost/index.htm>
- Miliaras, E.S., 1974: *Power plants with air-cooled condensing systems*. MIT Press, Cambridge, Massachusetts, 237 pp.
- Quoilin, S., 2007: *Experimental study and modelling of a low temperature rankine cycle for small scale cogeneration*. University of Liege, Dissertation, 129 pp.
- Sun, Da-Wen, 2006: An overview of refrigeration cycles. In: Sun, Da-Wen., *Handbook of frozen food processing and packaging*. CRC Press, Boca Raton, 57-81.

APPENDIX A: Aqueous lithium bromide solubility

Table of solubility of pure LiBr in water
(Herold et al., 1996)

Temperature [°C]	Solubility [X in %]	Temperature [°C]	Solubility [X in %]
-53.60	45.20	24.29	60.63
-49.32	48.03	33.14	62.50
-42.12	49.63	38.26	63.96
-36.32	50.09	44.27	65.17
-32.96	50.50	50.35	65.82
-29.17	51.20	57.58	66.16
-25.24	51.70	63.42	66.55
-16.11	51.95	70.90	67.37
-13.47	53.70	71.69	67.39
-8.94	54.75	82.68	68.32
-4.54	55.92	83.11	68.27
1.11	56.81	91.36	68.99
5.10	57.22	91.82	69.05
9.93	58.08	101.05	70.04
19.99	58.67	102.02	70.08

Dong-Seon Kim (Kim, 2007) did a polynomial fit for this solubility table and groups it in four regions. Region IV, the formula seems to be miss-typed thus separated polynomial fit was done replacing Kim's original formula.

Region I, $X_w < 48.5\%$

$$T = -398.3 + 25.107X_w - 0.253X_w^2$$

Region II, $48.5 < X_w < 57.2\%$

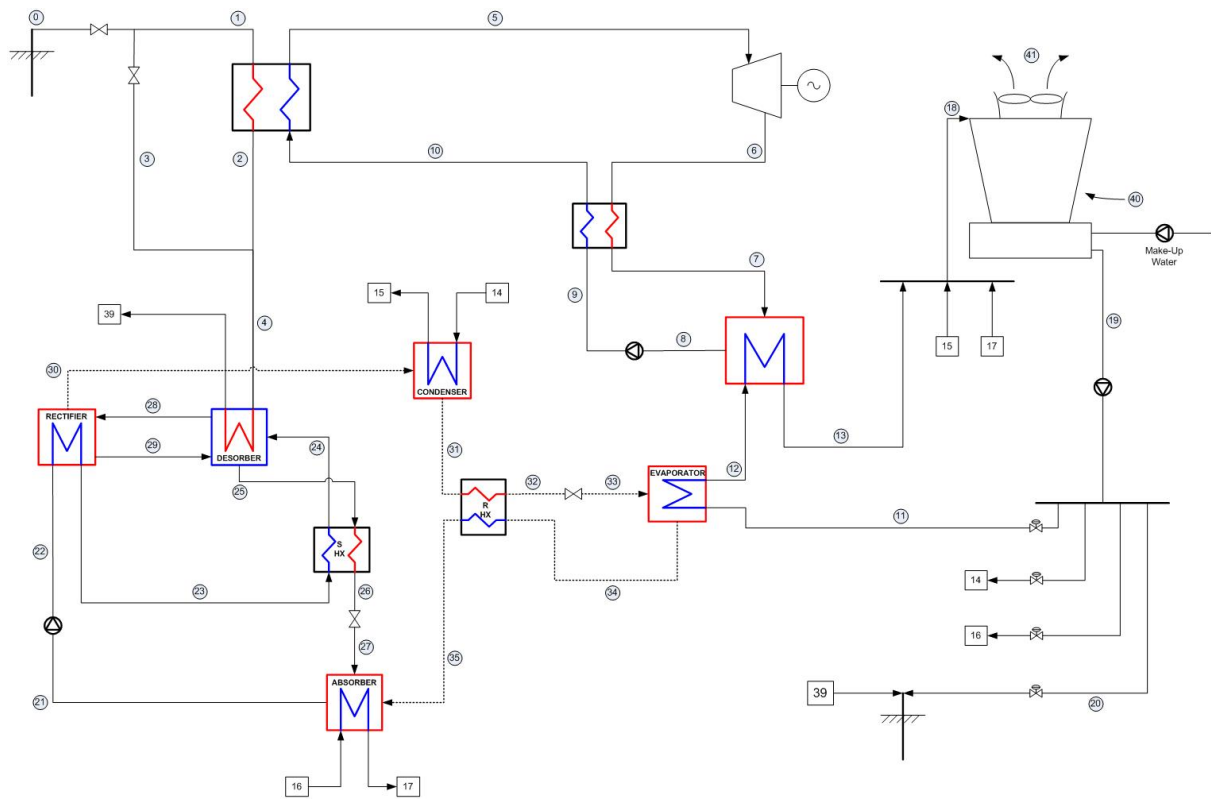
$$T = -919.4 + 38.51957477X_w - 0.3080928653X_w^2$$

Region III, $57.2 < X_w < 65.5\%$

$$T = -1159.4 + 42.7386184X_w - 0.308288545X_w^2$$

Region IV, $X_w > 65.5\%$

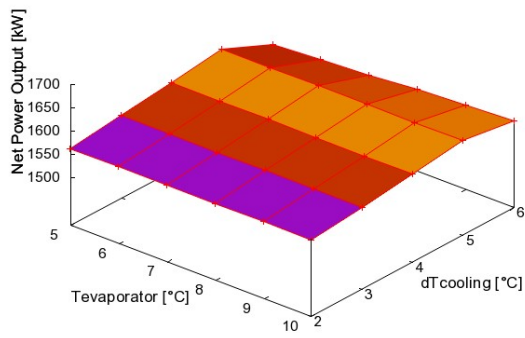
$$T = -2046.536869 + 58.34181996X_w - 0.3391180069X_w^2 \text{ (Re-calculated version)}$$



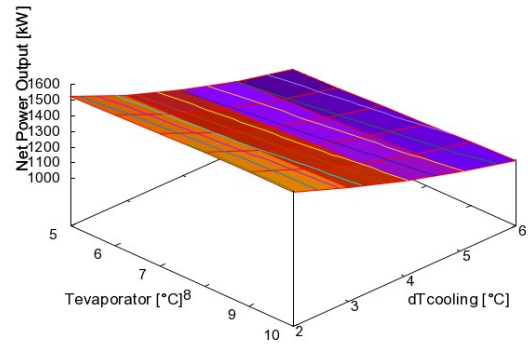
Organic Rankine cycle geothermal power plant with single effect water-ammonia ARS

APPENDIX C: Simulation results

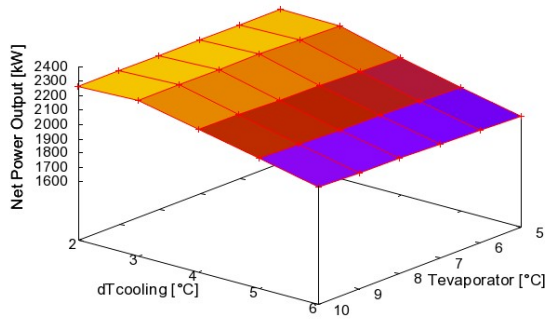
SF-LiBr Net Power Output- Full Resource



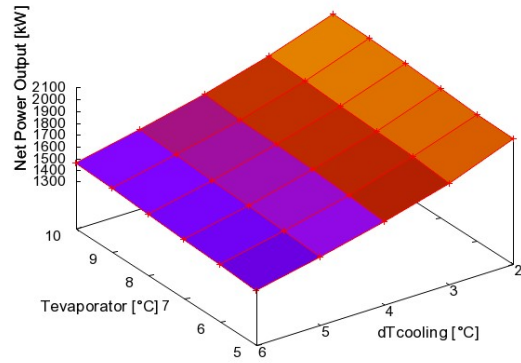
SF-NH3 Net Power Output- Full Resource



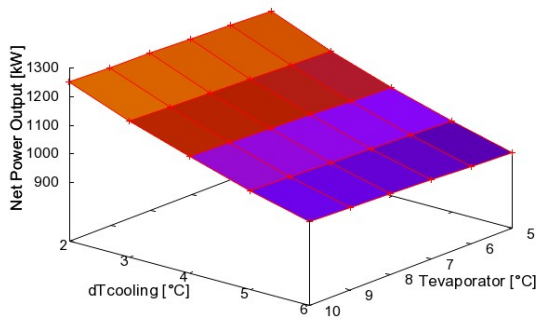
DF-LiBr Net Power Output- Full Resource



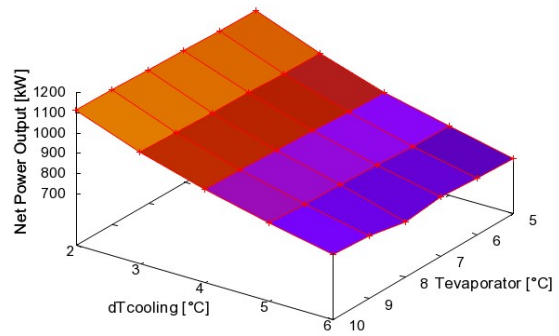
DF-NH3 Net Power Output- Full Resource



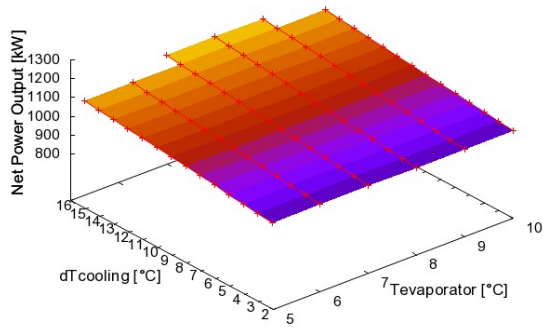
ORC-LiBr Net Power Output- Full Resource



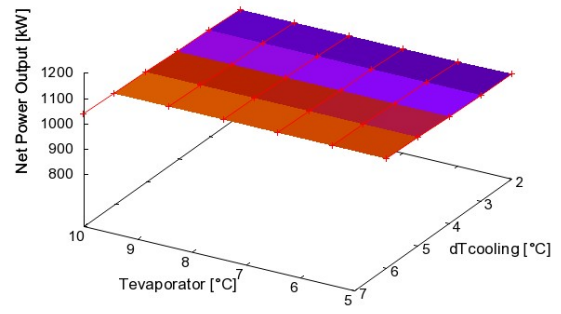
ORC-NH3 Net Power Output- Full Resource



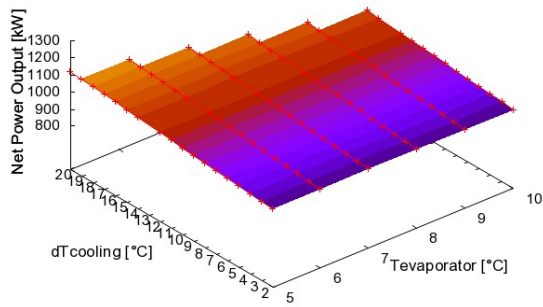
SF-LiBr Net Power Output- 1MW



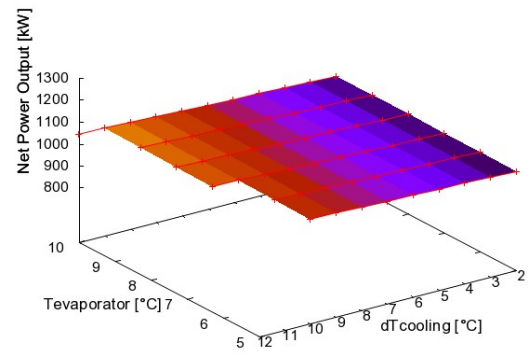
SF-NH3 Net Power Output- 1MW



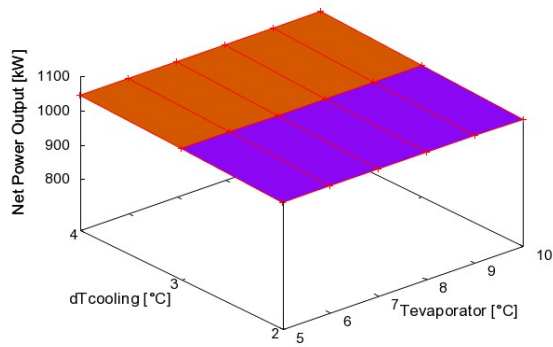
DF-LiBr Net Power Output- 1MW



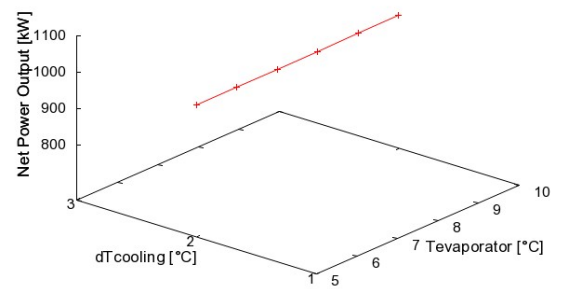
DF-NH3 Net Power Output- 1MW



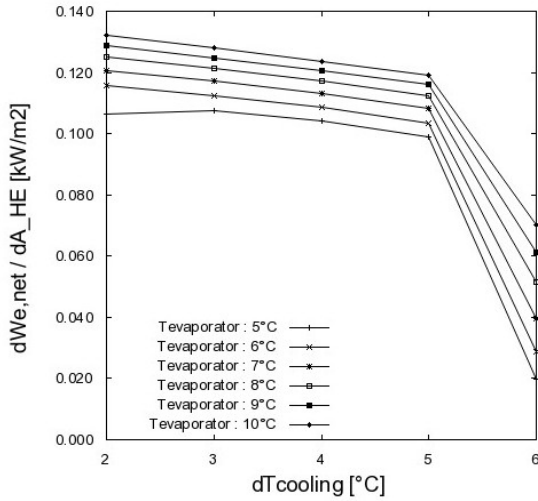
ORC-LiBr Net Power Output- 1MW



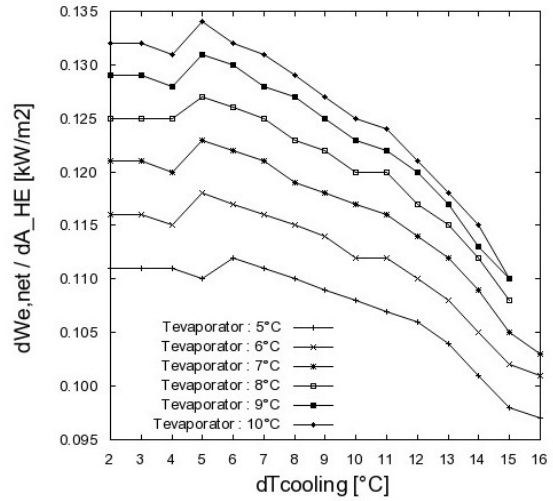
ORC-NH3 Net Power Output- 1MW



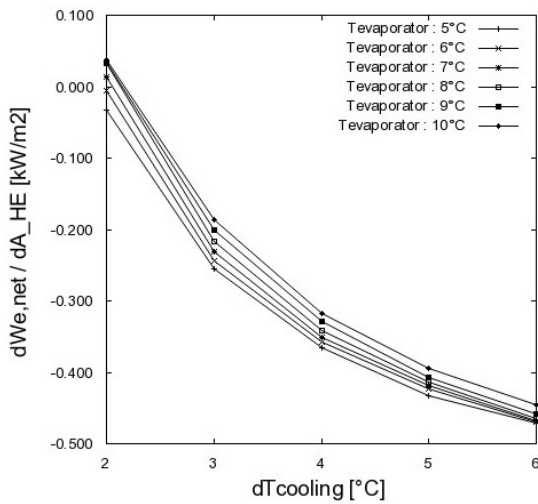
Power-Area Ratio for SF-LiBr - Full Resource



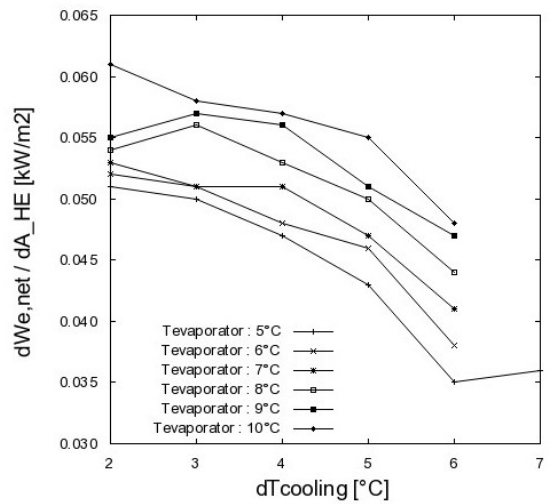
Power-Area Ratio for SF-LiBr - 1MW



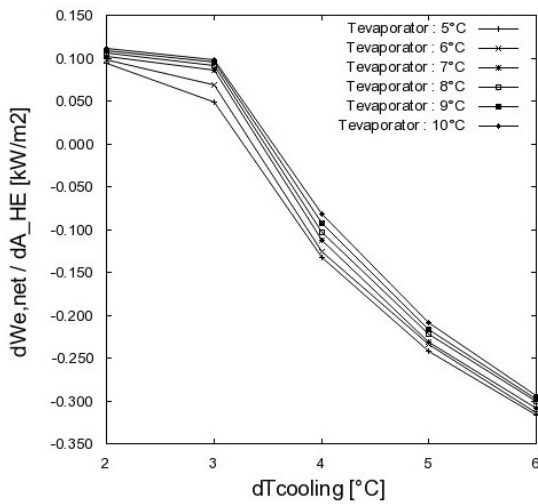
Power-Area Ratio for SF-NH3 - Full Resource



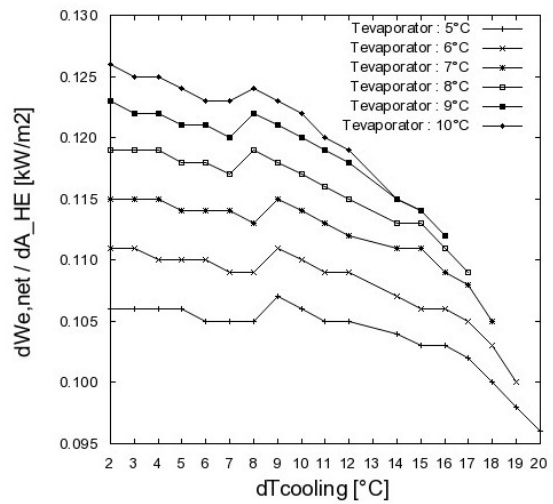
Power-Area Ratio for SF-NH3 - 1MW



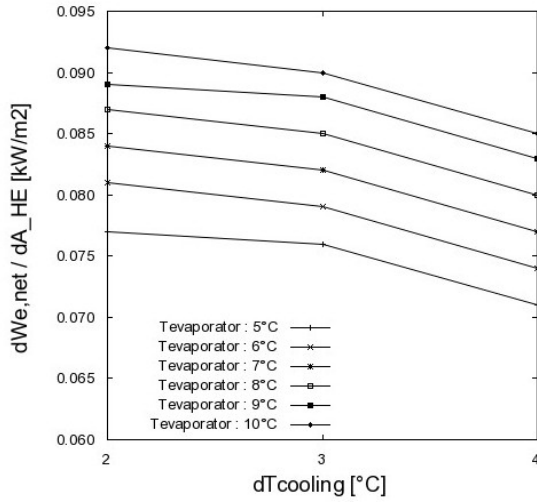
Power-Area Ratio for DF-LiBr - Full Resource



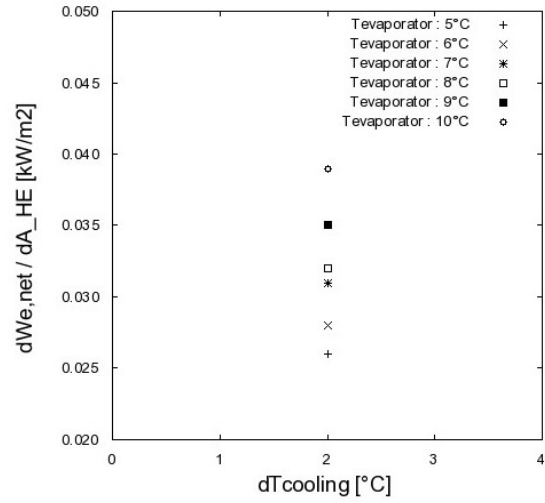
Power-Area Ratio for DF-LiBr - 1MW



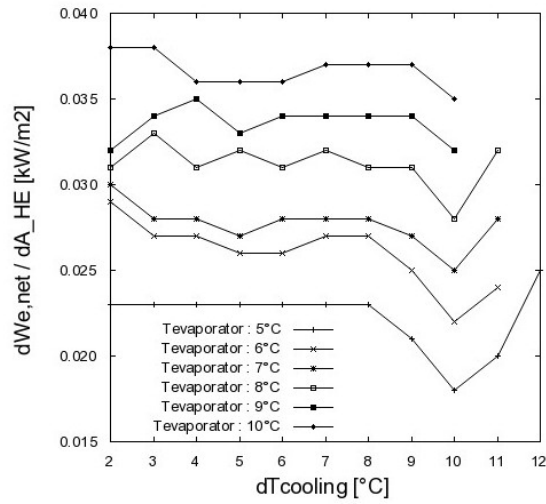
Power-Area Ratio for ORC-LiBr - 1MW



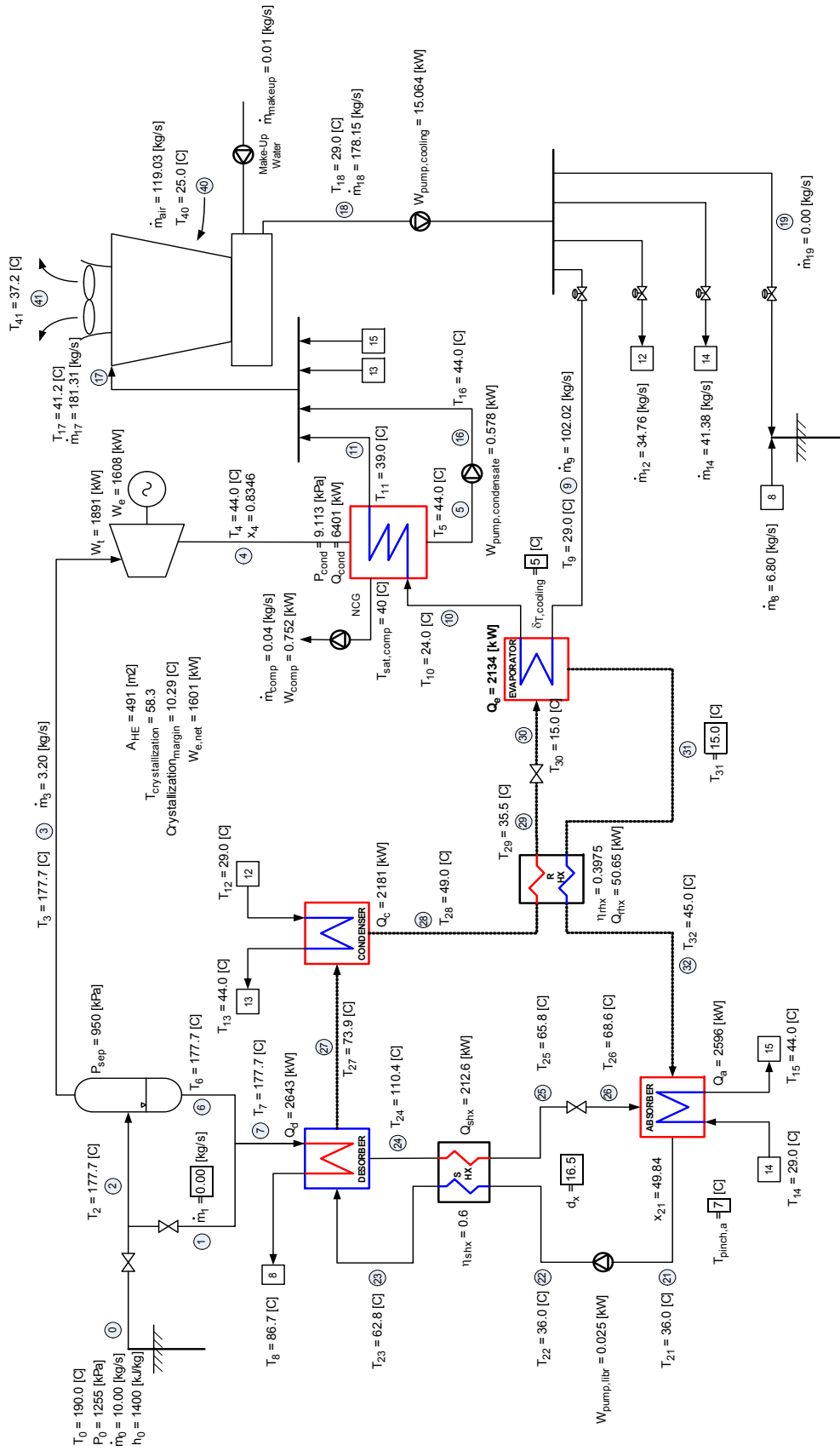
Power-Area Ratio for ORC-NH3 - 1MW



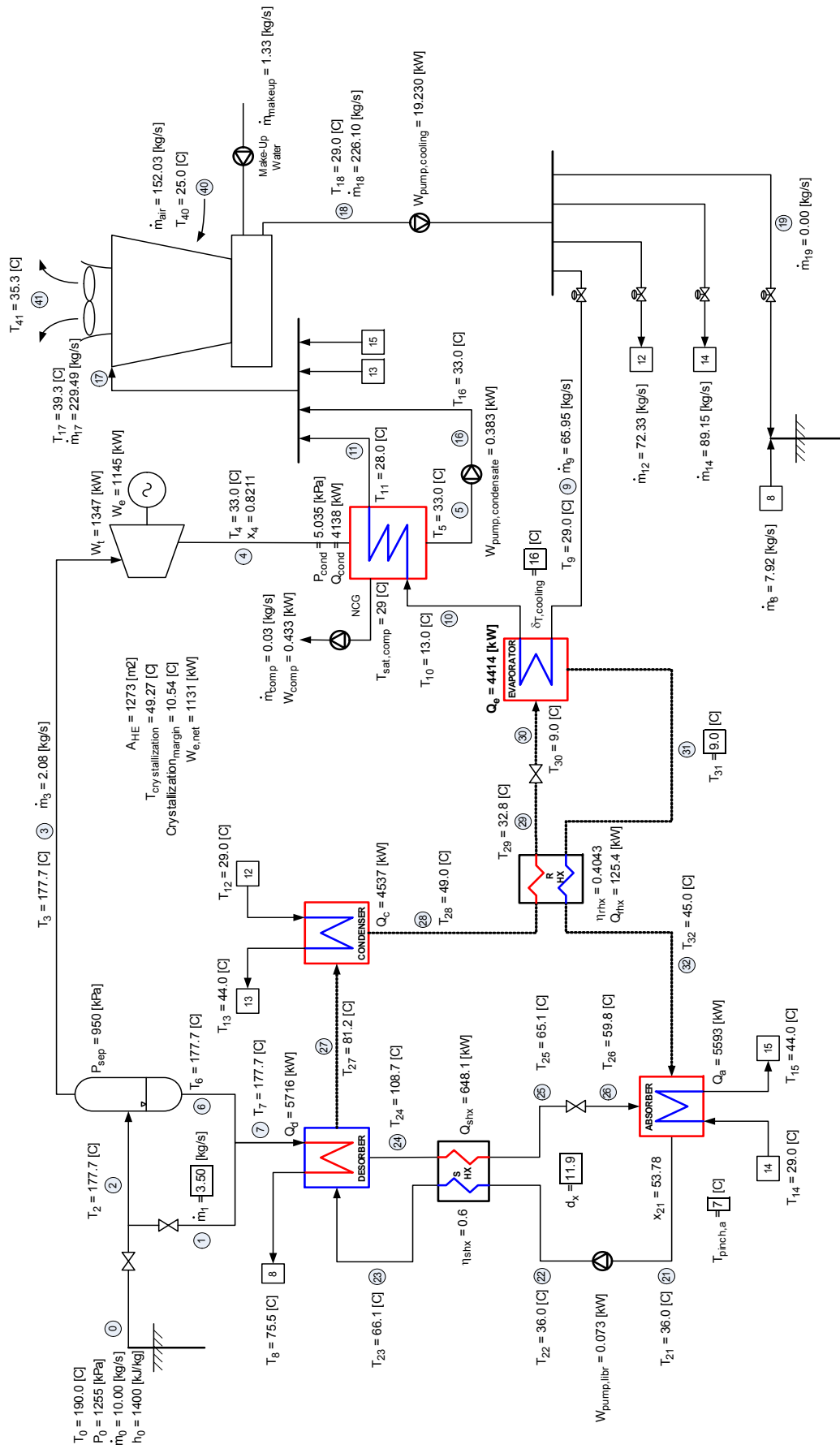
Power-Area Ratio for DF-NH3 - 1MW



APPENDIX D: Optimum design parameters



Single flash and lithium bromide ARS diagram – Full Resource Scenario



Single flash and lithium bromide ARS diagram – 1 MW scenario

Parameters for integrated single flash-lithium bromide system – Full resource

Nr.	h[i] [kJ/kg]	m_dot[i] [kg/s]	P[i] [kPa]	T[i] [C]	x[i]
0	1400	10	1255	190	
1	1400	0	950	177.7	
2	1400	10	950	177.7	0.32
3	2775	3.2	950	177.7	1
4	2184	3.2	9.113	44	0.8346
5	184.3	3.16	9.113	44	0
6	752.7	6.8	950	177.7	0
7	752.7	6.8	950	177.7	
8	364	6.8	950	86.7	
9	121.6	102.02	141.3	29	
10	100.7	102.02	141.3	24	
11	163.4	102.02	141.3	39	
12	121.6	34.76	141.3	29	
13	184.3	34.76	141.3	44	
14	121.6	41.38	141.3	29	
15	184.3	41.38	141.3	44	
16	184.4	3.16	181.3	44	
17	172.6	181.31	181.3	41.2	
18	121.6	178.15	101.3	29	
19		0			
20					
21	73.02	3.61	1.706	36	49.84
22	73.02	3.61	11.75	36	49.84
23	132	3.61	11.75	62.8	49.84
24	278.4	2.71	11.75	110.4	66.34
25	199.9	2.71	11.75	65.8	66.34
26	199.9	2.71	1.706	68.6	66.34
27	2637	0.9	11.75	73.9	100
28	205.2	0.9	11.75	49	0
29	148.7	0.9	11.75	35.5	0
30	148.7	0.9	1.706	15	0.03476
31	2528	0.9	1.706	15	1
32	2585	0.9	1.706	45	100
33					
34					
35					
36					
37					
38					
39					
40	63.23		101.3	25	
41	144.2		101.3	37.2	

Parameters for integrated single flash-lithium bromide system – 1 MW

Nr.	h[i] [kJ/kg]	m_dot[i] [kg/s]	P[i] [kPa]	T[i] [C]	x[i]
0	1400	10	1255	190	
1	1400	3.5	950	177.7	
2	1400	6.5	950	177.7	0.32
3	2775	2.08	950	177.7	1
4	2128	2.08	5.035	33	0.8211
5	138.3	2.05	5.035	33	0
6	752.7	4.42	950	177.7	0
7	1039	7.92	950	177.7	
8	317	7.92	950	75.5	
9	121.6	65.95	141.3	29	
10	54.68	65.95	141.3	13	
11	117.4	65.95	141.3	28	
12	121.6	72.33	141.3	29	
13	184.3	72.33	141.3	44	
14	121.6	89.15	141.3	29	
15	184.3	89.15	141.3	44	
16	138.5	2.05	181.3	33	
17	164.7	229.49	181.3	39.3	
18	121.6	226.1	101.3	29	
19		0			
20					
21	81.43	10.24	1.148	36	53.78
22	81.43	10.24	11.75	36	53.78
23	144.7	10.24	11.75	66.1	53.78
24	272	8.38	11.75	108.7	65.68
25	194.7	8.38	11.75	65.1	65.68
26	194.7	8.38	1.148	59.8	65.68
27	2651	1.85	11.75	81.2	100
28	205.2	1.85	11.75	49	0
29	137.6	1.85	11.75	32.8	0
30	137.6	1.85	1.148	9	0.04022
31	2517	1.85	1.148	9	1
32	2585	1.85	1.148	45	100
33					
34					
35					
36					
37					
38					
39					
40	63.23		101.3	25	
41	131		101.3	35.3	

APPENDIX E: EES source code

1. Single flash geothermal power plant with single effect lithium bromide-water ARS

\$UnitSystem SI MASS DEG KPA C KJ

Procedure crystallization(X_strong, P_low: T_crit, T_margin)

if (X_strong < 48.5) then

T_crit_K := -398.3 + 25.107 * X_strong - 0.253 * X_strong^2

else

if (X_strong >= 48.5) and (X_strong < 57.2) then

T_crit_K := -919.4 + 38.51957477 * X_strong - 0.3080928653 * X_strong^2

else

if (X_strong >= 57.2) and (X_strong < 65.5) then

T_crit_K := -1159.4 + 42.7386184 * X_strong - 0.308288545 * X_strong^2

else

if (X_strong >= 65.5) then

T_crit_K := -2046.536869 + 58.34181996 * X_strong - 0.3391180069 * X_strong^2

endif

endif

endif

endif

T_crit := ConvertTemp('K', 'C', T_crit_K)

T_real := T_LIBR('SI', P_low, x_strong)

T_margin := T_real - T_crit

If (T_margin < 10) then

Call Error('Crystallization margin is less than 10C. Lower your d_x input value')

Else

Endif

end

Procedure makeupwater(m_dot_CT_in, m_dot_CT_out, m_dot_condensate: m_dot_makeup)

if (m_dot_CT_out < (m_dot_CT_in - m_dot_condensate)) then

m_dot_makeup := m_dot_CT_in - m_dot_CT_out - m_dot_condensate

else

m_dot_makeup := 0

endif

end

=====
POWER GENERATION
=====

"Heat Source Information"

T[0] = 190 [C]

m_dot[0] = 10 [kg/s]

P[0] = pressure(steam_IAPWS, h=h[0], T=T[0])

h[0] = 1400 [kJ/kg]

s[0] = entropy(steam_IAPWS, P=P[0], h=h[0])

"Separator"

P_sep = 950 [kPa]

P[1] = P_sep

P[2] = P_sep

P[3] = P_sep

P[6] = P_sep

```

x[2] = (h[2] - h[6]) / (h[3] - h[6])
x[3] = 1
x[6] = 0
m_dot[0] = m_dot[1] + m_dot[2]
m_dot[3] = x[2] * m_dot[2]
m_dot[6] = (1 - x[2]) * m_dot[2]
h[1] = h[0]
h[2] = h[0]
h[3] = enthalpy(steam_IAPWS, P=P[3], x=x[3])
h[6] = enthalpy(steam_IAPWS, P=P[6], x=x[6])
s[1] = entropy(steam_IAPWS, P=P[1], h=h[1])
s[2] = entropy(steam_IAPWS, P=P[2], x=x[2])
s[3] = entropy(steam_IAPWS, P=P[3], h=h[3])
s[6] = entropy(steam_IAPWS, P=P[6], x=x[6])
T[1] = temperature(steam_IAPWS, P=P[1], h=h[1])
T[2] = temperature(steam_IAPWS, P=P[2], h=h[2])
T[3] = temperature(steam_IAPWS, P=P[3], h=h[3])
T[6] = temperature(steam_IAPWS, P=P[6], h=h[6])

```

"Turbine"

```

eta_g = 0.85
eta_t = 0.85
W_t = m_dot[3] * (h[3] - h[4])
W_e = eta_g * W_t

```

"Condenser"

```

delta_T_cond = 20 [C]
TTD = 5 [C]
T_cond = T[10] + delta_T_cond
P_cond = pressure(steam_IAPWS, T=T_cond, x=1)
P[4] = P_cond
P[5] = P_cond
x[4] = quality(steam_IAPWS, P=P[4], h=h[4])
x[5] = 0
s[4] = entropy(steam_IAPWS, P=P[4], h=h[4])
h_4_s = enthalpy(steam_IAPWS, P=P[4], s=s[3])
h[4] = h[3] - eta_t * (h[3] - h_4_s)
h[5] = enthalpy(steam_IAPWS, P=P[5], x=x[5])
T[4] = temperature(steam_IAPWS, h=h[4], s=s[4])
T[5] = temperature(steam_IAPWS, P=P[5], x=x[5])
m_dot[4] = m_dot[3]
m_dot[5] = m_dot[4] - m_dot_comp
Q_cond = m_dot[4] * (h[4] - h[5])

```

```

T[11] = T_cond - TTD
h[11] = enthalpy(water, T=T[11], P=P[11])
m_dot[4] * (h[4] - h[5]) = m_dot[10] * (h[11] - h[10])
m_dot[11] = m_dot[10]
P[11] = P[10]

```

"NCG"

```

eta_comp = 0.85
T_sat_comp = T_cond - 4 [C]
P_sat_comp = pressure(steam_IAPWS, T=T_sat_comp, x=1)
MM_steam = molarmass(steam_IAPWS)
MM_NCG = molarmass(CO2)

```



```

m_dot_NCG = 0.15 / 100 * m_dot[2]
m_dot_steam = (MM_steam * P_sat_comp) / (MM_NCG * (P_cond - P_sat_comp)) * m_dot_NCG
m_dot_comp = m_dot_NCG + m_dot_steam
c_p_steam = cp(steam, T=T_sat_comp, P=P_sat_comp)
c_p_NCG = cp(CO2, T=T_sat_comp)
c_p = c_p_NCG + (c_p_steam - c_p_NCG) * (P_sat_comp * MM_steam) / (P_cond * (MM_NCG + MM_steam))
c_v_steam = cv(steam, T=T_sat_comp, P=P_sat_comp)
c_v_NCG = cv(CO2, T=T_sat_comp)
R_steam = c_p_steam - c_v_steam
R_NCG = c_p_NCG - c_v_NCG
R = R_NCG + (R_steam - R_NCG) * (P_sat_comp * MM_steam) / (P_cond * (MM_NCG + MM_steam))
delta_h_comp = c_p * T_sat_comp * ((P_env/P_cond)^(R/c_p) - 1)
W_comp = (m_dot_comp * delta_h_comp) / eta_comp

```

"Condenser Plot"

```

T_plot_cond_hot[0] = T[5]
T_plot_cond_hot[1] = T[4]
T_plot_cond_cool[0] = T[10]
T_plot_cond_cool[1] = T[11]
Q_plot_cond[0] = 0
Q_plot_cond[1] = Q_cond

```

"Cooling Tower"

```

T_env = 25 [C]
P_env = 101.3 [kPa]
P_CT_low = P_env {P environment}
P_CT_mid = P_env + 40 [kPa] {P environment +
losses from outlet CT to ARS machine}
P_CT_high = P_env + 80 [kPa] {Total losses from
outlet CT to the top of CT inlet}

```

```

P[16] = P_CT_high
P[17] = P_CT_high
P[18] = P_CT_low
m_dot[16] = m_dot[5]
m_dot[17] = m_dot[11] + m_dot[13] + m_dot[15] + m_dot[16]
V[5] = Volume(Water, T=T[5], P=P[5])
W_pump_condensate = (m_dot[5] * V[5] * (P[16] - P[5])) / eta_pump
m_dot[5] * h[5] + W_pump_condensate = m_dot[16] * h[16]
T[16] = temperature(water, h=h[16], P=P[16])
m_dot[17] * h[17] = m_dot[11] * h[11] + m_dot[13] * h[13] + m_dot[15] * h[15] + m_dot[16] * h[16]
T[17] = temperature(water, h=h[17], P=P[17])
T[18] = T_env + 4 [C]
h[18] = enthalpy(water, T=T[18], P=P[18])

```

```

P[40] = P_env
P[41] = P_env
T[40] = T_env
T[41] = T[17] - 4 [C]
RH[40] = 0.75
RH[41] = 1
omega[40] = HumRat(AirH2O, T=T[40], r=RH[40], P=P[40])
omega[41] = HumRat(AirH2O, T=T[41], r=RH[41], P=P[41])
h[40] = enthalpy(AirH2O, T=T[40], r=RH[40], P=P[40])

```

```

h[41] = enthalpy(AirH2O, T=T[41], r=RH[41], P=P[41])
m_dot[17] + m_dot_air * omega[40] = m_dot[18] + m_dot_air * omega[41]
m_dot[17] * h[17] + m_dot_air * h[40] = m_dot[18] * h[18] + m_dot_air * h[41]

```

```

V[18] = Volume(Water, T=T[18], P=P[18])
W_pump_cooling = ((m_dot[18] + m_dot_makeup) * V[18] * (P_CT_high - P[18])) / eta_pump

```

```

m_dot[18] + m_dot_makeup = m_dot[9] + m_dot[12] + m_dot[14] + m_dot[19]

```

"Make Up Water"

```

Call makeupwater(m_dot[17], m_dot[18], m_dot[5]: m_dot_makeup)

```

```

=====
                        CHILLER
=====

```

\$IfNot DiagramWindow

```

d_x = 10
T_pinch_a = 9 [C]
T[31] = 10 [C]
m_dot[1] = 4.58 [kg/s]
delta_T_cooling = 5 [C]
$EndIf

```

"Absorber"

```

P[21] = P[31]
P[26] = P[31]
x[21] = X_LIBR('SI', T[21], P[21])
x[26] = x[24]
m_dot[21] = m_dot[26] + m_dot[32]
m_dot[21] * x[21] = m_dot[26] * x[26]
T[21] = T[14] + T_pinch_a
h[21] = H_LIBR('SI', T[21], x[21])
h[26] = h[25]
P[26] = P_LIBR('SI', T[26], x[26])
Q_a = m_dot[32] * h[32] + m_dot[26] * h[26] - m_dot[21] * h[21]
Q_a = m_dot[14] * (h[15] - h[14])

```

"Gain m14"

```

P[14] = P_CT_mid
P[15] = P[14]
T[14] = T[18]
T[15] = T[14] + 15 [C]
h[14] = enthalpy(water, T=T[14], P=P[14])
h[15] = enthalpy(water, T=T[15], P=P[15])
m_dot[15] = m_dot[14]

```

```

LMTD_a = ((T[26] - T[15]) - (T[21] - T[14])) / (ln((T[26] - T[15]) / (T[21] - T[14])))
U_a = 0.85 [kW/m2-C]
Q_a = U_a * A_a * LMTD_a

```

"Pump"

```

eta_pump = 0.95
P[22] = P[28]
x[22] = x[21]
m_dot[22] = m_dot[21]

```

$V[21] = V_LIBR('SI', T[21], x[21]) * \text{convert}(\text{cm}^3/\text{g}, \text{m}^3/\text{kg})$
 $W_pump_libr = (m_dot[21] * V[21] * (P[22] - P[21])) / \eta_{pump}$
 $m_dot[21] * h[21] + W_pump_libr = m_dot[22] * h[22]$
 $h[22] = H_LIBR('SI', T[22], x[22])$

"Gain h22"

"Solution Heat Exchanger"

$P[23] = P[28]$
 $P[25] = P[28]$
 $x[25] = x[24]$
 $x[23] = x[21]$
 $m_dot[23] = m_dot[21]$
 $m_dot[25] = m_dot[26]$
 $\eta_{shx} = 0.6$
 $T[25] = T[22] * \eta_{shx} + (1 - \eta_{shx}) * T[24]$
 $h[25] = H_LIBR('SI', T[25], x[25])$
 $Q_{shx} = m_dot[22] * (h[23] - h[22])$
 $Q_{shx} = m_dot[24] * (h[24] - h[25])$
 $h[23] = H_LIBR('SI', T[23], x[23])$
 $LMTD_{shx} = ((T[24] - T[23]) - (T[25] - T[22])) / (\ln((T[24] - T[23]) / (T[25] - T[22])))$
 $U_{shx} = 1.1 \text{ [kW/m}^2\text{-C]}$
 $Q_{shx} = U_{shx} * A_{shx} * LMTD_{shx}$

"Gain h23"

"Desorber"

$x[24] = x[21] + d_x$
 $x[27] = \text{quality}(\text{steam_IAPWS}, T=T[27], h=h[27])$
 $P[24] = P[28]$
 $P[27] = P[28]$
 $T[24] = T_LIBR('SI', P[24], x[24])$
 $T_g = T_LIBR('SI', P[23], x[23])$
 $T[27] = T_g$
 $h[24] = H_LIBR('SI', T[24], x[24])$
 $h[27] = \text{enthalpy}(\text{steam_IAPWS}, T=T[27], P=P[27])$
 $m_dot[27] = m_dot[31]$
 $m_dot[24] = m_dot[26]$
 $Q_d = m_dot[27] * h[27] + m_dot[24] * h[24] - m_dot[23] * h[23]$
 $Q_d = m_dot[7] * (h[7] - h[8])$

"Gain h8"

$P[7] = P_sep$
 $P[8] = P[7]$
 $T[7] = \text{temperature}(\text{steam_IAPWS}, P=P[7], h=h[7])$
 $T[8] = \text{temperature}(\text{steam_IAPWS}, P=P[8], h=h[8])$
 $m_dot[7] = m_dot[1] + m_dot[6]$
 $m_dot[7] * h[7] = m_dot[1] * h[1] + m_dot[6] * h[6]$
 $m_dot[8] = m_dot[7]$

$LMTD_d = ((T[7] - T[24]) - (T[8] - T[23])) / (\ln((T[7] - T[24]) / (T[8] - T[23])))$
 $U_d = 0.85 \text{ [kW/m}^2\text{-C]}$
 $Q_d = U_d * A_d * LMTD_d$

"Condenser"

$x[28] = 0$
 $T[28] = T[12] + 20 \text{ [C]}$
 $P[28] = \text{Pressure}(\text{steam_IAPWS}, T=T[28], x=x[28])$
 $h[28] = \text{enthalpy}(\text{steam_IAPWS}, P=P[28], x=x[28])$
 $m_dot[28] = m_dot[31]$
 $Q_c = m_dot[27] * (h[27] - h[28])$

$$Q_c = m_{\text{dot}}[12] * (h[13] - h[12])$$

"Gain m12"

$$P[12] = P_{\text{CT_mid}}$$

$$P[13] = P[12]$$

$$T[12] = T[18]$$

$$T[13] = T[12] + 15 \text{ [C]}$$

$$h[12] = \text{enthalpy}(\text{water}, T=T[12], P=P[12])$$

$$h[13] = \text{enthalpy}(\text{water}, T=T[13], P=P[13])$$

$$m_{\text{dot}}[13] = m_{\text{dot}}[12]$$

$$\text{LMTD}_c = ((T[27] - T[13]) - (T[28] - T[12])) / (\ln((T[27] - T[13]) / (T[28] - T[12])))$$

$$U_c = 1.4 \text{ [kW/m}^2\text{-C]}$$

$$Q_c = U_c * A_c * \text{LMTD}_c$$

"Refrigerant Heat Exchanger"

$$\text{eta}_{\text{rhx}} = (T[28] - T[29]) / (T[28] - T[31])$$

$$P[29] = P[28]$$

$$P[32] = P[31]$$

$$m_{\text{dot}}[29] = m_{\text{dot}}[31]$$

$$m_{\text{dot}}[32] = m_{\text{dot}}[31]$$

$$x[29] = \text{quality}(\text{steam_IAPWS}, T=T[29], h=h[29])$$

$$x[32] = \text{quality}(\text{steam_IAPWS}, T=T[32], h=h[32])$$

$$T[32] = T[28] - 4 \text{ [C]}$$

$$h[32] = \text{enthalpy}(\text{steam_IAPWS}, T=T[32], P=P[32])$$

$$m_{\text{dot}}[31] * h[31] + m_{\text{dot}}[28] * h[28] = m_{\text{dot}}[29] * h[29] + m_{\text{dot}}[32] * h[32] \quad \text{"Gain h29"}$$

$$T[29] = \text{temperature}(\text{steam_IAPWS}, h=h[29], P=P[29])$$

$$Q_{\text{rhx}} = m_{\text{dot}}[28] * (h[28] - h[29])$$

$$\text{LMTD}_{\text{rhx}} = ((T[28] - T[32]) - (T[29] - T[31])) / (\ln((T[28] - T[32]) / (T[29] - T[31])))$$

$$U_{\text{rhx}} = 1.1 \text{ [kW/m}^2\text{-C]}$$

$$Q_{\text{rhx}} = U_{\text{rhx}} * A_{\text{rhx}} * \text{LMTD}_{\text{rhx}}$$

"Evaporator"

$$x[30] = \text{quality}(\text{steam_IAPWS}, T=T[30], h=h[30])$$

$$x[31] = 1$$

$$P[31] = \text{pressure}(\text{steam_IAPWS}, T=T[31], x=x[31])$$

$$P[30] = P[31]$$

$$h[31] = \text{enthalpy}(\text{steam_IAPWS}, T=T[31], x=x[31])$$

$$h[30] = h[29]$$

$$Q_e = m_{\text{dot}}[31] * (h[31] - h[30])$$

$$m_{\text{dot}}[30] = m_{\text{dot}}[31]$$

$$T[30] = \text{temperature}(\text{steam_IAPWS}, P=P[30], h=h[30])$$

$$Q_e = m_{\text{dot}}[9] * (h[9] - h[10])$$

"Gain m9"

$$P[9] = P_{\text{CT_mid}}$$

$$P[10] = P[9]$$

$$T[9] = T[18]$$

$$T[10] = T[9] - \text{delta}_T_{\text{cooling}}$$

$$h[9] = \text{enthalpy}(\text{water}, T=T[9], P=P[9])$$

$$h[10] = \text{enthalpy}(\text{water}, T=T[10], P=P[10])$$

$$m_{\text{dot}}[9] = m_{\text{dot}}[10]$$

$$\text{LMTD}_e = ((T[9] - T[31]) - (T[10] - T[30])) / (\ln((T[9] - T[31]) / (T[10] - T[30])))$$

$$U_e = 1.5 \text{ [kW/m}^2\text{-C]}$$

$$Q_e = U_e * A_e * \text{LMTD}_e$$

Call crystallization(x[26], P[26]: T_crystallization, Crystallization_margin)

$A_{HE} = A_a + A_{shx} + A_d + A_c + A_{rhx} + A_e$

$COP_{chiller} = Q_e / (Q_d + W_{pump_libr})$

$Q_{in} = m_{dot}[2] * h[2]$

$\eta_{plant_thermal} = W_e / Q_{in}$

$h_{env} = \text{enthalpy}(\text{steam_IAPWS}, P=P_{env}, T=T_{env})$

$s_{env} = \text{entropy}(\text{steam_IAPWS}, P=P_{env}, T=T_{env})$

$EX = h[0] - h_{env} - T_{env} * (s[0] - s_{env})$

$\eta_{plant_EX} = W_e / EX$

$W_{e_net} = W_e - W_{pump_libr} - W_{pump_cooling} * ((m_{dot}[12] + m_{dot}[14]) / m_{dot}[18])$

2. Double flash geothermal power plant with single effect water-ammonia ARS

\$UnitSystem SI MASS DEG KPA C KJ

Procedure TPX(T_c, P, x: h, s, v, Q)

$T_k = T_c + 273.15$

$P_b = P * \text{convert}(\text{kPa}, \text{bar})$

Call NH3H2O(123, T_k, P_b, x: T, P, x, h, s, u, v, Q)

End

Procedure TPQ(T_c, P, Q: x, h, s, v)

$T_k = T_c + 273.15$

$P_b = P * \text{convert}(\text{kPa}, \text{bar})$

Call NH3H2O(128, T_k, P_b, Q: T, P, x, h, s, u, v, Q)

End

Procedure TXQ(T_c, x, Q: P_k, h, s, v)

$T_k = T_c + 273.15$

Call NH3H2O(138, T_k, x, Q: T, P, x, h, s, u, v, Q)

$P_k = P * \text{convert}(\text{bar}, \text{kPa})$

End

Procedure PXQ(P, x, Q: T_c, h, s, v)

$P_b = P * \text{convert}(\text{kPa}, \text{bar})$

Call NH3H2O(238, P_b, x, Q: T, P, x, h, s, u, v, Q)

$T_c = T - 273.15$

End

Procedure PXH(P, x, h: T_c, s, v, Q)

$P_b = P * \text{convert}(\text{kPa}, \text{bar})$

Call NH3H2O(234, P_b, x, h: T, P, x, h, s, u, v, Q)

$T_c = T - 273.15$

End

Procedure deltaxnh3(x_strong, P_low, P_high, T_pump_out, eta_shx: d_x)

$dx := x_strong$

$Q5 := 0$

REPEAT

$dx := dx - 0.01$

$x_weak := x_strong - dx$

Call PXQ(P_high, x_weak, Q5: T5, h5, s5, v5)

```

T6:= T_pump_out * eta_shx + (1 - eta_shx) * T5
Call TPX(T6, P_high, x_weak: h6, s6, v6, Q6)
Call PXH(P_low, x_weak, h6: T7, s7, v7, Q7)
UNTIL (T6 > T7)
d_x:= dx
end

Procedure makeupwater(m_dot_CT_in, m_dot_CT_out, m_dot_condensate: m_dot_makeup)
  if (m_dot_CT_out < (m_dot_CT_in - m_dot_condensate)) then
    m_dot_makeup:= m_dot_CT_in - m_dot_CT_out - m_dot_condensate
  else
    m_dot_makeup:= 0
  endif
end

```

=====
POWER GENERATION
=====

T_cooling_water = 25 [C]

```

$IfNot ParametricTable
P_sep_H = 390 [kPa]
P_sep_L = 320 [kPa]
$EndIf

```

eta_g = 0.85
eta_t = 0.85

"Heat Source Information"

```

T[0] = 190 [C]
m_dot[0] = 10 [kg/s]
h[0] = 1400 [kJ/kg]
s[0] = entropy(steam_IAPWS, P=P[0], h=h[0])
P[0] = pressure(steam_IAPWS, h=h[0], T=T[0])

```

"High Pressure Separator"

```

P[2] = P_sep_H
P[3] = P_sep_H
P[5] = P_sep_H
x[2] = (h[2] - h[5]) / (h[3] - h[5])
x[3] = 1
x[5] = 0
m_dot[0] = m_dot[1] + m_dot[2]
m_dot[3] = x[2] * m_dot[2]
m_dot[5] = (1 - x[2]) * m_dot[2]
h[2] = h[0]
h[3] = enthalpy(steam_IAPWS, P=P[3], x=x[3])
h[5] = enthalpy(steam_IAPWS, P=P[5], x=x[5])
s[2] = entropy(steam_IAPWS, P=P[2], x=x[2])
s[3] = entropy(steam_IAPWS, P=P[3], h=h[3])
s[5] = entropy(steam_IAPWS, P=P[5], x=x[5])
T[2] = temperature(steam_IAPWS, P=P[2], h=h[2])
T[3] = temperature(steam_IAPWS, P=P[3], h=h[3])
T[5] = temperature(steam_IAPWS, P=P[5], h=h[5])

```

"High Pressure Turbine"

$x[4] = 0.85$
 $P[4] = P_{sep_L}$
 $m_dot[4] = m_dot[3]$
 $s[4] = \text{entropy}(\text{steam_IAPWS}, P=P[4], h=h[4])$
 $h[4] = \text{enthalpy}(\text{steam_IAPWS}, P=P[4], x=x[4])$
 $T[4] = \text{temperature}(\text{steam_IAPWS}, P=P[4], x=x[4])$
 $W_t_H = m_dot[3] * (h[3] - h[4])$
 $W_e_H = \eta_g * W_t_H$

"Low Pressure Separator"

$P[6] = P_{sep_L}$
 $P[7] = P_{sep_L}$
 $P[8] = P_{sep_L}$
 $P[11] = P_{sep_L}$
 $x[7] = (h[7] - h[11]) / (h[8] - h[11])$
 $x[8] = 1$
 $x[11] = 0$
 $h[6] = h[5]$
 $h[8] = \text{enthalpy}(\text{steam_IAPWS}, P=P[8], x=x[8])$
 $h[11] = \text{enthalpy}(\text{steam_IAPWS}, P=P[11], x=x[11])$
 $T[6] = \text{temperature}(\text{steam_IAPWS}, P=P[6], h=h[6])$
 $T[7] = \text{temperature}(\text{steam_IAPWS}, P=P[7], h=h[7])$
 $T[11] = \text{temperature}(\text{steam_IAPWS}, P=P[11], h=h[11])$
 $m_dot[6] = m_dot[5]$
 $m_dot[7] = m_dot[6] + m_dot[4]$
 $m_dot[4] * h[4] + m_dot[6] * h[6] = m_dot[7] * h[7]$
 $m_dot[8] = x[7] * m_dot[7]$
 $m_dot[11] = (1 - x[7]) * m_dot[7]$

"Low Pressure Turbine"

$x[9] = \text{quality}(\text{steam_IAPWS}, P=P[9], h=h[9])$
 $m_dot[9] = m_dot[8]$
 $s[8] = \text{entropy}(\text{steam_IAPWS}, P=P[8], h=h[8])$
 $s[9] = \text{entropy}(\text{steam_IAPWS}, P=P[9], h=h[9])$

$P[9] = P_{cond}$
 $h_{9_s} = \text{enthalpy}(\text{steam_IAPWS}, P=P[9], s=s[8])$
 $h[9] = h[8] - \eta_t * (h[8] - h_{9_s})$
 $T[8] = \text{temperature}(\text{steam_IAPWS}, P=P[8], h=h[8])$
 $T[9] = \text{temperature}(\text{steam_IAPWS}, P=P[9], h=h[9])$
 $W_t_L = m_dot[8] * (h[8] - h[9])$
 $W_e_L = \eta_g * W_t_L$

"Condenser"

$\Delta T_{cond} = 20 \text{ [C]}$
 $T_{cond} = T[15] + \Delta T_{cond}$
 $P_{cond} = \text{pressure}(\text{steam_IAPWS}, T=T_{cond}, x=1)$

$P[10] = P_{cond}$
 $x[10] = 0$
 $h[10] = \text{enthalpy}(\text{steam_IAPWS}, P=P[10], x=x[10])$
 $T[10] = \text{temperature}(\text{steam_IAPWS}, P=P[10], x=x[10])$
 $m_dot[10] = m_dot[9] - m_dot_{comp}$
 $Q_{cond} = m_dot[9] * (h[9] - h[10])$

$$Q_{\text{cond}} = m_{\text{dot}}[15] * (h[16] - h[15])$$

$$P[16] = P[15]$$

$$T[16] = T[15] + 12$$

$$m_{\text{dot}}[16] = m_{\text{dot}}[15]$$

$$h[16] = \text{enthalpy}(\text{water}, T=T[16], P=P[16])$$

"NCG"

$$\text{eta_comp} = 0.85$$

$$T_{\text{sat_comp}} = T_{\text{cond}} - 4 \text{ [C]}$$

$$P_{\text{sat_comp}} = \text{pressure}(\text{steam_IAPWS}, T=T_{\text{sat_comp}}, x=1)$$

$$\text{MM_steam} = \text{molarmass}(\text{steam_IAPWS})$$

$$\text{MM_NCG} = \text{molarmass}(\text{CO2})$$

$$m_{\text{dot_NCG}} = 0.15 / 100 * m_{\text{dot}}[2]$$

$$m_{\text{dot_steam}} = (\text{MM_steam} * P_{\text{sat_comp}}) / (\text{MM_NCG} * (P_{\text{cond}} - P_{\text{sat_comp}})) * m_{\text{dot_NCG}}$$

$$m_{\text{dot_comp}} = m_{\text{dot_NCG}} + m_{\text{dot_steam}}$$

$$c_{\text{p_steam}} = \text{cp}(\text{steam}, T=T_{\text{sat_comp}}, P=P_{\text{sat_comp}})$$

$$c_{\text{p_NCG}} = \text{cp}(\text{CO2}, T=T_{\text{sat_comp}})$$

$$c_{\text{p}} = c_{\text{p_NCG}} + (c_{\text{p_steam}} - c_{\text{p_NCG}}) * (P_{\text{sat_comp}} * \text{MM_steam}) / (P_{\text{cond}} * (\text{MM_NCG} + \text{MM_steam}))$$

$$c_{\text{v_steam}} = \text{cv}(\text{steam}, T=T_{\text{sat_comp}}, P=P_{\text{sat_comp}})$$

$$c_{\text{v_NCG}} = \text{cv}(\text{CO2}, T=T_{\text{sat_comp}})$$

$$R_{\text{steam}} = c_{\text{p_steam}} - c_{\text{v_steam}}$$

$$R_{\text{NCG}} = c_{\text{p_NCG}} - c_{\text{v_NCG}}$$

$$R = R_{\text{NCG}} + (R_{\text{steam}} - R_{\text{NCG}}) * (P_{\text{sat_comp}} * \text{MM_steam}) / (P_{\text{cond}} * (\text{MM_NCG} + \text{MM_steam}))$$

$$\text{delta_h_comp} = c_{\text{p}} * T_{\text{sat_comp}} * ((P_{\text{env}}/P_{\text{cond}})^{(R/c_{\text{p}})} - 1)$$

$$W_{\text{comp}} = (m_{\text{dot_comp}} * \text{delta_h_comp}) / \text{eta_comp}$$

"Condenser Plot"

$$T_{\text{plot_cond_hot}}[0] = T[10]$$

$$T_{\text{plot_cond_hot}}[1] = T[9]$$

$$T_{\text{plot_cond_cool}}[0] = T[15]$$

$$T_{\text{plot_cond_cool}}[1] = T[16]$$

$$Q_{\text{plot_cond}}[0] = 0$$

$$Q_{\text{plot_cond}}[1] = Q_{\text{cond}}$$

$$Q_{\text{in}} = m_{\text{dot}}[2] * h[2]$$

$$\text{eta_plant} = W_{\text{e_TOT}} / Q_{\text{in}}$$

$$h_{\text{env}} = \text{enthalpy}(\text{steam_IAPWS}, P=P_{\text{env}}, T=T_{\text{env}})$$

$$s_{\text{env}} = \text{entropy}(\text{steam_IAPWS}, P=P_{\text{env}}, T=T_{\text{env}})$$

$$\text{EX} = h[0] - h_{\text{env}} - T_{\text{env}} * (s[0] - s_{\text{env}})$$

$$\text{eta_plant_EX} = W_{\text{e_TOT}} / \text{EX}$$

$$W_{\text{e_TOT}} = W_{\text{e_H}} + W_{\text{e_L}}$$

"Cooling Tower"

$$T_{\text{env}} = 25 \text{ [C]}$$

$$P_{\text{env}} = 101.3 \text{ [kPa]}$$

$$P_{\text{CT_low}} = P_{\text{env}}$$

{P environment}

$$P_{\text{CT_mid}} = P_{\text{env}} + 40 \text{ [kPa]}$$

{P environment + losses from outlet CT to

ARS machine}

$$P_{\text{CT_high}} = P_{\text{env}} + 80 \text{ [kPa]}$$

{Total losses from outlet CT to the top of CT

inlet}

$P[36] = P_CT_high$
 $P[37] = P_CT_high$
 $P[38] = P_CT_low$
 $m_dot[36] = m_dot[10]$
 $m_dot[37] = m_dot[16] + m_dot[18] + m_dot[20] + m_dot[36]$
 $V[10] = Volume(Water, T=T[10], P=P[10])$
 $W_pump_condensate = (m_dot[10] * V[10] * (P[36] - P[10])) / eta_pump$
 $m_dot[10] * h[10] + W_pump_condensate = m_dot[36] * h[36]$
 $T[36] = temperature(water, h=h[36], P=P[36])$
 $m_dot[37] * h[37] = m_dot[16] * h[16] + m_dot[18] * h[18] + m_dot[20] * h[20] + m_dot[36] * h[36]$
 $T[37] = temperature(water, h=h[37], P=P[37])$
 $T[38] = T_env + 4 [C]$
 $h[38] = enthalpy(water, T=T[38], P=P[38])$

$P[40] = P_env$
 $P[41] = P_env$
 $T[40] = T_env$
 $T[41] = T[37] - 4 [C]$
 $RH[40] = 0.75$
 $RH[41] = 1$
 $omega[40] = HumRat(AirH2O, T=T[40], r=RH[40], P=P[40])$
 $omega[41] = HumRat(AirH2O, T=T[41], r=RH[41], P=P[41])$
 $h[40] = enthalpy(AirH2O, T=T[40], r=RH[40], P=P[40])$
 $h[41] = enthalpy(AirH2O, T=T[41], r=RH[41], P=P[41])$
 $m_dot[37] + m_dot_air * omega[40] = m_dot[38] + m_dot_air * omega[41]$
 $m_dot[37] * h[37] + m_dot_air * h[40] = m_dot[38] * h[38] + m_dot_air * h[41]$

$V[38] = Volume(Water, T=T[38], P=P[38])$
 $W_pump_cooling = ((m_dot[38] + m_dot_makeup) * V[38] * (P_CT_high - P[38])) / eta_pump$

$m_dot[38] + m_dot_makeup = m_dot[14] + m_dot[17] + m_dot[19] + m_dot[39]$

"Make Up Water"

Call makeupwater(m_dot[37], m_dot[38], m_dot[10]: m_dot_makeup)

=====
 CHILLER
 =====

\$IfNot DiagramWindow

$d_x = 0.1$
 $T_pinch_a = 9 [C]$
 $T[34] = 10 [C]$
 $m_dot[1] = 0 [kg/s]$
 $delta_T_cooling = 10 [C]$

\$EndIf

{Call deltaxnh3(x[21], P[21], P[23], T[23], eta_shx: d_x)}

"Absorber"

$T[21] = T[19] + T_pinch_a$
 $x[27] = x[25]$
 $Q[21] = 0$
 $P[21] = P[34]$
 $P[27] = P[34]$

Call TPQ(T[21], P[21], Q[21]: x[21], h[21], s[21], v[21])
 $m_{\dot{21}} = m_{\dot{27}} + m_{\dot{35}}$
 $m_{\dot{21}} * x[21] = m_{\dot{27}} * x[27] + m_{\dot{35}} * x[35]$
 $h[27] = h[26]$
 Call PXH(P[27], x[27], h[27]: T[27], s[27], v[27], Q[27])
 $Q_a = m_{\dot{27}} * h[27] + m_{\dot{35}} * h[35] - m_{\dot{21}} * h[21]$
 $Q_a = m_{\dot{19}} * (h[20] - h[19])$

"Gain m19"

$P[19] = P_{CT_mid}$
 $P[20] = P[19]$
 $T[19] = T[38]$
 $T[20] = T[19] + 15 \text{ [C]}$
 $h[19] = \text{enthalpy}(\text{water}, T=T[19], P=P[19])$
 $h[20] = \text{enthalpy}(\text{water}, T=T[20], P=P[20])$
 $m_{\dot{20}} = m_{\dot{19}}$

$LMTD_a = ((T[27] - T[20]) - (T[21] - T[19])) / \ln((T[27] - T[20]) / (T[21] - T[19]))$
 $U_a = 0.85 \text{ [kW/m}^2\text{-C]}$
 $Q_a = U_a * A_a * LMTD_a$

"Pump"

$\eta_{pump} = 0.95$
 $x[22] = x[21]$
 $P[22] = P[31]$
 $m_{\dot{22}} = m_{\dot{21}}$
 $W_{pump_nh3} = (m_{\dot{21}} * v[21] * (P[22] - P[21])) / \eta_{pump}$
 $h[22] * m_{\dot{22}} = h[21] * m_{\dot{21}} + W_{pump_nh3}$
 Call PXH(P[22], x[22], h[22]: T[22], s[22], v[22], Q[22])

"Solution Heat Exchanger"

$\eta_{shx} = 0.6$
 $x[26] = x[25]$
 $P[23] = P[31]$
 $P[26] = P[31]$
 $m_{\dot{26}} = m_{\dot{25}}$
 $T[26] = T[23] * \eta_{shx} + (1 - \eta_{shx}) * T[25]$
 Call TPX(T[26], P[26], x[26]: h[26], s[26], v[26], Q[26])
 $m_{\dot{23}} * h[23] + m_{\dot{25}} * h[25] = m_{\dot{24}} * h[24] + m_{\dot{26}} * h[26]$
 Call PXH(P[24], x[24], h[24]: T[24], s[24], v[24], Q[24])
 $Q_{shx} = m_{\dot{25}} * (h[25] - h[26])$

$LMTD_{shx} = ((T[25] - T[24]) - (T[26] - T[23])) / \ln((T[25] - T[24]) / (T[26] - T[23]))$
 $U_{shx} = 1.1 \text{ [kW/m}^2\text{-C]}$
 $Q_{shx} = U_{shx} * A_{shx} * LMTD_{shx}$

"Desorber"

$x[24] = x[21]$
 $x[25] = x[24] - d_x$
 $Q[25] = 0$
 Call PXQ(P[25], x[25], Q[25]: T[25], h[25], s[25], v[25])
 $P[24] = P[31]$
 $P[25] = P[31]$
 $P[30] = P[31]$
 Call PXQ(P[30], x[30], Q[30]: T[30], h[30], s[30], v[30])
 $m_{\dot{30}} = m_{\dot{34}}$
 $m_{\dot{24}} = m_{\dot{21}}$
 $m_{\dot{25}} = m_{\dot{27}}$

$$Q_d = m_dot[25] * h[25] + m_dot[28] * h[28] - m_dot[24] * h[24] - m_dot[29] * h[29]$$

$$Q_d = m_dot[12] * (h[12] - h[13])$$

$$P[1] = P_sep_L$$

$$P[12] = P_sep_L$$

$$P[13] = P[12]$$

$$h[1] = h[0]$$

$$T[12] = \text{temperature}(\text{steam_IAPWS}, P=P[12], h=h[12])$$

$$T[13] = \text{temperature}(\text{steam_IAPWS}, h=h[13], P=P[13])$$

$$m_dot[12] * h[12] = m_dot[1] * h[1] + m_dot[11] * h[11]$$

$$m_dot[12] = m_dot[1] + m_dot[11]$$

$$m_dot[13] = m_dot[12]$$

$$LMTD_d = ((T[12] - T[25]) - (T[13] - T[24])) / \ln((T[12] - T[25]) / (T[13] - T[24]))$$

$$U_d = 0.85 \text{ [kW/m}^2\text{-C]}$$

$$Q_d = U_d * A_d * LMTD_d$$

"Rectifier"

$$Q[28] = 1$$

$$Q[29] = 0$$

$$Q[30] = 1$$

$$P[28] = P[31]$$

$$P[29] = P[31]$$

$$x[28] = 0.9444$$

$$x[30] = 0.999634$$

$$\text{Call PXQ}(P[28], x[28], Q[28]: T[28], h[28], s[28], v[28])$$

$$T[29] = T[28]$$

$$\text{Call TPQ}(T[29], P[29], Q[29]: x[29], h[29], s[29], v[29])$$

$$m_dot[28] = m_dot[29] + m_dot[30]$$

$$m_dot[28] * x[28] = m_dot[29] * x[29] + m_dot[30] * x[30]$$

$$Q_r = m_dot[28] * h[28] - m_dot[29] * h[29] - m_dot[30] * h[30]$$

$$Q_r = m_dot[22] * (h[23] - h[22])$$

$$x[23] = x[22]$$

$$m_dot[23] = m_dot[22]$$

$$\text{Call PXH}(P[23], x[23], h[23]: T[23], s[23], v[23], Q[23])$$

$$LMTD_r = ((T[28] - T[23]) - (T[30] - T[22])) / \ln((T[28] - T[23]) / (T[30] - T[22]))$$

$$U_r = 1.0 \text{ [kW/m}^2\text{-C]}$$

$$Q_r = U_r * A_r * LMTD_r$$

"Condenser"

$$x[31] = x[30]$$

$$T[31] = T[17] + 15 \text{ [C]}$$

$$Q[31] = 0$$

$$\text{Call TXQ}(T[31], x[31], Q[31]: P[31], h[31], s[31], v[31])$$

$$m_dot[31] = m_dot[34]$$

$$Q_c = m_dot[30] * (h[30] - h[31])$$

$$Q_c = m_dot[17] * (h[18] - h[17])$$

"Gain m17"

$$P[17] = P_CT_mid$$

$$P[18] = P[17]$$

$$T[17] = T[38]$$

$$T[18] = T[30] - 5 \text{ [C]}$$

$h[17] = \text{enthalpy}(\text{water}, T=T[17], P=P[17])$
 $h[18] = \text{enthalpy}(\text{water}, T=T[18], P=P[18])$
 $m_dot[18] = m_dot[17]$

$LMTD_c = ((T[30] - T[18]) - (T[31] - T[17])) / \ln((T[30] - T[18]) / (T[31] - T[17]))$
 $U_c = 1.4 \text{ [kW/m}^2\text{-C]}$
 $Q_c = U_c * A_c * LMTD_c$

"Refrigerant Heat Exchanger"

$\eta_{rhx} = (T[31] - T[32]) / (T[31] - T[34])$
 $P[32] = P[31]$
 $P[35] = P[34]$
 $x[32] = x[30]$
 $x[35] = x[30]$
 $T[35] = T[31] - 4 \text{ [C]}$
 Call TPX(T[35], P[35], x[35]: h[35], s[35], v[35], Q[35])
 $m_dot[31] * h[31] + m_dot[34] * h[34] = m_dot[32] * h[32] + m_dot[35] * h[35]$ "Gain h32"
 Call PXH(P[32], x[32], h[32]: T[32], s[32], v[32], Q[32])
 $m_dot[32] = m_dot[34]$
 $m_dot[35] = m_dot[34]$
 $Q_rhx = m_dot[31] * h[31] - m_dot[32] * h[32]$

$LMTD_rhx = ((T[31] - T[35]) - (T[32] - T[34])) / \ln((T[31] - T[35]) / (T[32] - T[34]))$
 $U_rhx = 1.1 \text{ [kW/m}^2\text{-C]}$
 $Q_rhx = U_rhx * A_rhx * LMTD_rhx$

"Evaporator"

$x[33] = x[30]$
 $x[34] = x[30]$
 $P[33] = P[34]$
 $Q[34] = 1$
 Call TXQ(T[34], x[34], Q[34]: P[34], h[34], s[34], v[34])
 $h[33] = h[32]$
 Call PXH(P[33], x[33], h[33]: T[33], s[33], v[33], Q[33])
 $Q_e = m_dot[34] * (h[34] - h[33])$
 $m_dot[33] = m_dot[34]$
 $Q_e = m_dot[14] * (h[14] - h[15])$ "Gain m14"

$P[14] = P_CT_mid$
 $P[15] = P[14]$
 $T[14] = T[38]$
 $T[15] = T[14] - \text{delta_T_cooling}$
 $h[14] = \text{enthalpy}(\text{water}, T=T[14], P=P[14])$
 $h[15] = \text{enthalpy}(\text{water}, T=T[15], P=P[15])$
 $m_dot[14] = m_dot[15]$

$LMTD_e = ((T[14] - T[34]) - (T[15] - T[33])) / \ln((T[14] - T[34]) / (T[15] - T[33]))$
 $U_e = 1.5 \text{ [kW/m}^2\text{-C]}$
 $Q_e = U_e * A_e * LMTD_e$

$A_HE = A_a + A_shx + A_d + A_r + A_c + A_rhx + A_e$
 $m_dot_cooling = m_dot[14] + m_dot[17] + m_dot[19]$

$COP_chiller = Q_e / (Q_d + W_pump_nh3)$

$W_e_net = W_e_TOT - W_pump_nh3 - W_pump_cooling * ((m_dot[17] + m_dot[19]) / m_dot[38])$